TECHNICAL REPORT-RD-WS-93-1

SELECTIVE NITRATIONS: THE LASER-INDUCED NITRATION OF THREE CYCLOALKANES: II

Ann E. Stanley
Judith M. Bonicamp
Susan E. Godbey
Larry M. Ludwick
Weapons Sciences Directorate
Research, Development, and Engineering Center

MARCH 1993

U.S. ARMY MISSILE COMMAND
Redstone Arsenal, Alabama 35898-5000

DESTRUCTION NOTICE

FOR CLASSIFIED DOCUMENTS, FOLLOW THE PROCEDURES IN DoD 5200.22-M, INDUSTRIAL SECURITY MANUAL, SECTION II-19 OR DoD 5200.1-R, INFORMATION SECURITY PROGRAM REGULATION, CHAPTER IX. FOR UNCLASSIFIED, LIMITED DOCUMENTS, DESTROY BY ANY METHOD THAT WILL PREVENT DISCLOSURE OF CONTENTS OR RECONSTRUCTION OF THE DOCUMENT.

DISCLAIMER

THE FINDINGS IN THIS REPORT ARE NOT TO BE CONSTRUED AS AN OFFICIAL DEPARTMENT OF THE ARMY POSITION UNLESS SO DESIGNATED BY OTHER AUTHORIZED DOCUMENTS.

TRADE NAMES

USE OF TRADE NAMES OR MANUFACTURERS IN THIS REPORT DOES NOT CONSTITUTE AN OFFICIAL ENDORSEMENT OR APPROVAL OF THE USE OF SUCH COMMERCIAL HARDWARE OR SOFTWARE.

REPORT DOCUMENTATION PAGE

Form Approved
OMB No. 0704-0188

1a. REPORT SECURITY CLASSIFICATION Unclassified	1b. RESTRICTIVE MARKINGS
2a. SECURITY CLASSIFICATION AUTHORITY	3. DISTRIBUTION/AVAILABILITY OF REPORT *Approved for public release; distribution is unlimited.*
2b. DECLASSIFICATION/DOWNGRADING SCHEDULE	
4. PERFORMING ORGANIZATION REPORT NUMBER(S) Technical Report RD-WS-93-1	5. MONITORING ORGANIZATION REPORT NUMBER (S)
6a. NAME OF PERFORMING ORGANIZATION Weapons Sciences Directorate RD&E Center 6b. OFFICE SYMBOL (if applicable) AMSMI-RD-WS-CM	7a. NAME OF MONITORING ORGANIZATION
6c. ADDRESS (City, State, and ZIP Code) Commander, U. S. Army Missile Command ATTN: AMSMI-RD-WS-CM Redstone Arsenal, AL 35898-5248	7b. ADDRESS (City, State, and ZIP Code)
8a. NAME OF FUNDING/SPONSORING ORGANIZATION 8b. OFFICE SYMBOL (if applicable)	9. PROCUREMENT INSTRUMENT IDENTIFICATION NUMBER
8c. ADDRESS (City, State, and ZIP Code)	10. SOURCE OF FUNDING NUMBERS PROGRAM ELEMENT NO. / PROJECT NO. / TASK NO. / WORK UNIT ACCESSION NO.

11. TITLE (Include Security Classification)

SELECTIVE NITRATIONS: THE LASER-INDUCED NITRATION OF THREE CYCLOALKANES: II

12. PERSONAL AUTHOR(S)

ANN E. STANLEY, JUDITH M. BONICAMP, SUSAN E. GODBEY, AND LARRY M. LUDWICK

13a. TYPE OF REPORT	13b. TIME COVERED	14. DATE OF REPORT (Year, Month, Day)	15. PAGE COUNT
Final	FROM July 91 TO Sep 92	March 1993	99

16. SUPPLEMENTARY NOTATION

17. FIELD	COSATI CODES: GROUP	SUB-GROUP

18. SUBJECT TERMS (Continue on reverse if necessary and identify by block number)
Laser-containing Compounds; Hydrocarbons; Nitrogen Dioxide; Cyclopropane; Cyclobutane; Cyclopentane

19. ABSTRACT (Continue on reverse if necessary and identify by block number)

The army uses nitrated compounds as explosives and propellants. There is a special need for propellants with the chemical composition necessary to burn exactly with high energy production, but with a minimum of side products which create smoke. Laser-induced chemistry possesses the potential to drive some reactions in an efficient and selective manner, and may be useful in driving nitration reactions toward specific products. Reported here are the results of several successful attempts to laser-induce the reactions of nitrogen oxides with three cycloalkanes. Specifically, the tunable, continuous wave, carbon dioxide infrared laser was used to drive the reaction between nitrogen dioxide and cyclopropane, cyclobutane, and cyclopentane under a variety of reaction conditions. The spectrochemical analyses of the product mixtures are presented here. In addition to nitrocycloalkanes, other products resulting were either from ring cleavage, or from nitration or oxidation of ring fragments. By examining the effects of various reaction conditions on the product arrays, it was possible to find optimum conditions for producing the nitrocycloalkanes while minimizing side products.

20. DISTRIBUTION/AVAILABILITY OF ABSTRACT ☐ UNCLASSIFIED/UNLIMITED ☒ SAME AS RPT. ☐ DTIC USERS	21. ABSTRACT SECURITY CLASSIFICATION Unclassified
22a. NAME OF RESPONSIBLE INDIVIDUAL Ann E. Stanley	22b. TELEPHONE (Include Area Code) (205) 876-5937 22c. OFFICE SYMBOL AMSMI-RD-WS-CM

DD Form 1473, JUN 86 Previous editions are obsolete.

ACKNOWLEDGEMENTS

Judith M. Bonicamp, Susan E. Godbey, and Larry M. Ludwick would like to acknowledge financial support from the U. S. Army Missile Command under Battelle Contract Number DAAL03-86-D-0001, in partial performance of this work. Permanent address for Judith M. Bonicamp is Department of Chemistry and Physics, Middle Tennessee State University, Murfreesboro, TN 37132. Permanent address for Susan E. Godbey is Department of Chemistry, Eastern Kentucky University, Richmond, KY 40475. Permanent address for Larry M. Ludwick is Tuskegee University, Tuskegee, AL 36088.

Appreciation is extended to Dr. S. P. McManus of the University of Alabama in Huntsville for providing the sample of cyclobutane.

TABLE OF CONTENTS

LIST OF FIGURES

LIST OF FIGURES (cont'd)

LIST OF FIGURES (cont'd)

LIST OF FIGURES (cont'd)

LIST OF FIGURES (cont'd)

LIST OF FIGURES (cont'd)

LIST OF FIGURES (cont'd)

LIST OF FIGURES (cont'd)

LIST OF FIGURES (cont'd)

LIST OF FIGURES (cont'd)

LIST OF FIGURES (cont'd)

LIST OF FIGURES (cont'd)

LIST OF FIGURES (cont'd)

LIST OF FIGURES (cont'd)

LIST OF FIGURES (cont'd)

I. INTRODUCTION

Nitrogen-containing compounds are commonly used by the Army in propellants and explosives. The chemical and physical properties of these high energy formulations are governed by the molecular structures of the individual components. In the face of increasingly stringent performance requirements for these materials, improved methods of nitration are sought that will allow the molecular structures of the products to be selectively designed. Laser-induced chemistry is an excellent tool for this type of work.

As in the thermally driven, vapor phase nitration [1] of cyclopropane. the laser-induced reaction of nitrogen dioxide with these three nitrocycloalkanes very likely involves the replacement of hydrogen atoms by nitro groups. It is a bimolecular reaction of the cycloalkane and nitrogen dioxide which results in the formation of nitro compounds and some alcohols. There are competing reactions which involve the thermal isomerization of cyclopropane to propene, or in general, the thermal isomerization of the cycloalkane to alkenes. Above 390°, decomposition and oxidation of reaction mixtures occurred [1]. At lower temperatures, 335°-390°, and longer exposure times, the thermal isomerization, oxidation, and decomposition of the reaction mixture were minimized [1]. It is highly likely that a laser-induced process can be optimized in a similar manner with higher yield.

Previously, workers from this laboratory reported the successful nitration of several open-chain alkanes by nitrogen dioxide (NO_2) using a tunable, continuous wave (CW), CO_2 laser to drive the reactions [2]. Both the yields of nitroalkanes and the selectivity of the process were promising. Subsequently, we extended the CW, CO_2 laser-induced nitration process to a series of cyclic hydrocarbons, namely, cyclopropane, cyclobutane, and cyclopentane [3,4]. The products in these reactions were identified using gas chromatography-mass spectrometry (GC-MS) and infrared analyses. Under certain conditions nitrocycloalkanes could be formed without making significant amounts of other nitrated products. In this current work we report further on the nitration of the cycloalkanes, this time to describe the quantitative dependence of the nitrocycloalkanes in the product mixtures on changes in the pressures of reactants and on variations in the energy absorbed by the system with and without the photochemical sensitizer, sulfur hexafluoride, SF_6. The focus of the project was to optimize the yields of the nitrocycloalkanes while minimizing, if not eliminating, side products. Though the experiments were designed with this objective in mind, we were able to follow the formation of a number of side products in the course of monitoring the production of nitrocycloalkanes. Our discussion includes an evaluation of the synthetic utility and specificity of the laser driven nitration process based on this information.

The nitrocycloalkane products formed all have strong infrared absorption bands which are readily accessible to the output of the carbon dioxide laser. A major concern is whether these products might readily decompose in the beam or by collisional transfer, in a manner somewhat similar to the shock initiated pyrolysis of nitrocyclopropane [5]. The major product of this pyrolysis was

ethylene. However, it is known through theoretical studies [6] that the nitro group is electron withdrawing, thus the cyclopropyl ring is stabilized by the nitro moiety.

II. EXPERIMENTAL

Samples of cyclopropane, cyclopentane, 2,2-dimethylbutane, nitromethane, nitroethane, 1-nitropropane, 2-nitropropane, 2-methyl-2-nitropropane, 1-nitrobutane, 1-nitropentane, nitrocyclopentane, and nitrogen dioxide were obtained from Aldrich Chemical Company, Milwaukee, WI. The samples were of 98 percent or greater stated purity, except for 2-nitropropane, which was 94 percent stated purity, and cyclopropane which was 95 percent stated purity. The cyclobutane sample was provided by Dr. S. McManus, Department of Chemistry, University of Alabama at Huntsville. The purity of the samples was monitored with GC-MS, and the infrared spectra were compared with published spectra where available [8-12]. No further purification of the compounds was undertaken, with the exception of nitrogen dioxide and cyclobutane which were purified by trap-to-trap separation at –78.5 °C. Nitrocyclopropane was prepared by the method of Gilkut and Borden [13]. After distillation the sample was sent to the University of Alabama at Huntsville where its identity was verified by NMR analysis. All compounds were degassed at –196.8 °C.

A 100-mL stainless steel cell of exterior dimensions $5 \times 5 \times 10$ cm was used to hold reactants during irradiation. This cell was equipped with zinc selenide or potassium chloride windows on the long path through which the laser was directed, and AMTIR-1 windows on the short path for collecting the infrared spectra of reactants and products. The optical path lengths were 10.5 cm for the long path and 5 cm for the short path. The initial sample pressures were measured with a MKS Baratron electronic manometer, consisting of a Type 222B transducer and a Type PDR-5B power supply/digital readout. All nitration reactions followed the same general procedure. After evacuating the system to baseline pressure, the gas for the lowest pressure was admitted to the cell. Following removal of the gas from the vacuum line, the next higher pressure gas was admitted at a pressure greater than the final pressure desired. The cell valve was opened for 1-2 seconds to allow pressure equilibration and then closed. The gas in the vacuum system was then removed and, if necessary, a third gas component was introduced into the cell in the same manner. Using this technique a given gas mixture could be reproduced readily. The reproducibility was established by measuring the infrared absorbances of the components in the mixtures.

The infrared spectra were recorded on a Bomem DA3.002 interferometer equipped with a vacuum bench and either a deuterated TGS detector or a liquid nitrogen-cooled MCT detector and a KBr beamsplitter. The effective resolution was 1 cm^{-1}, and 32 scans were taken for each sample and reference. A medium apodization function was used [14].

A Coherent Radiation Model 41 CW CO_2 tunable laser provided the energy to drive the reactions, and it was operated in a single mode at various selected wavelengths and powers. The wavelength was verified with an Optical

Engineering CO_2 spectrum analyzer. The powers were measured by a Coherent Radiation Model 213 water-cooled power meter.

The reaction cell was positioned on a movable stage which could be translated along the laser path. All samples were irradiated with the cell positioned behind the focal point where the beam was slightly diverging. The zinc selenide windows allowed a beam transmittance of about 70 percent through the sample cell. The KCl windows allowed about 86 percent of the beam through the two windows to the power meter. The reported laser powers do not correct for this window absorption, nor for the difference in beam diameter at the sample, as opposed to the diameter at the power meter, where the beam is larger. The beam diameter was approximately 2 mm at the point of entry to the reaction cell.

The separation and analysis of the reaction products were accomplished using a Hewlett-Packard (HP) 5890 gas chromatograph equipped with a 0.250-mL gas sampling loop and interfaced to an HP 5970 series mass selective detector. The chromatographic column was an HP Ultra 2 (crosslinked 5 percent phenyl methyl silicone) of about 40 m length, having a 0.2-mm interior diameter and 0.22-μm film thickness. The volumetric flow rate was 1.6 cm^3/min (linear flow rate 10 m/min); the split ratio was 47:1; and the column head pressure was 10 psi. For chromatographic analysis two different temperature programs were used. With cyclopropane, cyclobutane, and some cyclopentane mixtures, the oven temperature was programmed to 140 °C (10°C/min) following 5 minutes at the initial temperature of 40 °C. For other cyclopentane reaction mixtures the initial oven temperature was 60 °C and programming to 160 °C (10°C/min) began immediately. Identification of the components of the chromatographic peaks was attempted using the computer search routine and the NBS43k Mass Spectra Library. Whenever possible component identities were verified by comparing the gas chromatographic retention times and the mass spectra to those of known samples. The separation of some highly volatile components was not possible with the chromatographic conditions used.

Irradiation of the cyclopentane reaction mixtures frequently produced visible condensation of liquid on the KCl windows. A procedure was developed to quantitate the amount of liquid formed. Following the removal of a gas sample to the gas sampling loop, the cell was opened and 2.0 mL of absolute ethanol was added using a 10.00 ml pipet. After rinsing the inside of the cell for 5-10 minutes, the ethanol solution was removed and placed in a septum sealed vial. Following each ethanol wash the KCl cell windows were polished to remove cloudiness. Liquid samples (0.5 ul) of the wash solution were injected on the GC using a 1.0 ul syringe. Several injections were averaged to give GC-MS total ion areas for the nitrocyclopentane, the only nitroalkane identified in the ethanol solution. A calibration curve from the GC-MS total ion areas of a series of standard solutions of nitrocyclopentane in absolute ethanol was used to quantify the nitrocyclopentane produced in the reaction.

The program XYmath (C. Taylor, P.O. Box 277875, Sacramento, CA 95827-7875) was used for curve-fitting of the GC-MS total ion areas and the infrared spectral integrals.

III. RESULTS AND DISCUSSION

The CW carbon dioxide infrared laser emits several intense bands of radiation in the region between 900 and 1100 cm^{-1}. Absorbance spectra for the three cycloalkanes [3] reveal vibrational bands for each compound that are accessible by the output of the CO_2 laser. These bands indicate why it was possible to initiate and sustain by laser excitation, the reaction of the hydrocarbons with nitrogen dioxide. In instances where the power output of the laser transition is low or the hydrocarbon absorption is weak at that frequency, an infrared sensitizer, sulfur hexafluoride, was used to initiate the reaction indirectly.

We irradiated mixtures of each cyclic hydrocarbon with nitrogen dioxide under variable conditions of laser powers, irradiation frequencies and times, and pressures of reactants or sensitizer. For each hydrocarbon we will present results which illustrate the impact of varying the conditions on the relative amounts of products formed.

A. Cyclopropane

Cyclopropane has two infrared absorption bands that are accessible to the laser, one at 866 cm^{-1}, the other at 1027 cm^{-1}. Although not on the absorption maximum, the CO_2 laser output from the P(18) line of the (00°1)-(02°0) transition at 1048.7 cm^{-1} could be varied easily from 20–50 W/cm^2, which was one reason why this line was a good choice for irradiation of cyclopropane mixtures. Other CO_2 output lines, in addition to being on the periphery of cyclopropane's absorption band, afforded limited laser power.

Infrared spectra were acquired for reaction mixtures before and after irradiation. The infrared spectra recorded before irradiation allowed us to monitor the reproducibility of the initial gas pressures. These spectra were integrated over regions corresponding to absorbance bands of cyclopropane (4511.3 - 4500.2 cm^{-1}) and nitrogen oxides (N_2O_4, 1296.0 - 1208.2 cm^{-1}; N_2O_4 and NO_2, 778.6-665.8 cm^{-1}). Figure 1 shows a linear relationship between the cyclopropane areas versus partial pressures of cyclopropane in the reaction mixtures. Figure 2 shows a similar relationship between the areas and the partial pressures for the nitrogen oxides.

When mixtures of cyclopropane and nitrogen oxides were irradiated the quantity of nitrogen oxides consumed depended on the initial pressure of cyclopropane, as determined by infrared spectral analysis. Figure 3 shows the depletion of nitrogen oxides (40 Torr) when the mixtures were irradiated at 30 W/cm^2 for 60 s. The amount of cyclopropane used during irradiation with

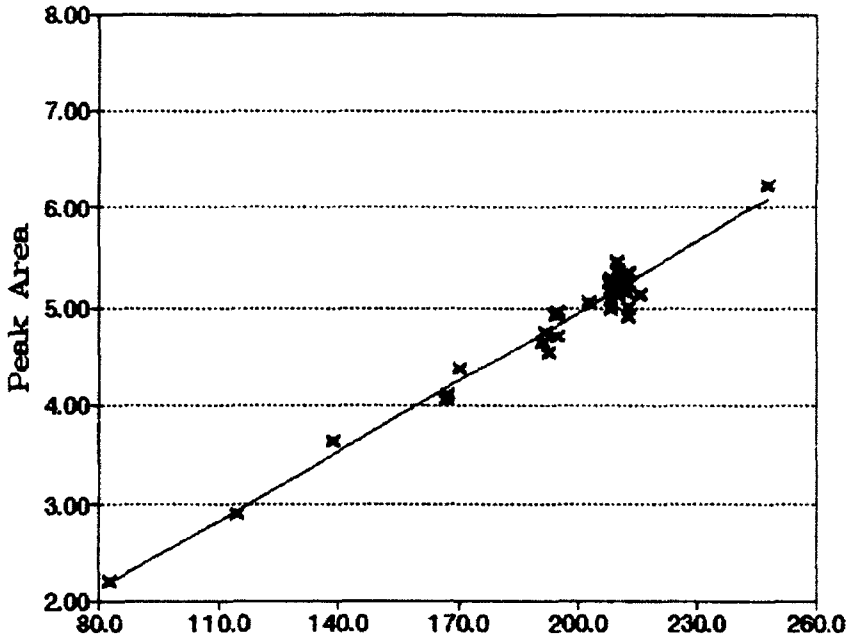

Figure 1. Areas of Cyclopropane Infrared Peak: Before Irradiation Versus Cyclopropane Pressure

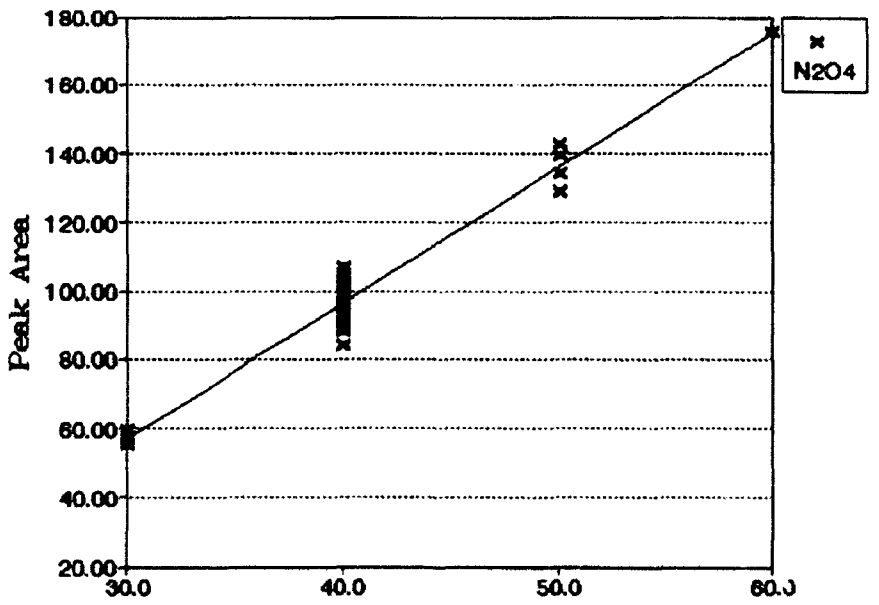

Figure 2a. Areas of Nitrogen Oxides: Before Irradiation Versus Nitrogen Oxides Pressure, N_2O_4 Infrared Peak Areas

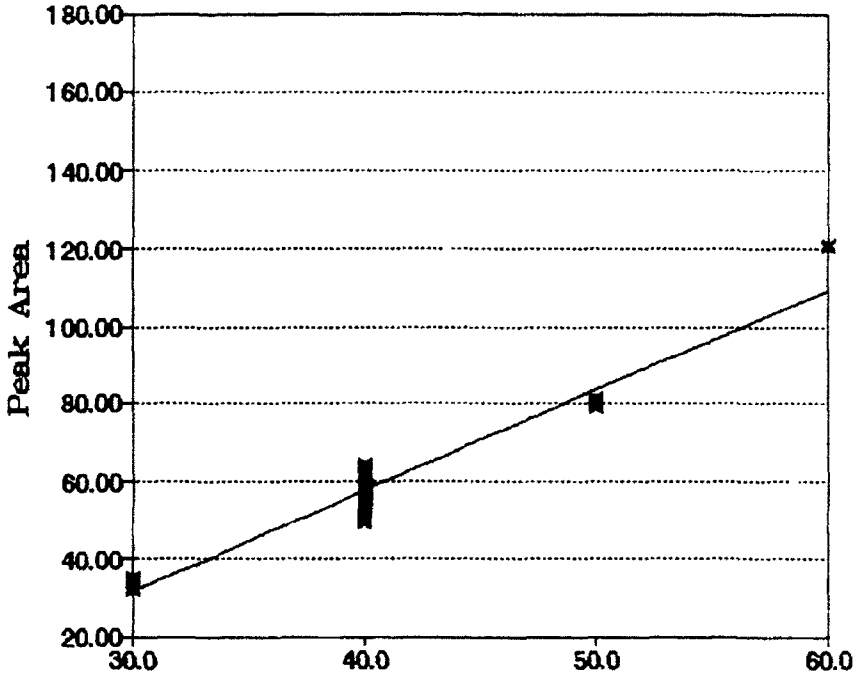

Figure 2b. Areas of Nitrogen Oxides: Before Irradiation Versus Nitrogen Oxides Pressure, $NO_2 + N_2O_4$ Infrared Peak Areas

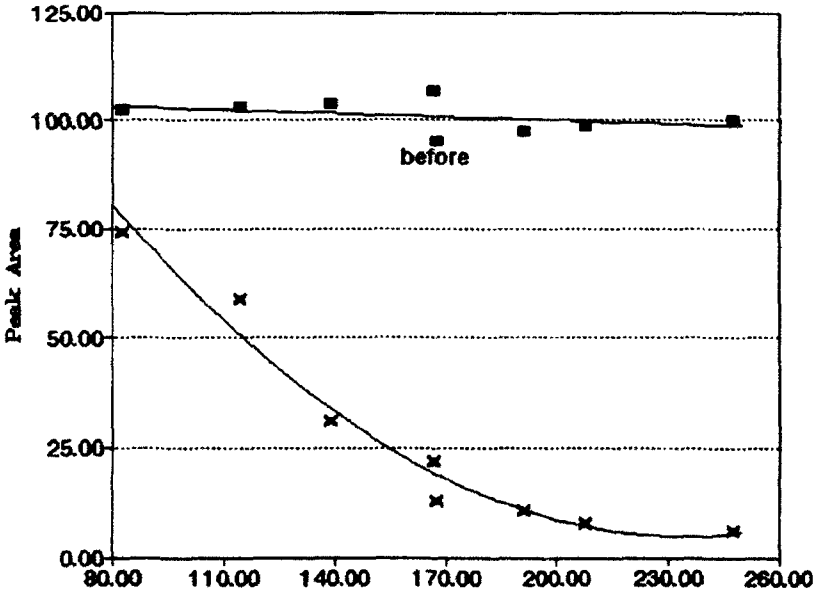

Figure 3a. Nitrogen Oxides (40 Torr) Versus Cyclopropane Pressure: Before and After Irradiation for 60 s at 30 W/cm^2 Using the P(18) Line of the (00°1)-(02°0) Transition, 1048.7 cm^{-1}, N_2O_4 Infrared Peak Areas

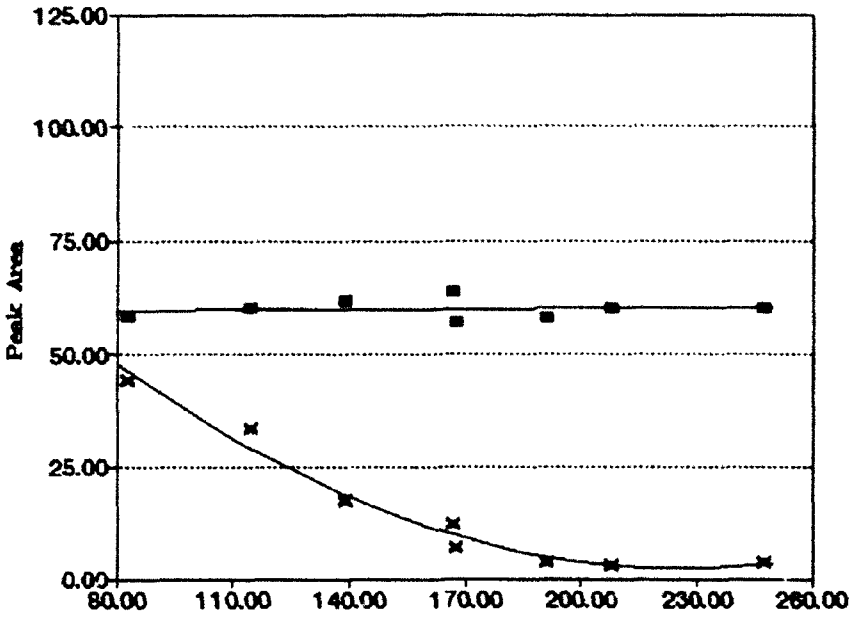

Figure 3b. Nitrogen Oxides (40 Torr) Versus Cyclopropane Pressure: Before and After Irradiation for 60 s at 30 W/cm^2 Using the P(18) Line of the (00°1)-(02°0) Transition, 1048.7 cm^{-1}, N_2O_4 + NO_2 Infrared Peak Areas

nitrogen oxide mixtures showed little dependence on the initial pressure of cyclopropane. Irradiation products identified from the infrared spectra include H_2O, HCN, CO_2, NNO, CO, NO, formic acid, ethene, and nitrocyclopropane [3]. The frequency regions over which integrals were acquired are in Table 1. Figure 4 shows the manner in which the formation of nitrocyclopropane depended on the initial pressure of cyclopropane, as determined by both gas phase infrared analysis, and GC-MS analysis using the gas sampling loop. At a constant nitrogen oxide pressure of 40 Torr, the nitrocyclopropane in the vapor phase of the product mixture increased up to a pressure of about 200 Torr of cyclopropane. Beyond this pressure if more nitrocyclopropane was produced it was in a condensed phase and was not detected by infrared or GC-MS analysis. No nitroalkanes besides nitrocyclopropane were detected under these conditions. Other products resulting were either from ring cleavage, or from nitration or oxidation of ring fragments. All of the ring-cleavage products showed a strong dependence on the partial pressure of cyclopropane (Figs. 5 - 9), with the production of formic acid, ethene and carbon dioxide leveling off as the cyclopropane pressure increased. Production of hydrogen cyanide and the fragment CO continued to increase as the cyclopropane pressure rose. Figures 10 and 11 show how the formation of NO and NNO depended on the cyclopropane pressure. The GC-MS analysis of the product mixtures revealed the presence of propene, 2-propenal, and acetonitrile, in addition to a large mixed gas peak. The mixed gas peak resulted from water and those highly volatile components not separable with the chromatographic conditions used, HCN, CO_2, NNO, CO, NO,

and ethene, in addition to unreacted nitrogen oxides. Production of mixed gases rose smoothly as the pressure of cyclopropane increased (Fig. 12). The product propene did not appear in the GC-MS traces until the cyclopropane pressure in the reaction mixtures was greater than about 120 Torr (Fig. 13).

Table 1. Infrared Frequency Regions (cm^{-1}) for Integrals of Reactants and Products in the Cyclopropane and Nitrogen Oxides Systems

Frequency Interval	Identity
4511.3 – 4500.2	Cyclopropane
2389.0 – 2292.5	CO_2
2254.0 – 2225.0	NNO
2224.6 – 2141.6	CO
1877.9 – 1824.4	NO
1390.9 – 1349.0	Nitrocyclopropane
1296.0 – 1208.2	N_2O_4
1140.2 – 1102.1	Formic Acid
952.1 – 943.5	Ethene
778.6 – 720.3	$N_2O_4 + NO_2$
716.4 – 708.7	HCN

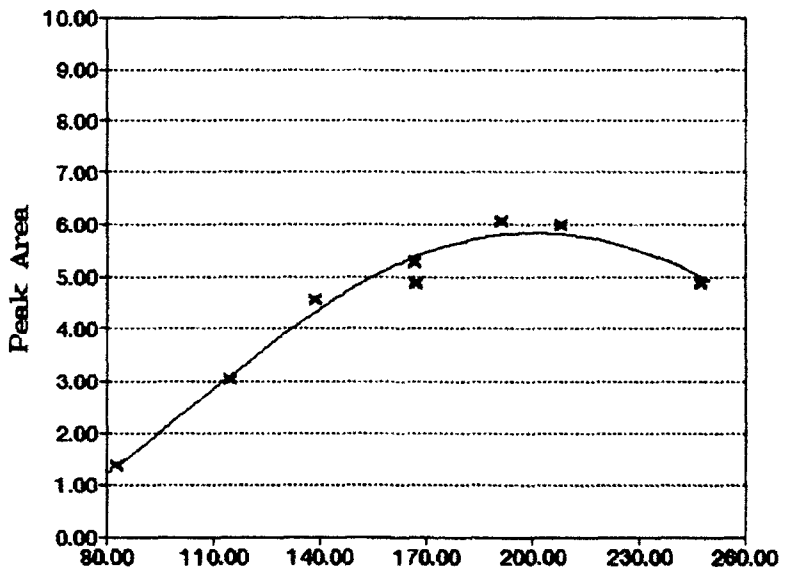

Figure 4a. Nitrocyclopropane Production Versus Cyclopropane Pressure: After Irradiation of Mixtures Containing 40 Torr of Nitrogen Oxides for 60s at 30 W/cm² Using the P(18) Line of the (00°1)-(02°0) Transition, 1048.7 cm⁻¹, Nitrocyclopropane Infrared Peak Areas

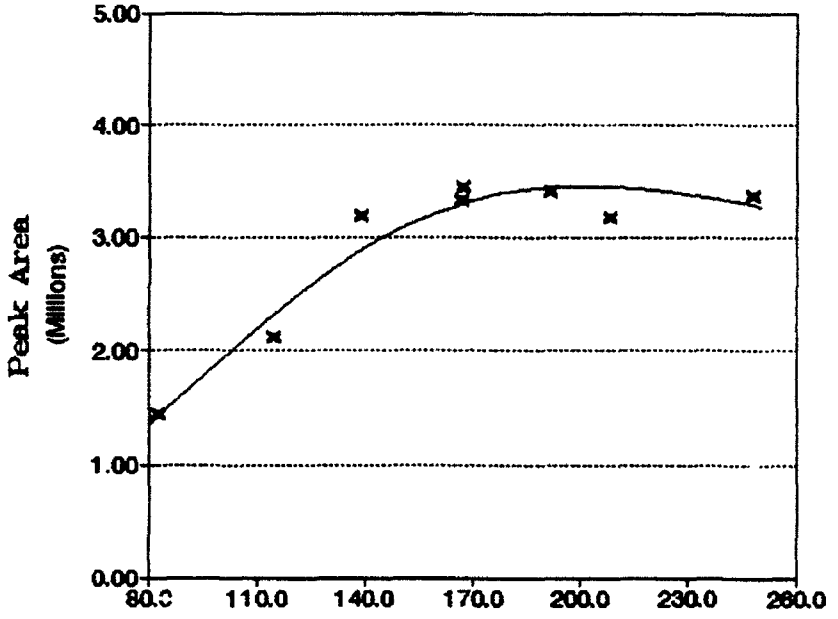

Figure 4b. Nitrocyclopropane Production Versus Cyclopropane Pressure: After Irradiation of Mixtures Containing 40 Torr of Nitrogen Oxides for 60 s at 30 W/cm^2 Using the P(18) Line of the (00°1)-(02°0) Transition, 1048.7 cm^{-1}, Nitrocyclopropane GC-MS Peak Areas

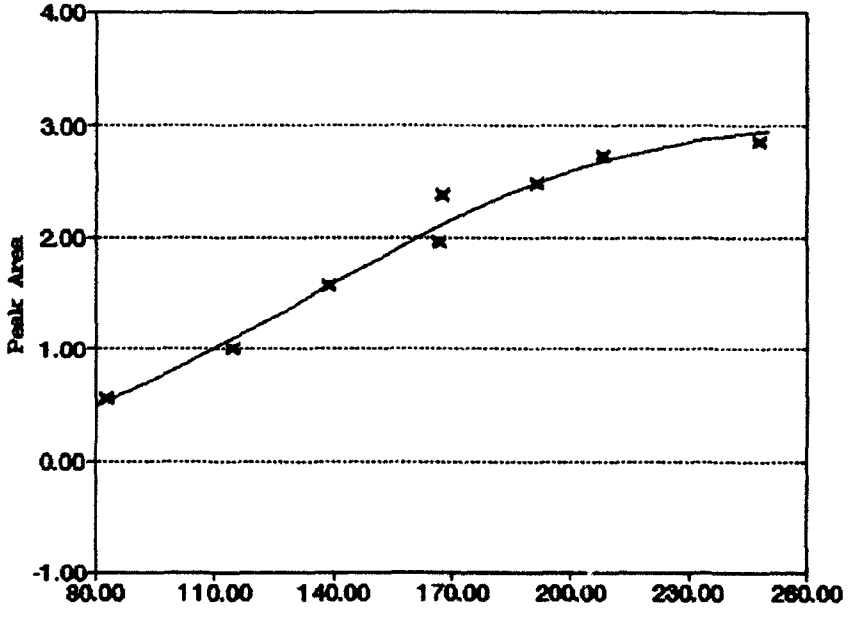

Figure 5. Ethene Production Versus Cyclopropane Pressure: Ethene Infrared Peak Areas After Irradiation of Mixtures Containing 40 Torr of Nitrogen Oxides for 60 s at 30 W/cm^2 Using the P(18) Line of the (00°1)-(02°0) Transition, 1048.7 cm^{-1}

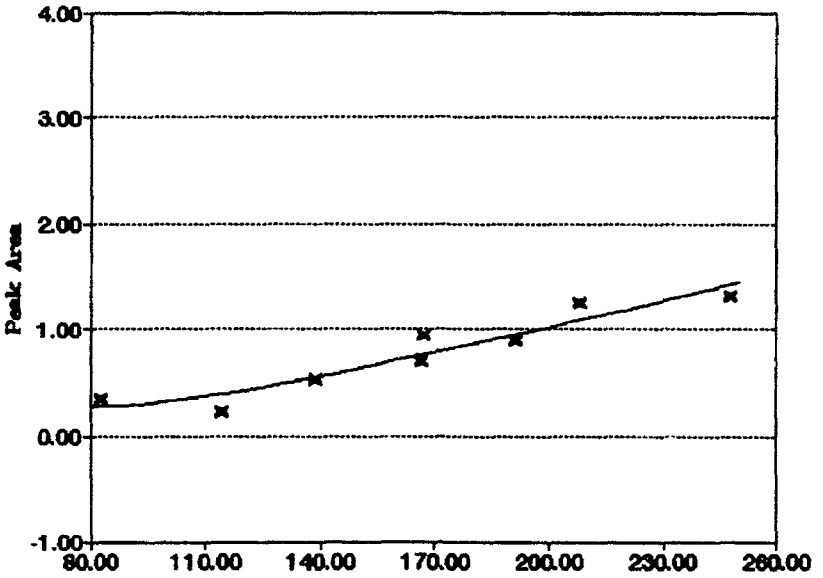

Figure 6. HCN Production Versus Cyclopropane Pressure: HCN Infrared Peak Areas After Irradiation of Mixtures Containing 40 Torr of Nitrogen Oxides for 60 s at 30 W/cm^2 Using the P(18) Line of the (00°1)-(02°0) Transition, 1048.7 cm^{-1}

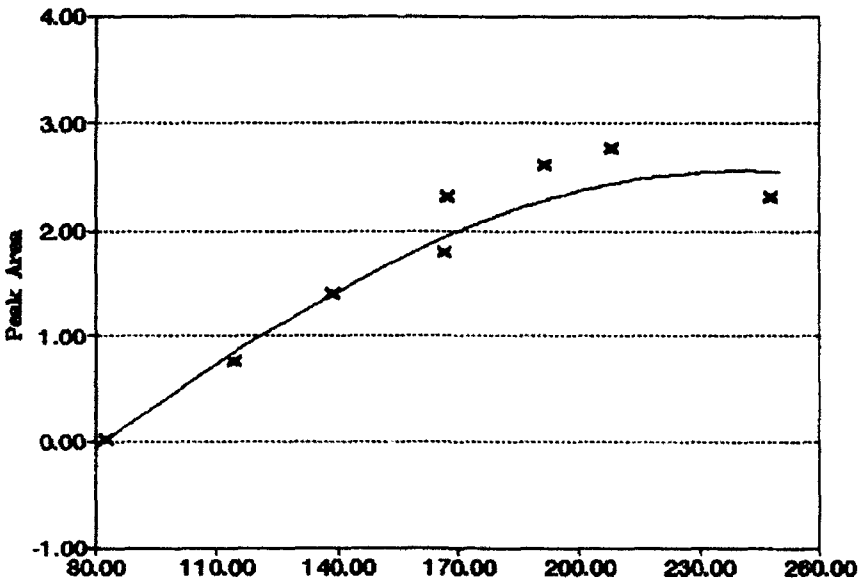

Figure 7. Formic Acid Production Versus Cyclopropane Pressure: Formic Acid Infrared Peak Areas After Irradiation of Mixtures Containing 40 Torr of Nitrogen Oxides for 60 s at 30 W/cm^2 Using the P(18) Line of the (00°1)-(02°0) Transition, 1048.7 cm^{-1}

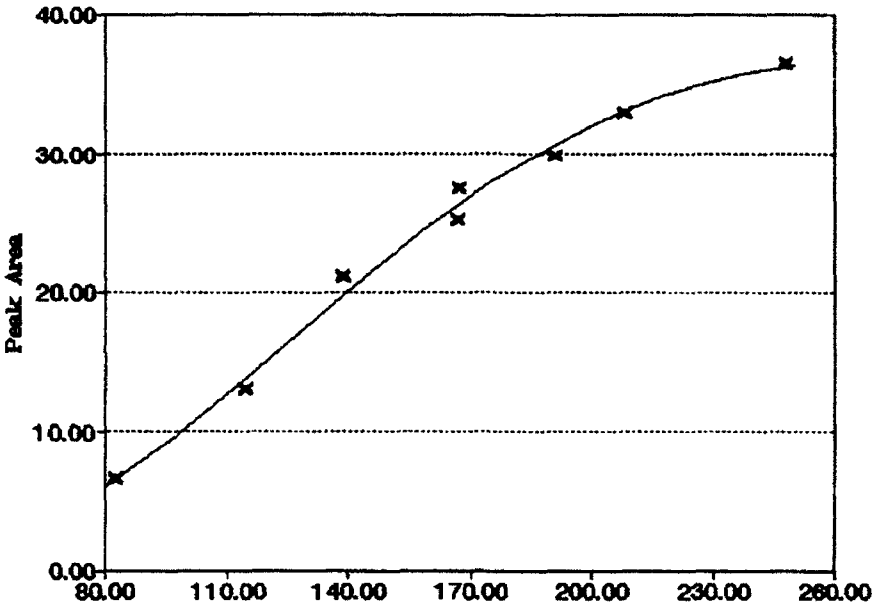

Figure 8. Carbon Dioxide Production Versus Cyclopropane Pressure: Carbon Dioxide Infrared Peak Areas After Irradiation of Mixtures Containing 40 Torr of Nitrogen Oxides for 60 s at 30 W/cm^2 Using the P(18) Line of the (00°1)-(02°0) Transition, 1048.7 cm^{-1}

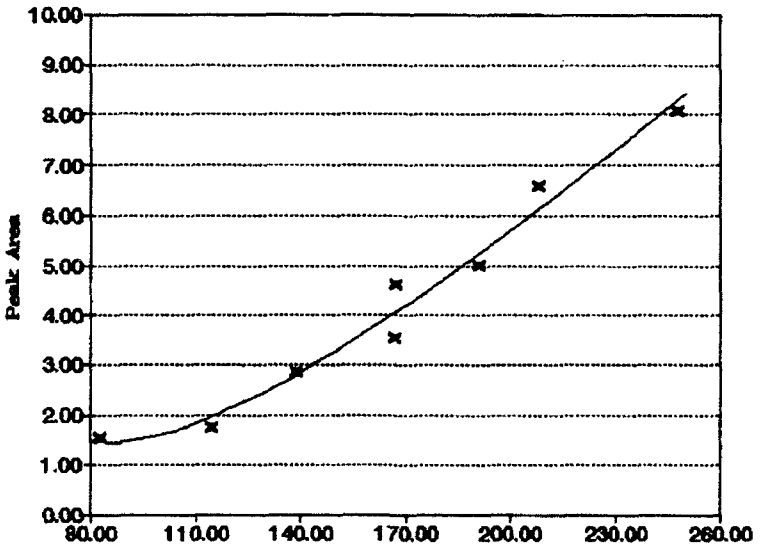

Figure 9. Carbon Monoxide Production Versus Cyclopropane Pressure: Carbon Monoxide Infrared Peak Areas After Irradiation of Mixtures Containing 40 Torr of Nitrogen Oxides for 60 s at 30 W/cm^2 Using the P(18) Line of the (00°1)-(02°0) Transition, 1048.7 cm^{-1}

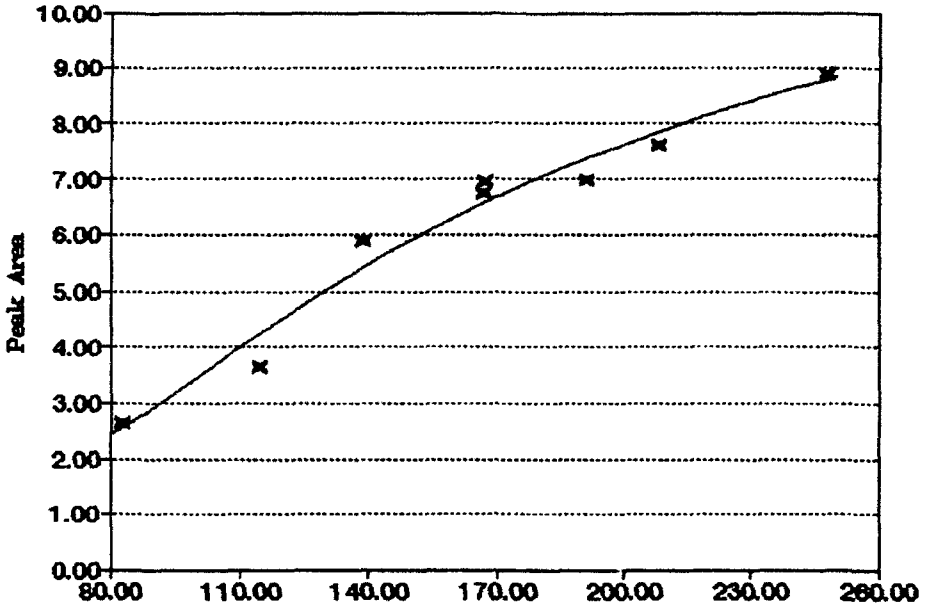

Figure 10. Nitrogen Monoxide Production Versus Cyclopropane Pressure: Nitrogen Monoxide Infrared Peak Areas After Irradiation of Mixtures Containing 40 Torr of Nitrogen Oxides for 60 s at 30 W/cm^2 Using the P(18)Line of the (00°1)-(02°0) Transition, 1048.7 cm^{-1}

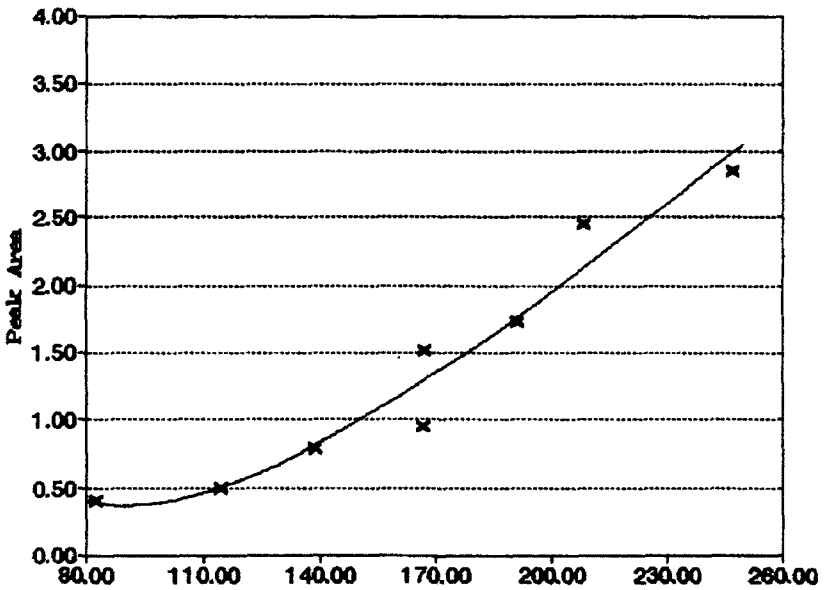

Figure 11. NNO Production Versus Cyclopropane Pressure: NNO Infrared Peak Areas After Irradiation of Mixtures Containing 40 Torr of Nitrogen Oxides for 60 s at 30 W/cm^2 Using the P(18) Line of the (00°1)-(02°0) Transition, 1048.7 cm^{-1}

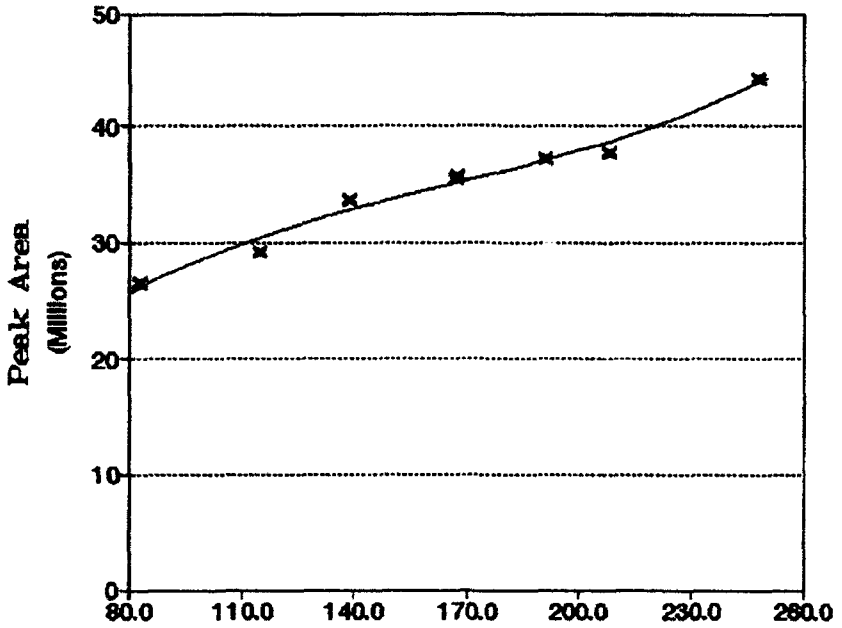

Figure 12. Mixed Gas Production Versus Cyclopropane Pressure: Mixed Gas GC-MS Peak Areas After Irradiation of Mixtures Containing 40 Torr of Nitrogen Oxides for 60 s at 30 W/cm^2 Using the P(18) Line of the (00°1)-(02°0) Transition, 1048.7 cm^{-1}

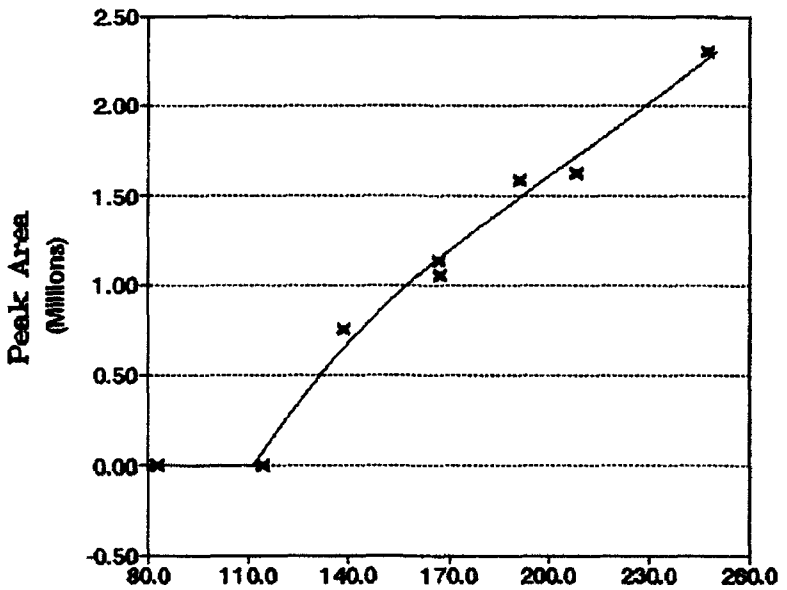

Figure 13. Propene Production Versus Cyclopropane Pressure: Propene GC-MS Peak Areas After Irradiation of Mixtures Containing 40 Torr of Nitrogen Oxides for 60 s at 30 W/cm^2 Using the P(18) Line of the (00°1)-(02°0) Transition, 1048.7 cm^{-1}

The infrared integrals and the GC-MS total ion areas allowed us to evaluate the effect on product formation of varying nitrogen oxide pressures at a constant partial pressure of cyclopropane, 200 Torr. When mixtures were irradiated at 30 W/cm^2 for 30 s, the amount of cyclopropane remaining in the product mixtures decreased as the nitrogen oxide pressure in the reaction mixtures rose (Fig. 14). Similarly, the greater the nitrogen oxide pressures initially, the more nitrogen

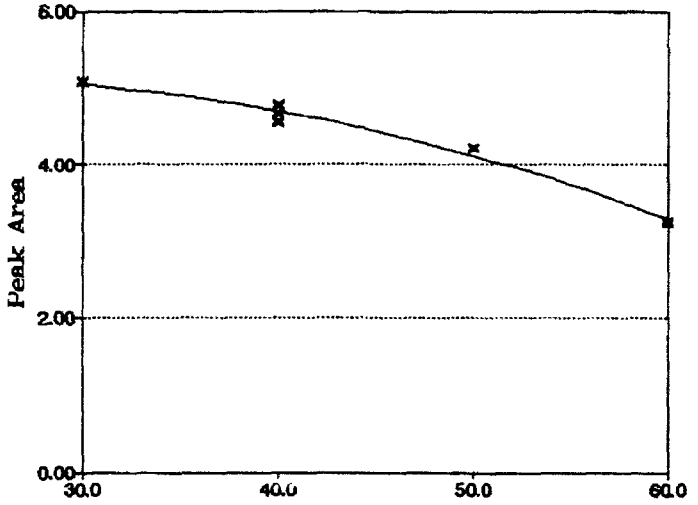

Figure 14a. Cyclopropane (200 Torr) Versus Nitrogen Oxides Pressure: After Irradiation for 30 s at 30 W/cm^2 Using the P(18) Line of the (00°1)-(02°0) Transition, 1048.7 cm^{-1}, Cyclopropane Infrared Peak Areas

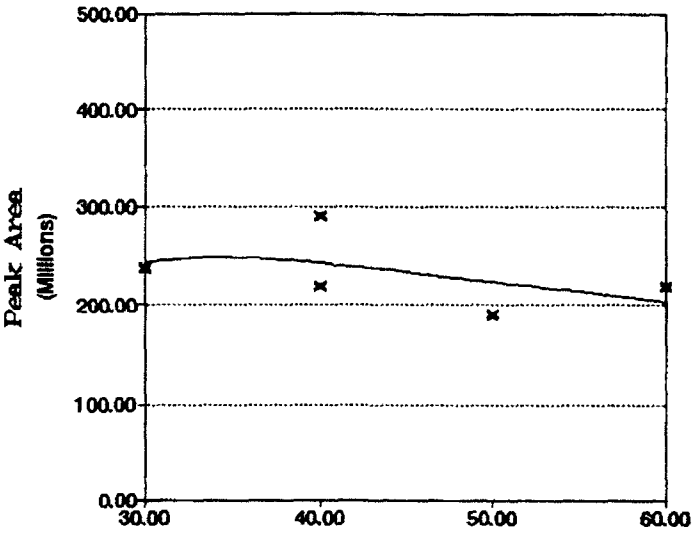

Figure 14b. Cyclopropane (200 Torr) Versus Nitrogen Oxides Pressure: After Irradiation for 30 s at 30 W/cm^2 Using the P(18) Line of the (00°1)-(02°0) Transition, 1048.7 cm^{-1}, Cyclopropane GC-MS Peak Areas

oxides were consumed, though the amount of nitrogen oxides remaining after irradiation was difficult to quantitate by infrared integrals. We believe that because nitrogen oxides participate in complex, temperature-dependent equilibria their infrared integrals are sensitive to small variations in cell temperature. The ring-cleavage products, ethene, HCN, formic acid, CO_2, and CO, (Figs. 15 – 19) increased in a near-linear manner with the pressure of nitrogen oxides, as did

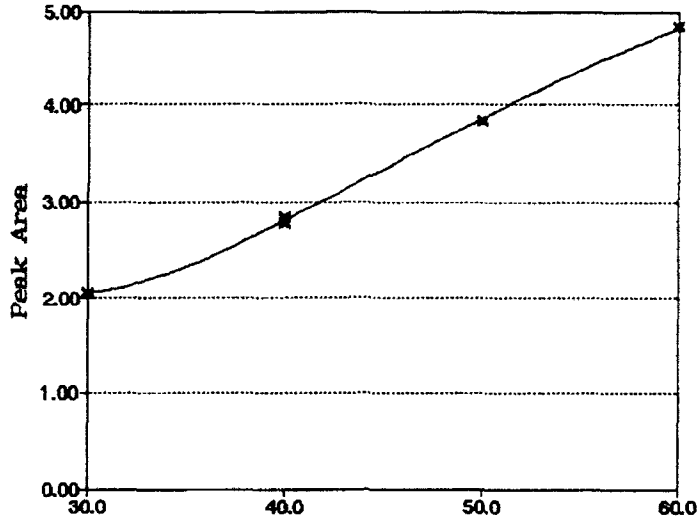

Figure 15. Ethene Production Versus Nitrogen Oxides Pressure: Ethene Infrared Peak Areas After Irradiation of Mixtures Containing 200 Torr of Cyclopropane for 30 s at 30 W/cm^2 Using the P(18) Line of the (00°1)-(02°0) Transition, 1048.7 cm^{-1}

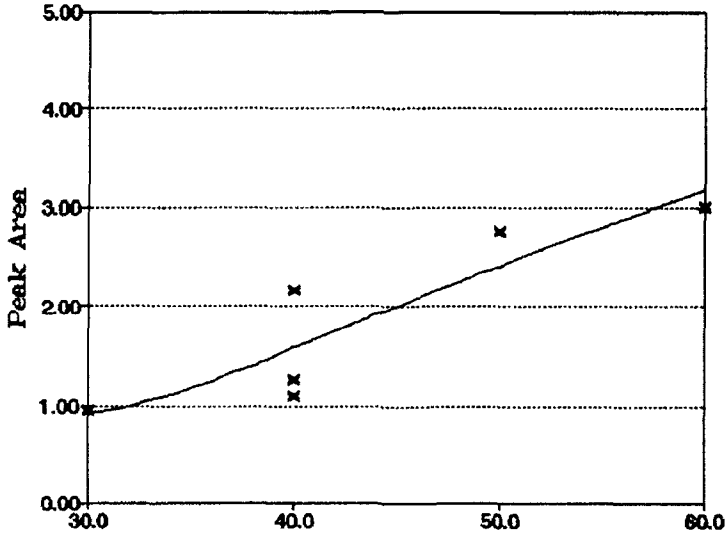

Figure 16. HCN Production Versus Nitrogen Oxides Pressure: HCN Infrared Peak Areas After Irradiation of Mixtures Containing 200 Torr of Cyclopropane for 30 s at 30 W/cm^2 Using the P(18) Line of the (00°1)-(02°0) Transition, 1048.7 cm^{-1}

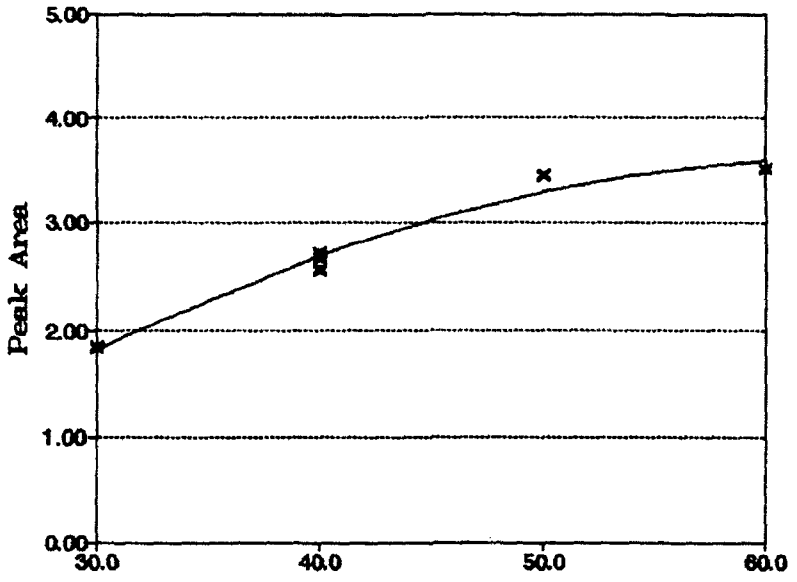

Figure 17. Formic Acid Production Versus Nitrogen Oxides Pressure: Formic Acid Infrared Peak Areas After Irradiation of Mixtures Containing 200 Torr of Cyclopropane for 30 s at 30 W/cm^2 Using the P(18) Line of the (00°1)-(02°0) Transition, 1048.7 cm^{-1}

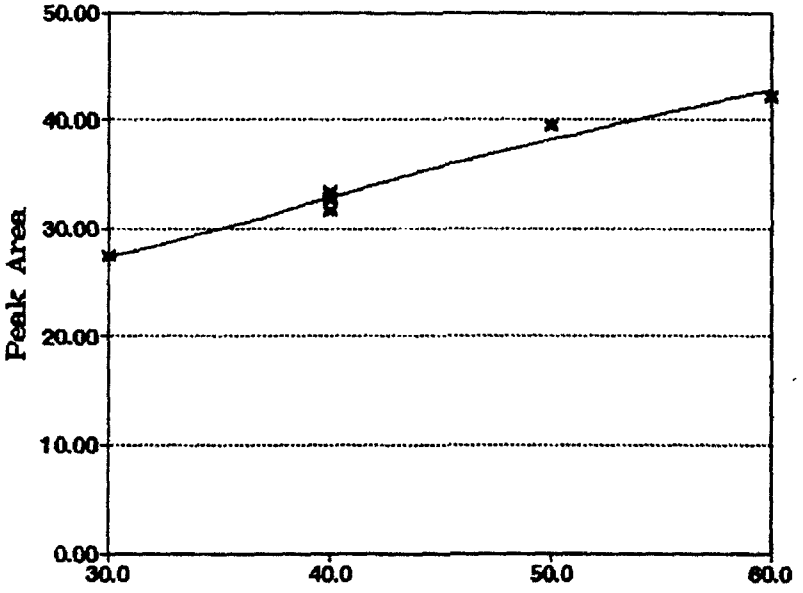

Figure 18. Carbon Dioxide Production Versus Nitrogen Oxides Pressure: Carbon Dioxide Infrared Peak Areas After Irradiation of Mixtures Containing 200 Torr of Cyclopropane for 30 s at 30 W/cm^2 Using the P(18) Line of the (00°1)-(02°0) Transition, 1048.7 cm^{-1}

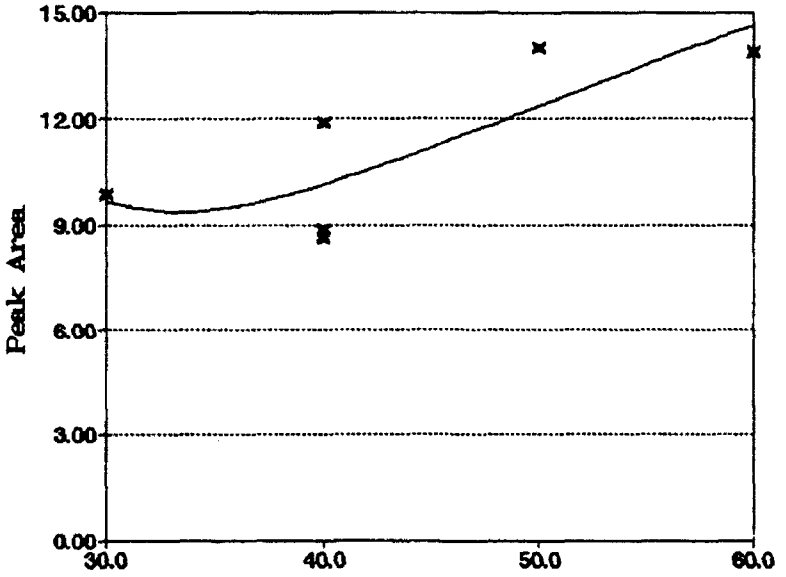

Figure 19. Carbon Monoxide Production Versus Nitrogen Oxides Pressure: Carbon Monoxide Infrared Peak Areas After Irradiation of Mixtures Containing 200 Torr of Cyclopropane for 30 s at 30 W/cm^2 Using the P(18) Line of the (00°1)-(02°0) Transition, 1048.7 cm^{-1}

the product NO (Fig. 20) and the mixed gas peak in the GC-MS analyses (Fig. 21). Increasing the nitrogen oxide pressure did not increase the nitrocyclopropane produced unless the product condensed on the cell walls. The infrared and GC-MS analyses of the vapor phase yielded nitrocyclopropane versus nitrogen oxide plots with production of nitrocyclopropane nearly flat as nitrogen dioxide pressure increased over the range 30.0 to 60.0 Torr. The GC-MS analysis of the product mixtures revealed the presence of a number of other components, propene, acetonitrile, propenitrile, and nitromethane, these products appearing when the nitrogen oxide pressure exceeded 40 Torr and increasing almost linearly thereafter (Figs. 22 through 25). Nitromethane was the only other nitroalkane produced from nitrogen oxide and cyclopropane mixtures. Figure 26 shows a similar dependence for the production of 2-propenal except that 2-propenal could be detected when the initial nitrogen oxide pressure was 30 Torr.

Conditions of higher laser power (50 W/cm^2) promoted the fragmentation of reactants and products. The infrared spectra showed additional products including methane, acetylene, and perhaps formaldehyde [3]. Propene and 2-propenal could now be identified in the infrared spectrum of the product mixture; whereas, in the preceding experiments, these products could not be detected in the infrared spectra, though they were present in the GC trace. In the 50 W/cm^2 product mixtures neither nitrocyclopropane nor any other nitroalkane could be detected in the infrared or in the GC-MS analyses.

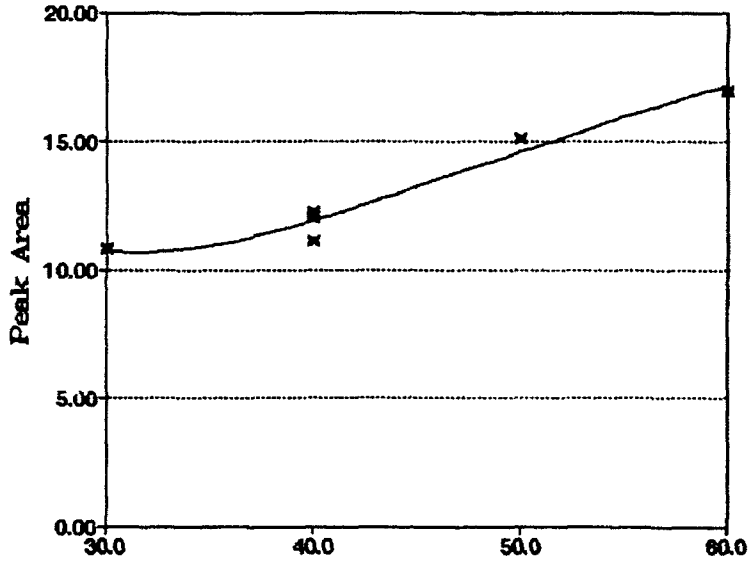

Figure 20. Nitrogen Monoxide Production Versus Nitrogen Oxides Pressure: Nitrogen Monoxide Infrared Peak Areas After Irradiation of Mixtures Containing 200 Torr of Cyclopropane for 30 s at 30 W/cm^2 Using the P(18) Line of the (00°1)-(02°0) Transition, 1048.7 cm^{-1}

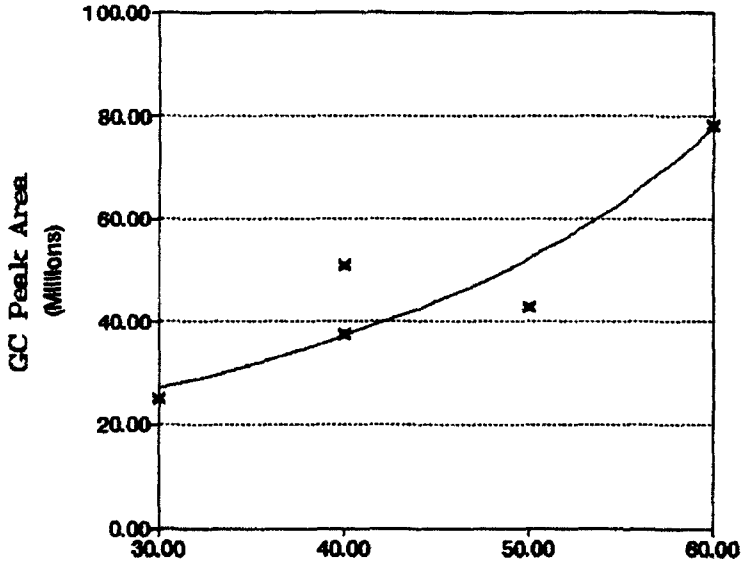

Figure 21. Mixed Gases Production Versus Nitrogen Oxides Pressure: Mixed Gas GC-MS Peak Areas After Irradiation of Mixtures Containing 200 Torr of Cyclopropane for 30 s at 30 W/cm^2 Using the P(18) Line of the (00°1)-(02°0) Transition, 1048.7 cm^{-1}

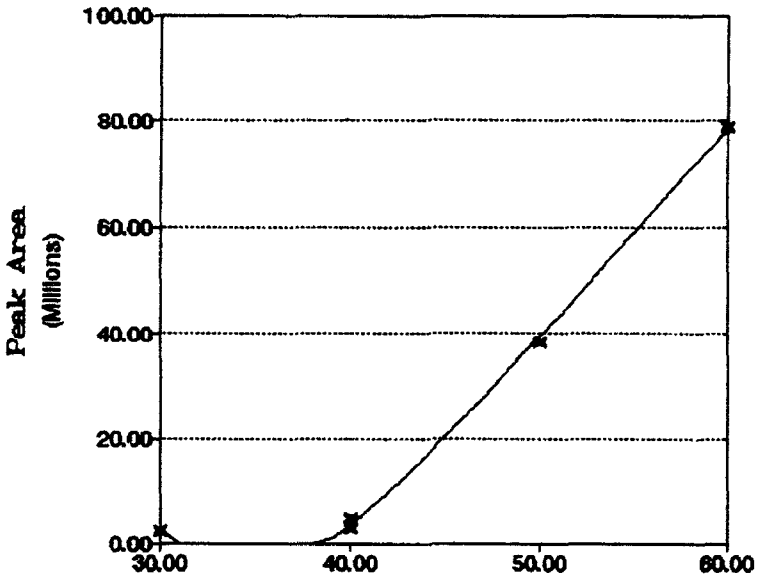

Figure 22. Propene Gases Production Versus Nitrogen Oxides Pressure: Propene GC-MS Peak Areas After Irradiation of Mixtures Containing 200 Torr of Cyclopropane for 30 s at 30 W/cm^2 Using the P(18) Line of the (00°1)-(02°0) Transition, 1048.7 cm^{-1}

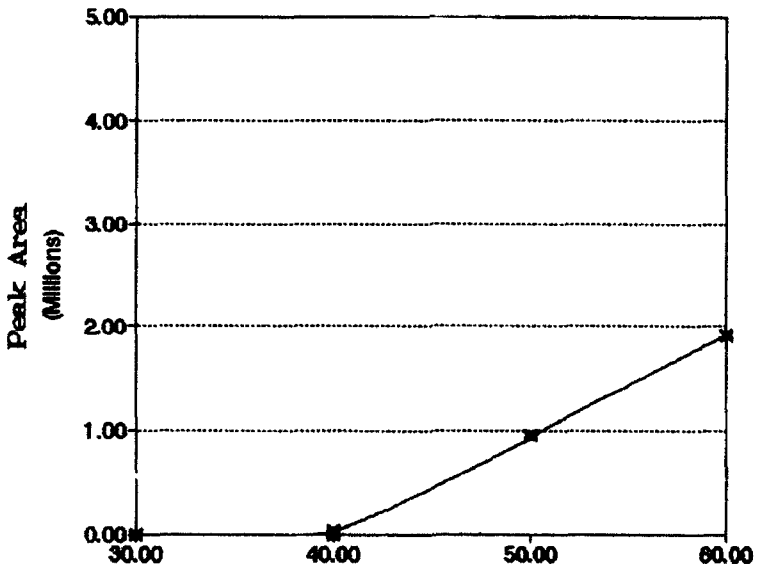

Figure 23. Acetonitrile Production Versus Nitrogen Oxides Pressure: Acetonitrile GC-MS Peak Areas After Irradiation of Mixtures Containing 200 Torr of Cyclopropane for 30 s at 30 W/cm^2 Using the P(18) Line of the (00°1)-(02°0) Transition, 1048.7 cm^{-1}

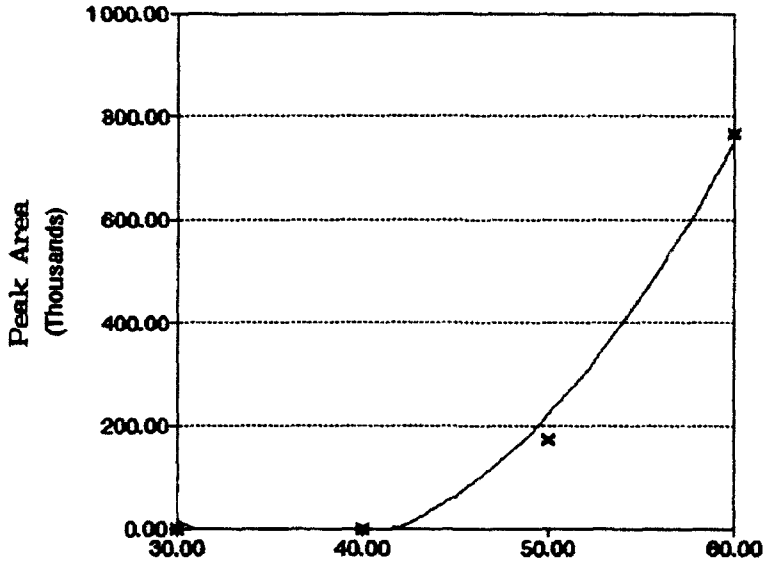

Figure 24. Propenitrile Production Versus Nitrogen Oxides Pressure: Propenitrile GC-MS Peak Areas After Irradiation of Mixtures Containing 200 Torr of Cyclopropane for 30 s at 30 W/cm^2 Using the P(18) Line of the (00°1)-(02°0) Transition, 1048.7 cm^{-1}

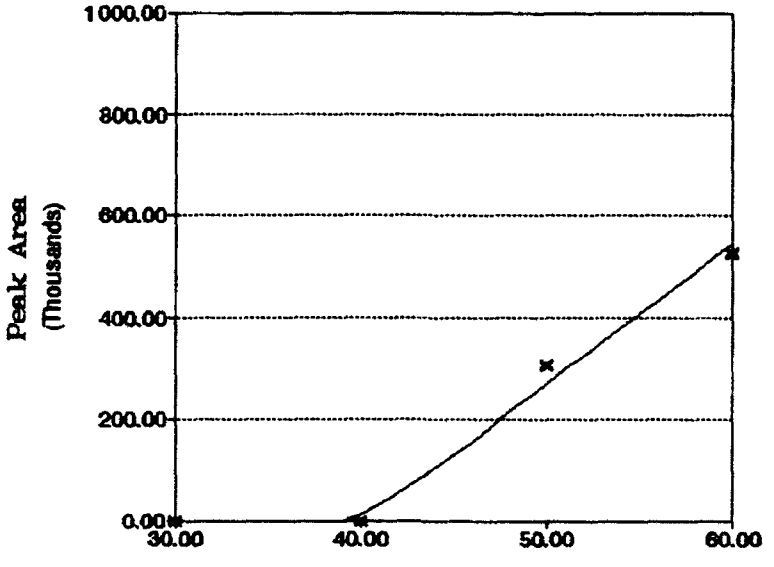

Figure 25. Nitromethane Production Versus Nitrogen Oxides Pressure: Nitromethane GC-MS Peak Areas After Irradiation of Mixtures Containing 200 Torr of Cyclopropane for 30 s at 30 W/cm^2 Using the P(18) Line of the (00°1)-(02°0) Transition, 1048.7 cm^{-1}

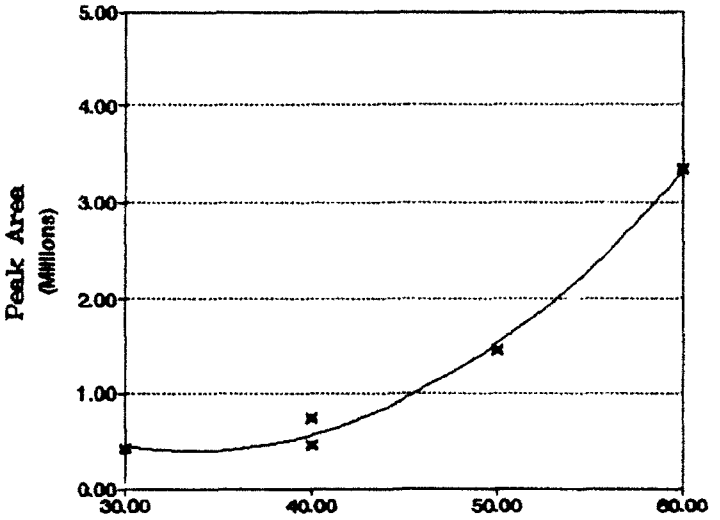

Figure 26. Propenal Production Versus Nitrogen Oxides Pressure: Propenal Peak Areas After Irradiation of Mixtures Containing 200 Torr of Cyclopropane for 30 s at 30 W/cm^2 Using the P(18) Line of the (00°1)-(02°0) Transition, 1048.7 cm^{-1}

A series of 30 second-irradiation experiments, in which the pressures of reactant gases were constant (cyclopropane, 212 Torr; nitrogen oxides, 50 Torr) but in which the irradiation power was varied, allowed us to assess the effects of moderate laser powers on the reaction. Figure 27 shows the response of

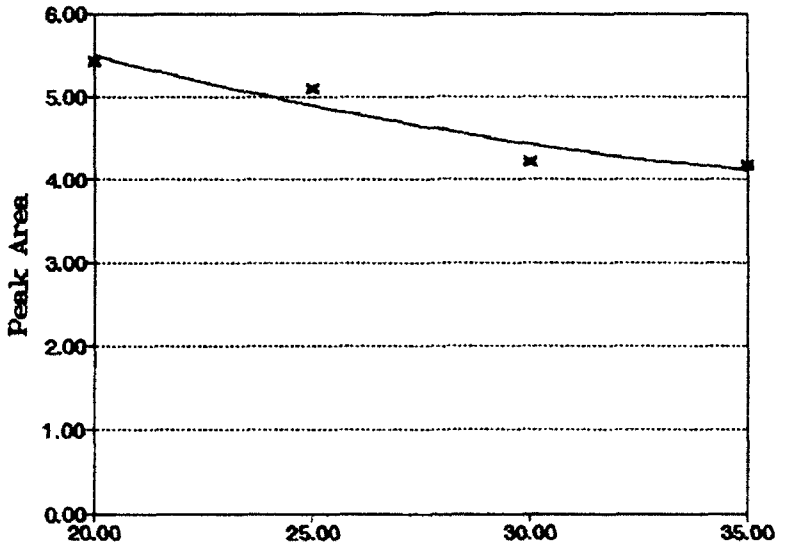

Figure 27a. Cyclopropane (212.5 Torr) Remaining Versus Incident Laser Power: After Irradiation of Mixtures Containing 50 Torr of Nitrogen Oxides for 30 s Using the P(18) Line of the (00°1)-(02°0) Transition, 1048.7 cm^{-1}, Cyclopropane Infrared Peak Areas

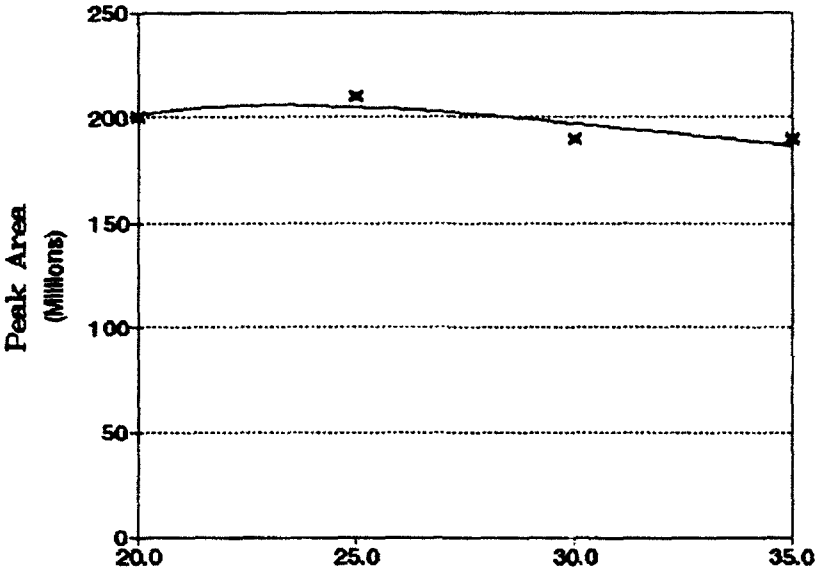

Figure 27b. Cyclopropane (212.5 Torr) Remaining Versus Incident Laser Power: After Irradiation of Mixtures Containing 50 Torr of Nitrogen Oxides for 30 s Using the P(18) Line of the (00°1)-(02°0) Transition, 1048.7 cm^{-1}, Cyclopropane GC-MS Peak Areas

cyclopropane to increasing irradiation power as determined from the infrared integrals and from the GC-MS total ion count. Nitrogen oxides showed stronger responses to increasing laser power and were completely depleted from the product mixtures when the laser power approached 35 W/cm^2 (Fig. 28). The amount of nitrocyclopropane in the gas phase reached a maximum between 25 - 30 W/cm^2. The decrease in nitrocyclopropane above 30 W/cm^2 (Fig. 29) is consistent with an increase in production of smaller molecules and fragments at higher laser powers, as described above for the 50 W/cm^2 experiments. Figures 30 through 32 show the dependence of the production of HCN, ethene, and formic acid, respectively, on irradiation power. The ethene and formic acid production leveled off as the power increased. Formic acid is a likely source in the product mixture of CO_2 and CO, whose production was favored as the laser power approached 35 W/cm^2 (Figs. 33 and 34). Production of NO leveled off before 35 W/cm^2 (Fig. 35), but production of NNO continued to rise linearly with increasing irradiation power (Fig. 36). The area of the mixed gas peak is plotted versus the irradiation power in Fig. 37. Its composition varies with the irradiation power as infrared analysis prior to gas chromatography of the product mixtures indicates: at low laser powers the peak consists of small molecules and unreacted nitrogen oxides, but at higher powers the peak is depleted of NO_2 and N_2O_4, and contains more of the species resulting from fragmentation and oxidation reactions, CO_2, CO, NO, NNO. Acetonitrile, propenitrile, and nitromethane were not detected by GC-MS until the laser power had been raised to 30 W/cm^2, after which the amount

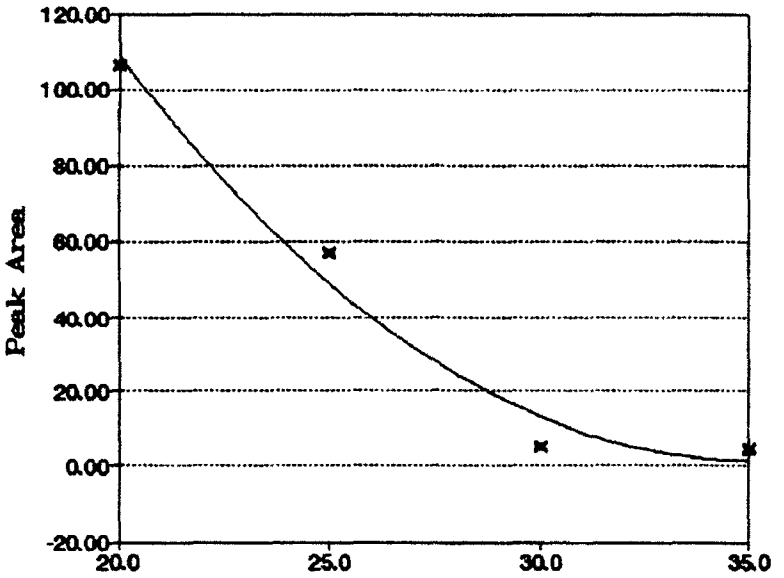

Figure 28a. Nitrogen Oxides (50 Torr) Remaining Versus Incident Laser Power: After Irradiation of Mixtures Containing 212.5 Torr of Cyclopropane for 30 s Using the P(18) Line of the (00°1)-(02°0) Transition, 1048.7 cm^{-1}, N_2O_4 Infrared Peak Areas

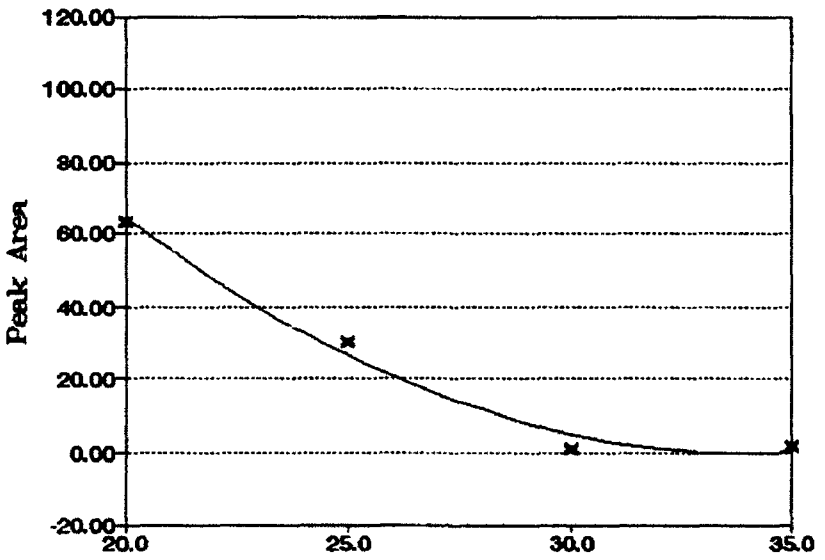

Figure 28b. Nitrogen Oxides (50 Torr) Remaining Versus Incident Laser Power: After Irradiation of Mixtures Containing 212.5 Torr of Cyclopropane for 30 s Using the P(18) Line of the (00°1)-(02°0) Transition, 1048.7 cm^{-1}, NO_2 Infrared Peak Areas

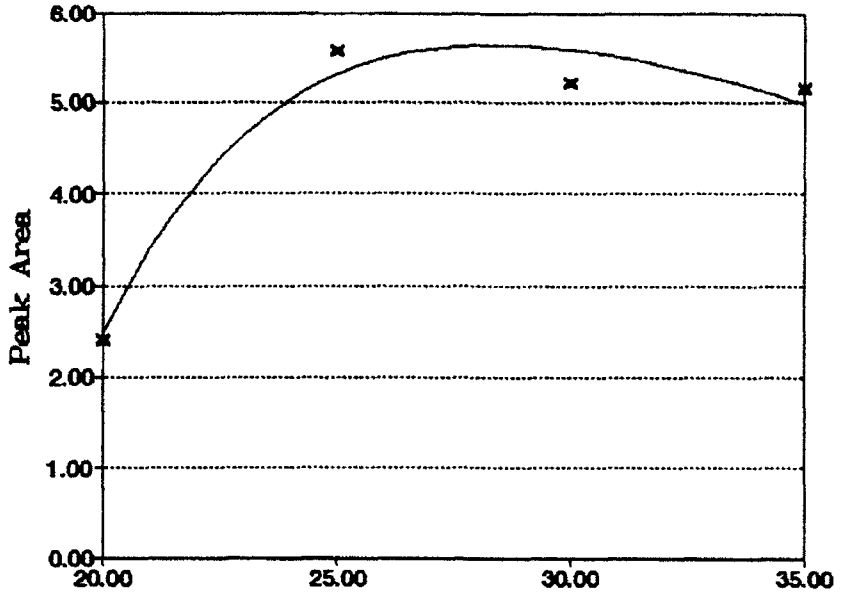

Figure 29a. Nitrocyclopropane Versus Incident Laser Power: After Irradiation of Mixtures Containing 212.5 Torr of Cyclopropane and 50 Torr of Nitrogen Oxides for 30 s Using the P(18) Line of the (00°1)-(02°0) Transition, 1048.7 cm^{-1}, Nitrocyclopropane Infrared Peak Areas

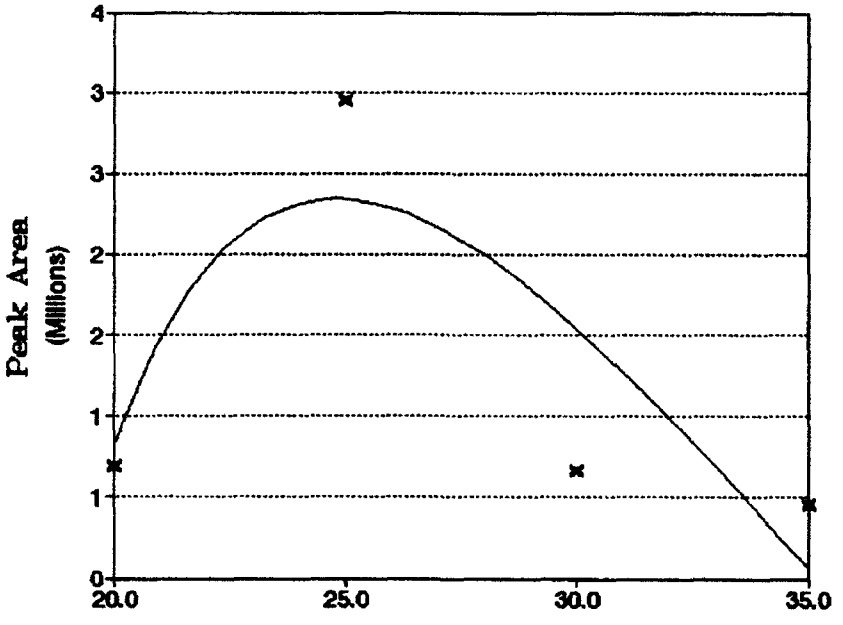

Figure 29b. Nitrocyclopropane Versus Incident Laser Power: After Irradiation of Mixtures Containing 212.5 Torr of Cyclopropane and 50 Torr of Nitrogen Oxides for 30 s Using the P(18) Line of the (00°1)-(02°0) Transition, 1048.7 cm^{-1}, Nitrocyclopropane GC-MS Peak Areas

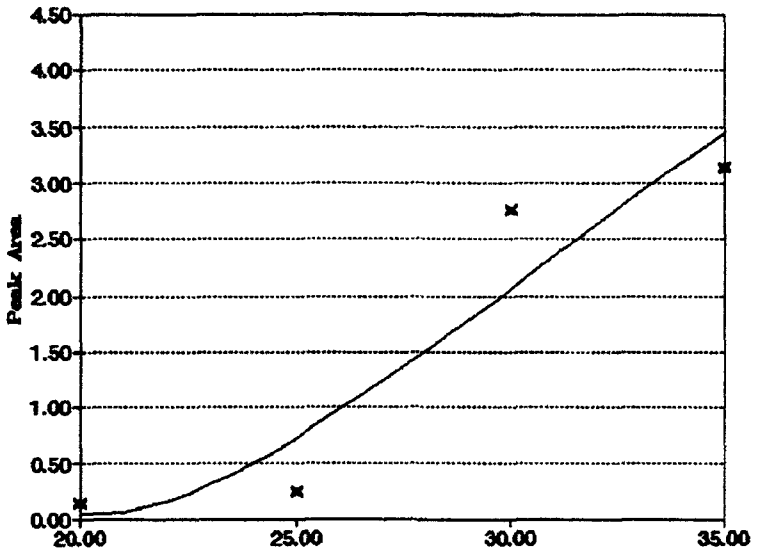

Figure 30. HCN Produced Versus Incident Laser Power: HCN Infrared Peak Areas After Irradiation of Mixtures Containing 212.5 Torr of Cyclopropane and 50 Torr of Nitrogen Oxides for 30 s Using the P(18) Line of the (00°1)-(02°0) Transition, 1048.7 cm^{-1}

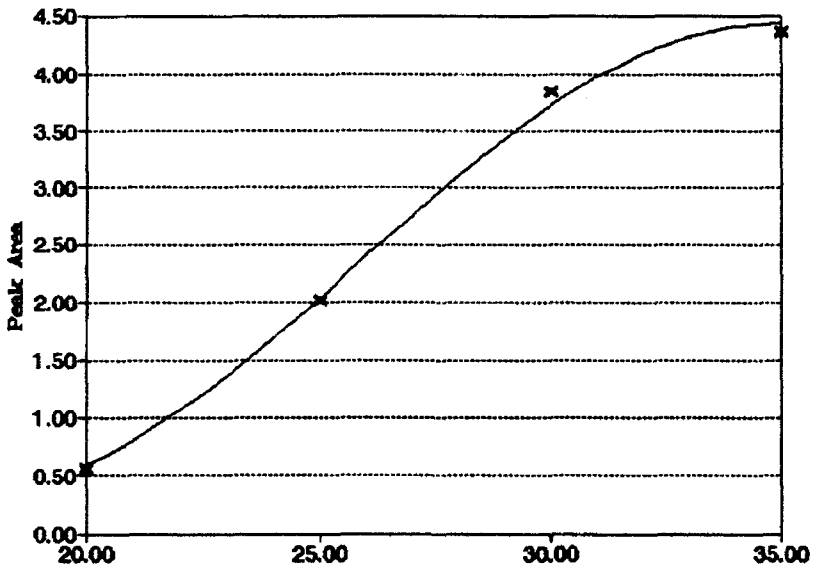

Figure 31. Ethene Produced Versus Incident Laser Power: Ethene Infrared Peak Areas After Irradiation of Mixtures Containing 212.5 Torr of Cyclopropane and 50 Torr of Nitrogen Oxides for 30 s Using the P(18) Line of the (00°1)-(02°0) Transition, 1048.7 cm^{-1}

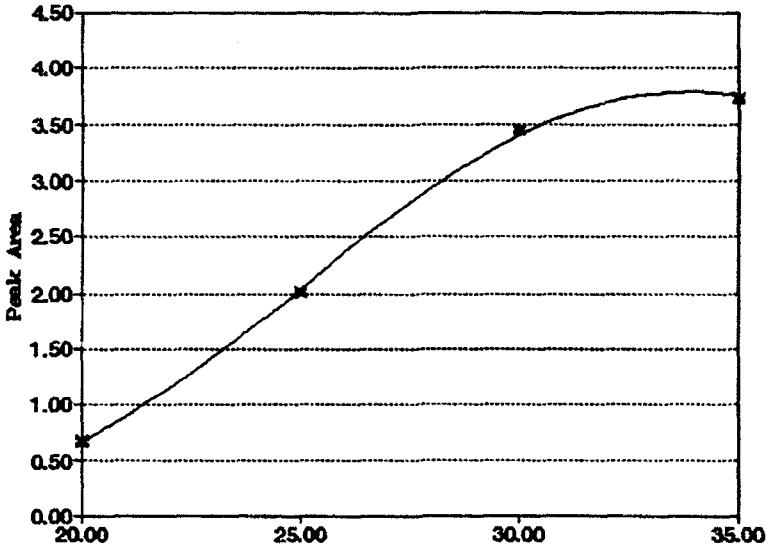

Figure 32. Formic Acid Produced Versus Incident Laser Power: Formic Acid Infrared Peak Areas After Irradiation of Mixtures Containing 212.5 Torr of Cyclopropane and 50 Torr of Nitrogen Oxides for 30 s Using the P(18) Line of the (00°1)-(02°0) Transition, 1048.7 cm^{-1}

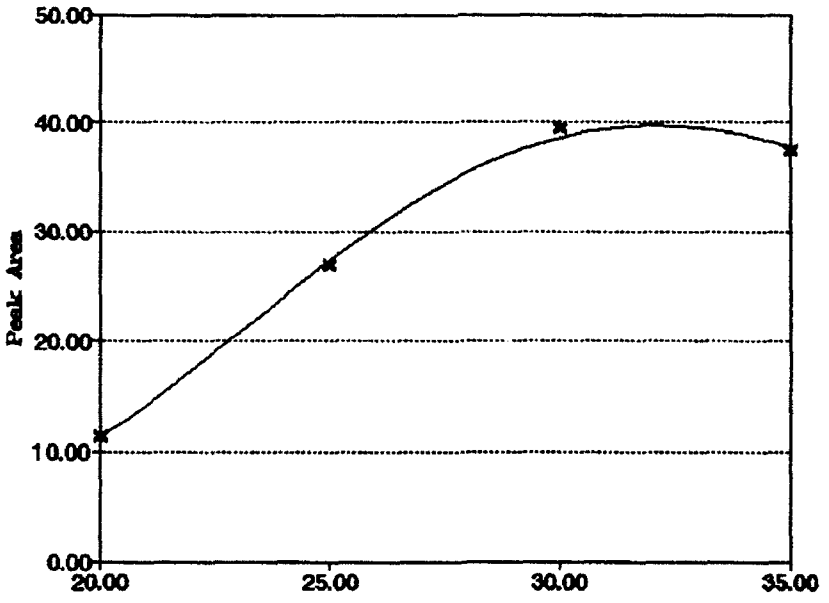

Figure 33. Carbon Dioxide Produced Versus Incident Laser Power: Carbon Dioxide Infrared Peak Areas After Irradiation of Mixtures Containing 212.5 Torr of Cyclopropane and 50 Torr of Nitrogen Oxides for 30 s Using the P(18) Line of the (00°1)-(02°0) Transition, 1048.7 cm^{-1}

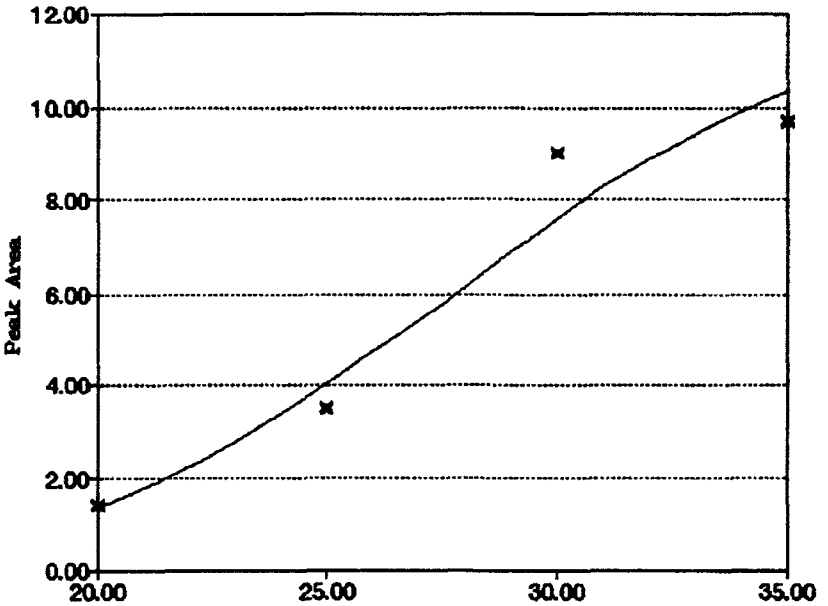

Figure 34. Carbon Monoxide Produced Versus Incident Laser Power: Carbon Monoxide Infrared Peak Areas After Irradiation of Mixtures Containing 212.5 Torr of Cyclopropane and 50 Torr of Nitrogen Oxides for 30 s Using the P(18) Line of the (00°1)-(02°0) Transition, 1048.7 cm^{-1}

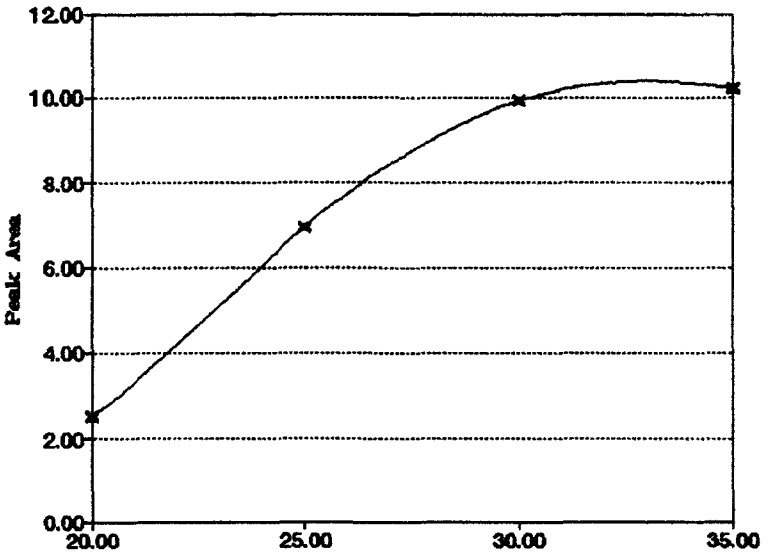

Figure 35. Nitrogen Monoxide Produced Versus Incident Laser Power: Nitrogen Monoxide Infrared Peak Areas After Irradiation of Mixtures Containing 212.5 Torr of Cyclopropane and 50 Torr of Nitrogen Oxides for 30 s Using the P(18) Line of the (00°1)-(02°0) Transition, 1048.7 cm^{-1}

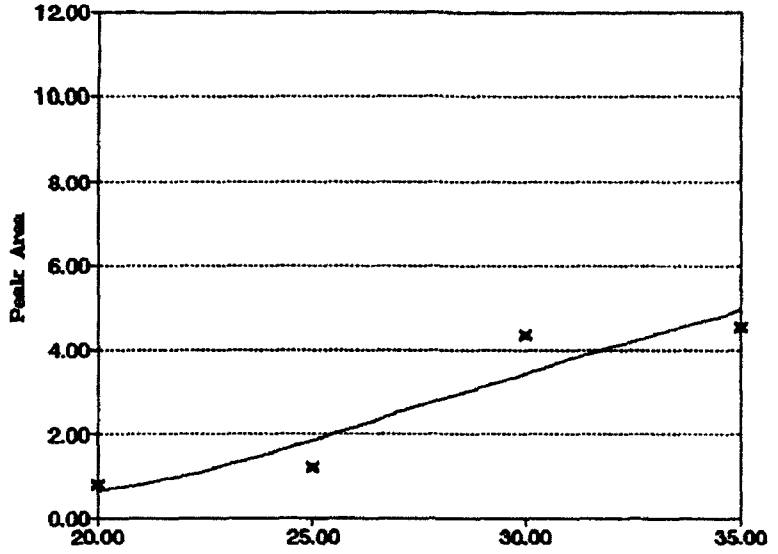

Figure 36. NNO Produced Versus Incident Laser Power: NNO Infrared Peak Areas After Irradiation of Mixtures Containing 212.5 Torr of Cyclopropane and 50 Torr of Nitrogen Oxides for 30 s Using the P(18) Line of the (00°1)-(02°0) Transition, 1048.7 cm^{-1}

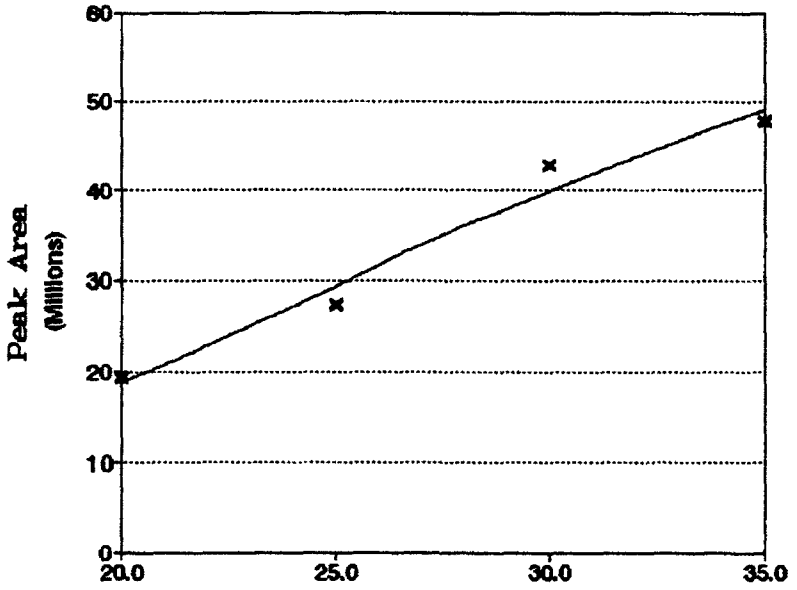

Figure 37. Mixed Gas Produced Versus Incident Laser Power: Mixed Gas GC-MS Peak Areas After Irradiation of Mixtures Containing 212.5 Torr of Cyclopropane and 50 Torr of Nitrogen Oxides for 30 s Using the P(18) Line of the (00°1)-(02°0) Transition, 1048.7 cm^{-1}

of each rose as the power increased, with nitromethane production falling again after 30 W/cm^2 (Figs. 38 through 40). Propene and 2-propenal could be detected by GC-MS at 20 and 25 W/cm^2, respectively, but their amounts remained low until the power was raised above 30 W/cm^2, beyond which their production was facilitated (Figs. 41 and 42).

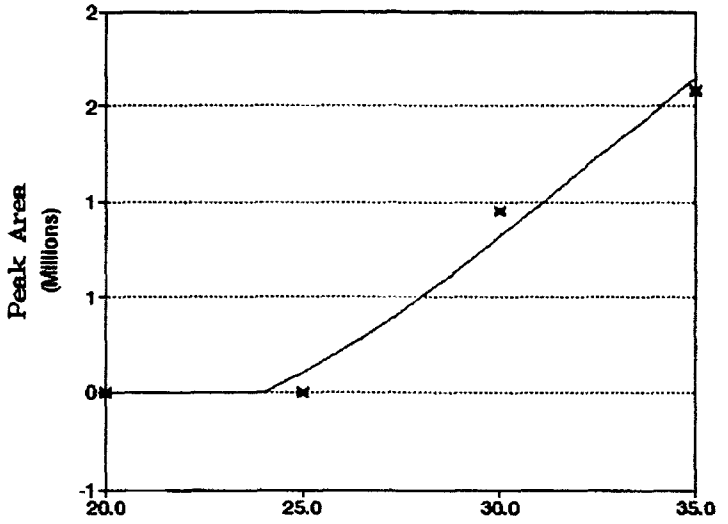

Figure 38. Acetonitrile Produced Versus Incident Laser Power: Acetonitrile GC-MS Peak Areas After Irradiation of Mixtures Containing 212.5 Torr of Cyclopropane and 50 Torr of Nitrogen Oxides for 30 s Using the P(18) Line of the (00°1)-(02°0) Transition, 1048.7 cm^{-1}

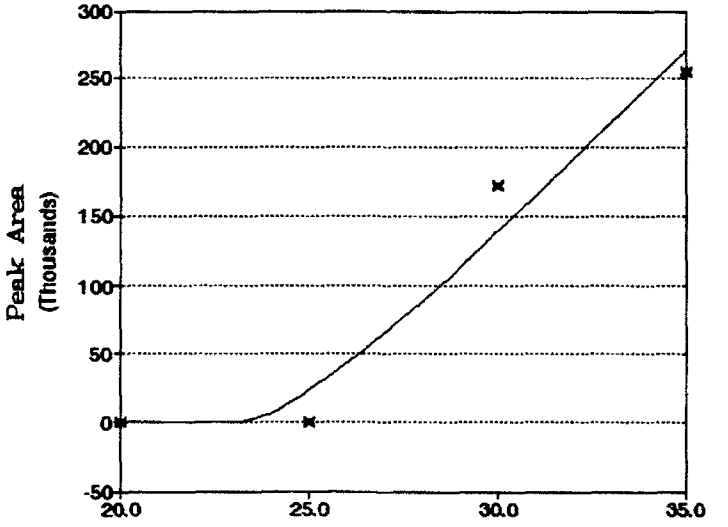

Figure 39. Propenitrile Produced Versus Incident Laser Power: Propenitrile GC-MS Peak Areas After Irradiation of Mixtures Containing 212.5 Torr of Cyclopropane and 50 Torr of Nitrogen Oxides for 30 s Using the P(18) Line of the (00°1)-(02°0) Transition, 1048.7 cm^{-1}

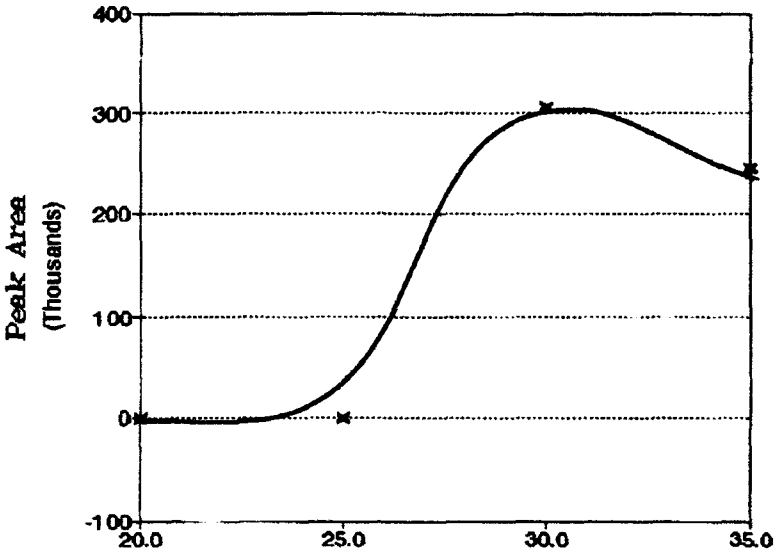

Figure 40. Nitromethane Produced Versus Incident Laser Power: Nitromethane GC-MS Peak Areas After Irradiation of Mixtures Containing 212.5 Torr of Cyclopropane and 50 Torr of Nitrogen Oxides for 30 s Using the P(18) Line of the (00°1)-(02°0) Transition, 1048.7 cm^{-1}

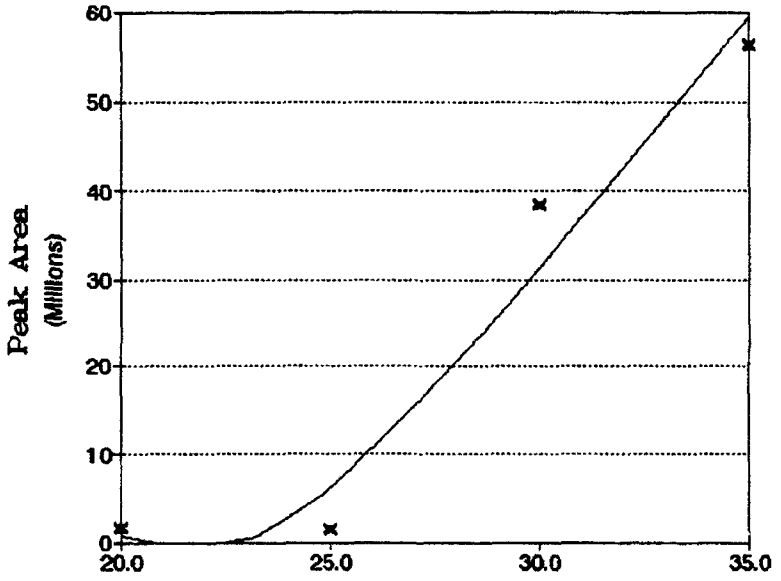

Figure 41. Propene Produced Versus Incident Laser Power: Propene GC-MS Peak Areas After Irradiation of Mixtures Containing 212.5 Torr of Cyclopropane and 50 Torr of Nitrogen Oxides for 30 s Using the P(18) Line of the (00°1)-(02°0) Transition, 1048.7 cm^{-1}

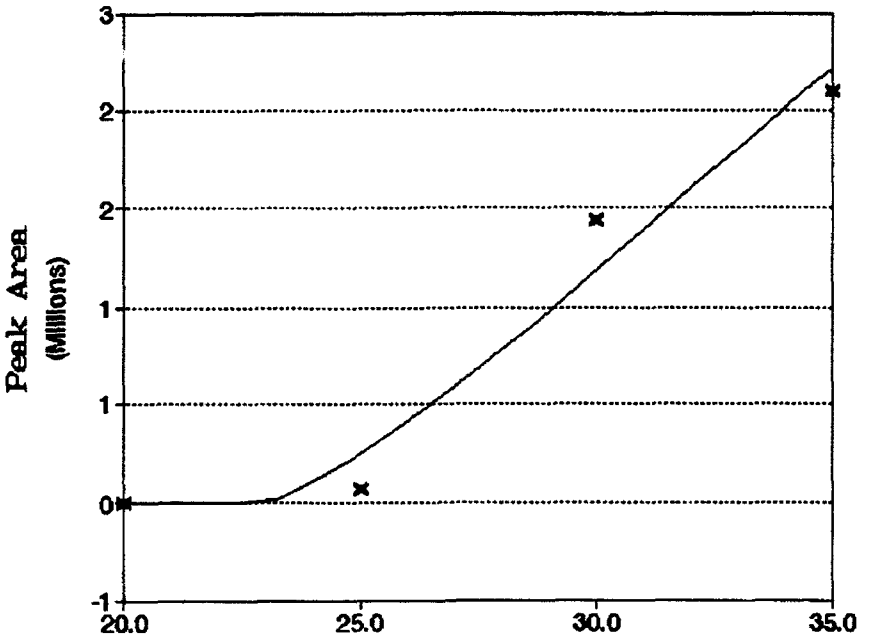

Figure 42. Propenal Produced Versus Incident Laser Power: Propenal GC-MS Peak Areas After Irradiation of Mixtures Containing 212.5 Torr of Cyclopropane and 50 Torr of Nitrogen Oxides for 30 s using the P(18) Line of the (00°1)-(02°0) Transition, 1048.7 cm^{-1}

We conducted a final set of experiments with fixed partial pressures of cyclopropane and nitrogen oxides (209 Torr and 40 Torr, respectively) and with the laser power set at 25 W/cm^2, in order to evaluate the effect of irradiation time on the product array. The choice of irradiation power was based on the previous experiments which showed that 25 W/cm^2 was appropriate for producing nitrocyclopropane. As Figure 43 shows, the amount of cyclopropane remaining after irradiation decreased slightly at longer irradiation times; however, the amount of nitrogen oxides remaining in the reaction mixture showed no clear dependence on irradiation time. The amount of nitrocyclopropane in the vapor phase showed little increase with irradiation time over the range studied. A number of other products were followed as irradiation time varied. Increasing the irradiation time from 20 to 30 s encouraged the formation of ethene, CO_2, CO, and NO, but their amounts showed little dependence on longer irradiation times. With the low laser power utilized, such small amounts of formic acid, HCN, and NNO were produced that we could not follow the time dependence of their formation. The GC-MS traces indicated that the maximum production of propene occurred at irradiation times of 20 to 30 s (Fig. 44), but that the mixed gas production rose until the irradiation time was about 45 s (Fig. 45).

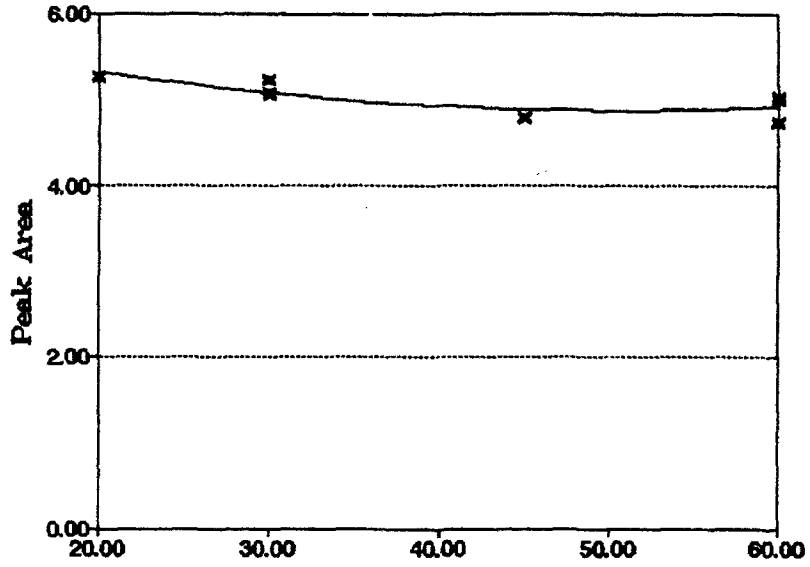

Figure 43a. Cyclopropane (209 Torr) Remaining Versus Irradiation Time: After Irradiation of Mixtures Containing 40 Torr of Nitrogen Oxides at 25 W/cm^2 Using the P(18) Line of the (00°1)-(02°0) Transition, 1048.7 cm^{-1}, Cyclopropane Infrared Peak Areas

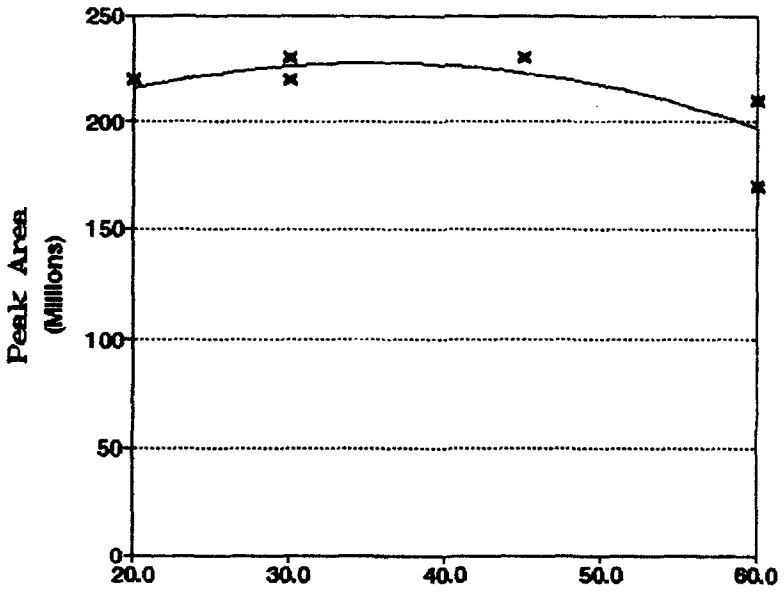

Figure 43b. Cyclopropane (209 Torr) Remaining Versus Irradiation Time: After Irradiation of Mixtures Containing 40 Torr of Nitrogen Oxides at 25 W/cm^2 Using the P(18) Line of the (00°1)-(02°0) Transition, 1048.7 cm^{-1}, Cyclopropane GC-MS Peak Areas

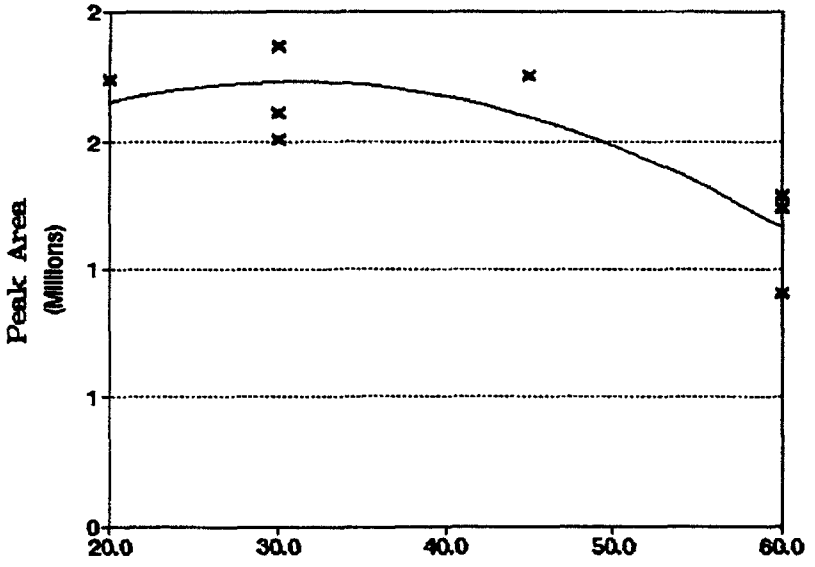

Figure 44. Propene Production Versus Irradiation Time: Propene GC-MS Peak Areas After Irradiation of Mixtures Containing 209 Torr of Cyclopropane and 40 Torr of Nitrogen Oxides at 25 W/cm^2 Using the P(18) Line of the (00°1)-(02°0) Transition, 1048.7 cm^{-1}

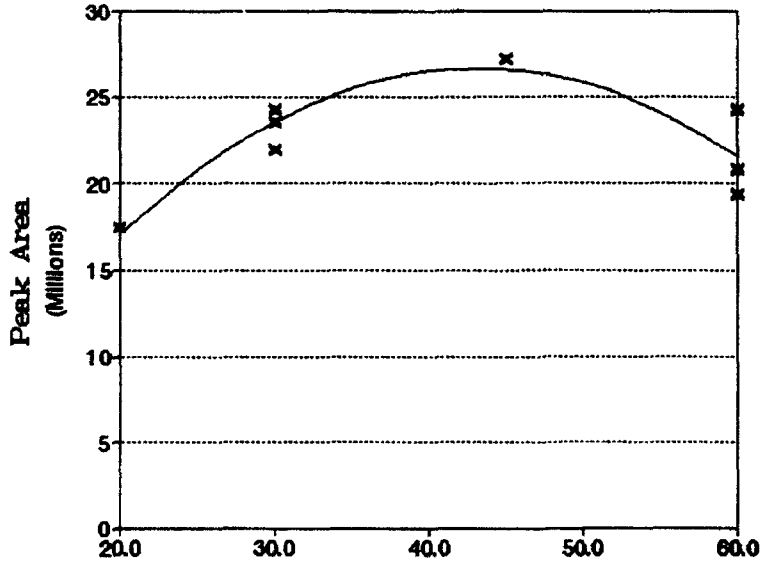

Figure 45. Mixed Gas Production Versus Irradiation Time: Mixed Gas GC-MS Peak Areas After Irradiation of Mixtures Containing 209 Torr of Cyclopropane and 40 Torr of Nitrogen Oxides at 25 W/cm^2 Using the P(18) line of the (00°1)-(02°0) transition, 1048.7 cm^{-1}

By careful selection of conditions we found it possible to produce nitrocyclopropane without making detectable amounts of any other nitrated products. A mixture of cyclopropane (191.1 Torr) and NO_2 (40.0 Torr) which had been irradiated at 30 W/cm^2 for 60 s, gave nitrocyclopropane, the only nitroalkane present, at a retention time of 10.8 min; any nitroalkane should appear in the GC trace at a retention time of greater than 5 min under the GC conditions we employed.

B. Cyclobutane

The infrared spectrum of cyclobutane shows a single, weak absorption centered at 900 cm^{-1} accessible to the CW carbon dioxide laser. Irradiation using the P(42) laser line of the (00°1)–(10°0) transition at 922.9 cm^{-1} was on the R branch near the maximum at 922 cm^{-1}. Because of the weak absorption and the limited laser power available, longer irradiation times were necessary to induce the nitration reaction. Table 2 presents the frequency intervals over which integrals were acquired for reactants and products. Figure 46 shows a linear relationship between the cyclobutane areas vs. partial pressures of cyclobutane in the reaction mixtures. Irradiation of 200 Torr of cyclobutane and 40.0 Torr of NO_2 using the P(42) line at 60 W/cm^2 for 60 s, yielded products identified by infrared analysis as H_2O, CO_2, CO, NO, formic acid, and ethene [3]. We have tentatively attributed other absorbances at 1560 and 1376 cm^{-1} to nitrocyclobutane. The amount of nitrogen oxides consumed during irradiation depended on the pressure of

Table 2. Infrared Frequency Regions (cm^{-1}) for Integrals of Reactants and Products in the Cyclobutane and Nitrogen Oxides Systems

Frequency Interval	Identity
2386.0 – 2293.0	CO_2
1956.0 – 1872.1	NO
1500.9 – 1400.1	Cyclobutane
1296.0 – 1228.0	N_2O_4
1140.2 – 1078.0	Formic Acid
952.7 – 945.9	Ethene
778.2 – 720.3	$N_2O_4 + NO_2$

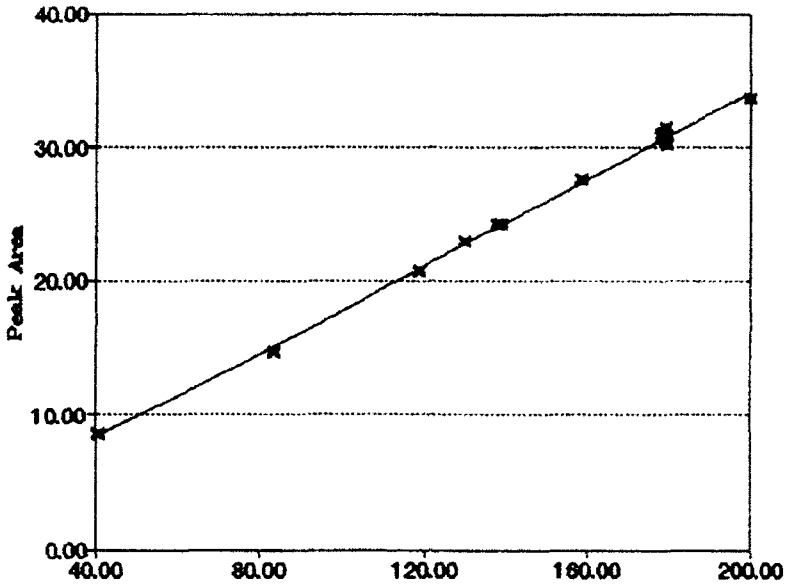

Figure 46. Areas of Cyclobutane Infrared Peak: Before Irradiation Versus Cyclobutane Pressure

cyclobutane as Figure 47 shows for nitrogen oxides at 40 Torr. The infrared region usually integrated for N_2O_4 (1296.0 - 1228.0 cm^{-1}) also includes a peak arising from cyclobutane. For this reason data is not included for the N_2O_4 peak. The amount

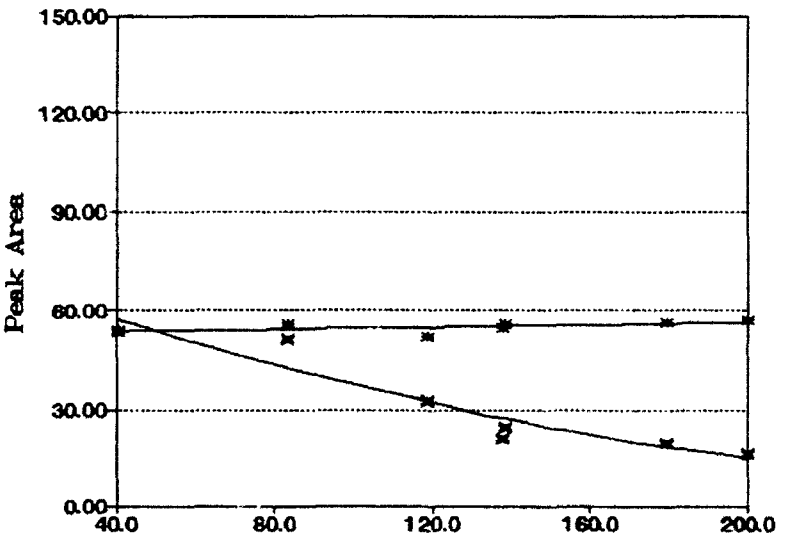

Figure 47. Nitrogen Oxides (40 Torr) Versus Cyclobutane Pressure: $N_2O_4 + NO_2$ Infrared Peak Areas Before and After Irradiation for 60 s at 60 W/cm^2 Using the P(42) Line of the (00°1)-(10°0) Transition, 922.9 cm^{-1}

of cyclobutane used during irradiation did not depend appreciably on the initial pressure of cyclobutane. Nitrocyclobutane and 1-nitropropane appeared in the GC trace at 13.6 min and 9.4 min, respectively. The amount of nitrocyclobutane produced showed a near-linear relationship to the partial pressure of cyclobutane in the reaction mixtures (Fig. 48). A similar dependence for the formation of 1-nitropropane, the only other nitroalkane identified by GC-MS analysis, is illustrated in Figure 49; however, no 1-nitropropane was detected until the cyclobutane pressure was greater than 80 Torr. Trends for the products arising from cleavage of the cyclobutane ring are illustrated in Figs. 50 through 53. The plots for formic acid, carbon dioxide and 2-butene show a similar dependence on the cyclobutane pressures in the reaction mixtures: as the cyclobutane pressure rose, the products increased then leveled off, or perhaps decreased. The production of ethene increased smoothly as the cyclobutane pressure increased. Although the fragment CO was identified in the infrared spectra, its formation was not followed due to the presence of relatively large cyclobutane absorbances overlying the CO absorption region. Nitrogen monoxide is another compound whose production appeared to level off at higher pressures of cyclobutane (Fig. 54). The mixed gas production as monitored from the GC-MS peak area was fairly constant as cyclobutane pressures ranged from 40 - 200 Torr, though the composition of the peak certainly varied as more nitrogen oxides reacted and low molecular weight, volatile products formed.

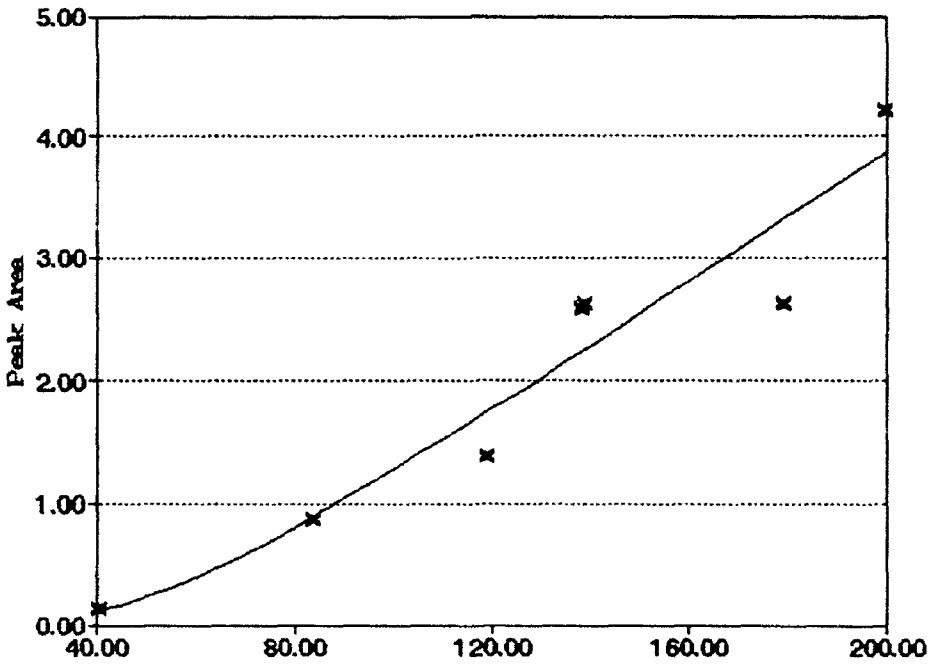

Figure 48a. Nitrocyclobutane Formation Versus Cyclobutane Pressure: After Irradiation of Mixtures Containing 40 Torr of Nitrogen Oxides for 60 s at 60 W/cm^2 Using the P(42) Line of the (00°1)-(10°0) Transition, 922.9 cm^{-1}, Nitrocyclobutane Infrared Peak Areas

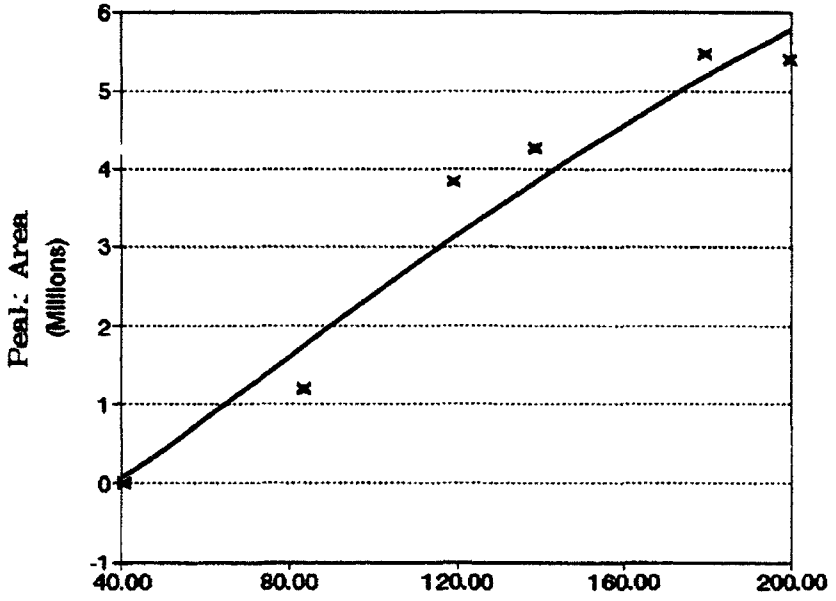

Figure 48b. Nitrocyclobutare Formation Versus Cyclobutane Pressure: After Irradiation of Mixtures Containing 40 Torr of Nitrogen Oxides for 60 s at 60 W/cm^2 Using the P(42) Line of the (00°1)-(10°0) Transition, 922.9 cm^{-1}, Nitrocyclobutane GC-MS Peak Areas

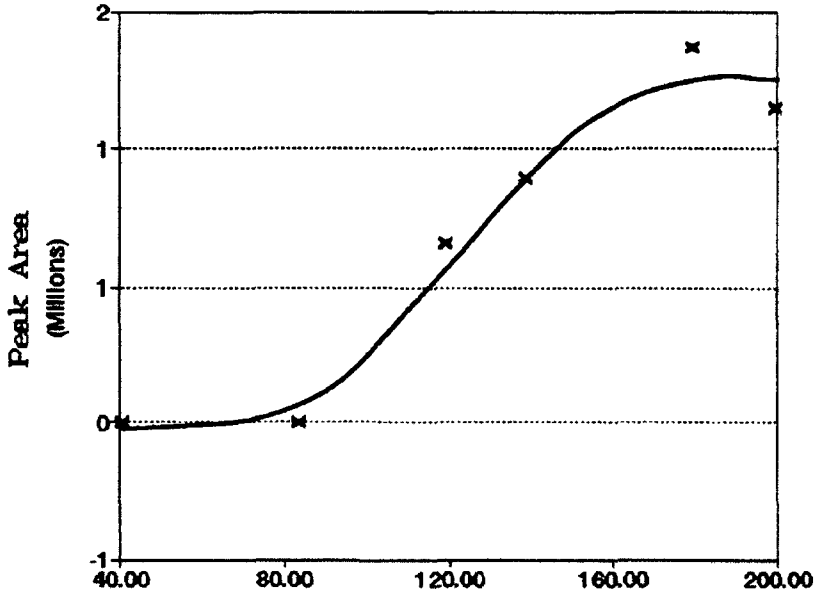

Figure 49. 1-Nitropropane Production Versus Cyclobutane Pressure: 1-Nitropropane GC-MS Peak Areas After Irradiation of Mixtures Containing 40 Torr of Nitrogen Oxides for 60 s at 60 W/cm^2 Using the P(42) Line of the (00°1)-(10°0) Transition, 922.9 cm^{-1}

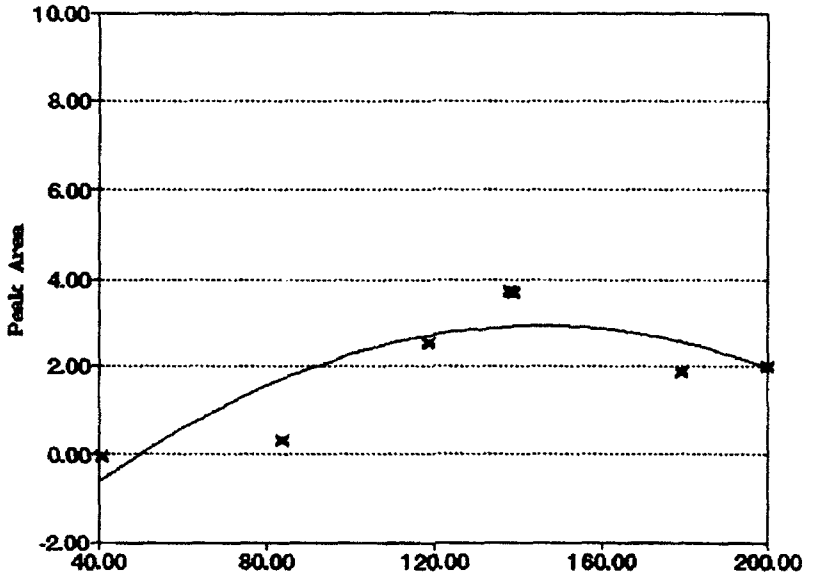

Figure 50. Formic Acid Production Versus Cyclobutane Pressure: Formic Acid Infrared Peak Areas After Irradiation of Mixtures Containing 40 Torr of Nitrogen Oxides for 60 s at 60 W/cm^2 Using the P(42) Line of the (00°1)-(10°0) Transition, 922.9 cm^{-1}

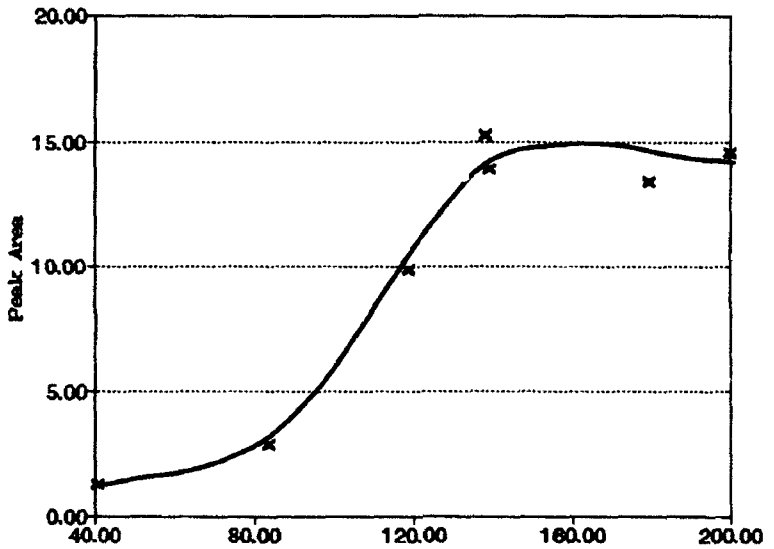

Figure 51. Carbon Dioxide Production Versus Cyclobutane Pressure: Carbon Dioxide Infrared Peak Areas After Irradiation of Mixtures Containing 40 Torr of Nitrogen Oxides for 60 s at 60 W/cm^2 Using the P(42) Line of the (00°1)-(10°0) Transition, 922.9 cm^{-1}

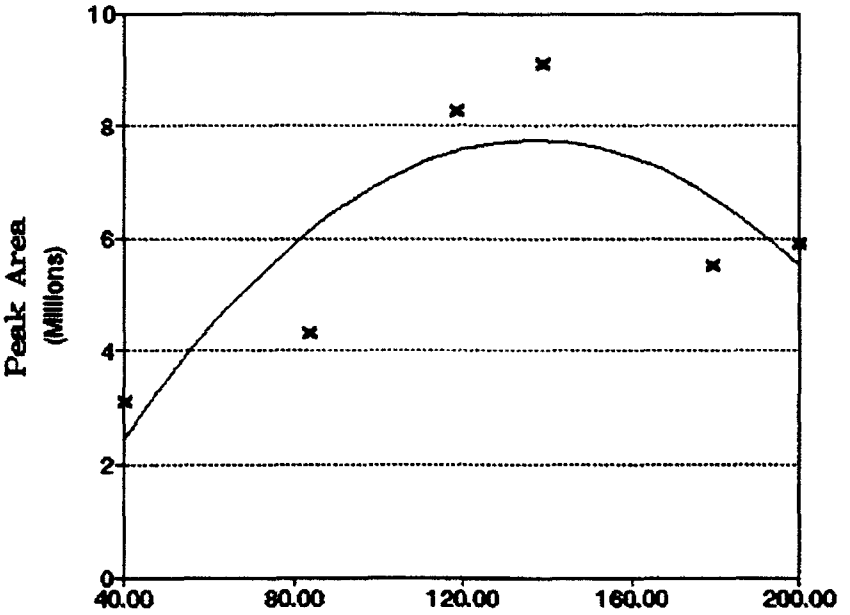

Figure 52. 2-Butene Production Versus Cyclobutane Pressure: 2-Butene GC-MS Peak Areas After Irradiation of Mixtures Containing 40 Torr of Nitrogen Oxides for 60 s at 60 W/cm^2 Using the P(42) Line of the (00°1)-(10°0) Transition, 922.9 cm^{-1}

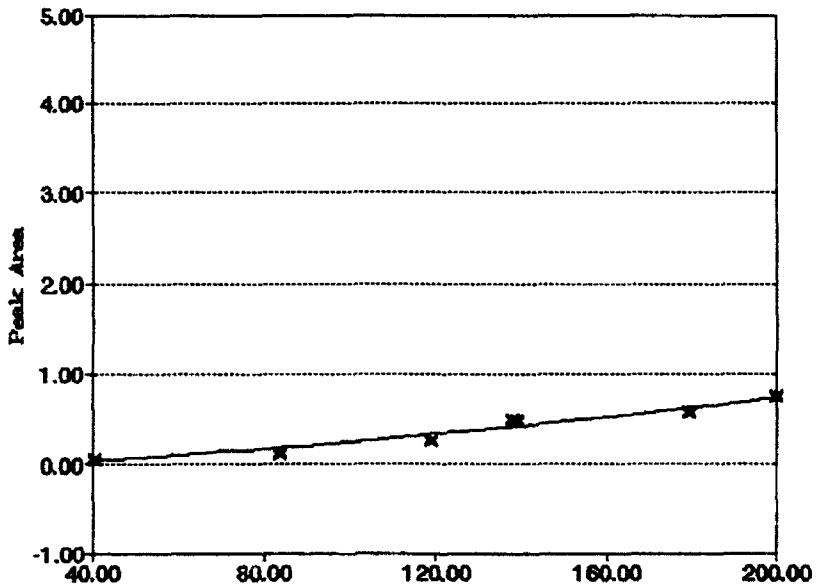

Figure 53. Ethene Production Versus Cyclobutane Pressure: Ethene Infrared Peak Areas After Irradiation of Mixtures Containing 40 Torr of Nitrogen Oxides for 60 s at 60 W/cm^2 Using the P(42) Line of the (00°1)-(10°0) Transition, 922.9 cm^{-1}

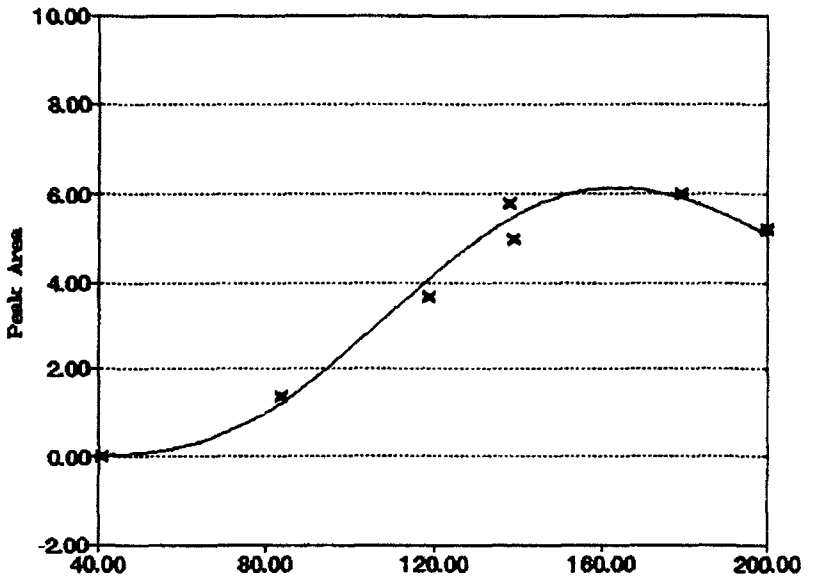

Figure 54. Nitrogen Monoxide Production Versus Cyclobutane Pressure: Nitrogen Monoxide Infrared Peak Areas After Irradiation of Mixtures Containing 40 Torr of Nitrogen Oxides for 60 s at 60 W/cm^2 Using the P(42) Line of the (00°1)-(10°0) Transition, 922.9 cm^{-1}

A series of 60 second irradiation experiments, in which the cyclobutane pressure was 179 Torr and nitrogen oxide pressure was 40 Torr, but in which the irradiation power was varied from 45 - 60 W/cm^2, allowed us to assess the effect of varying laser powers on the amounts of products formed. Our experiments were limited by the small quantity of cyclobutane on hand. The cyclobutane areas after irradiation were constant over the power range, but the decreased area of the nitrogen oxides peak (Fig. 55) shows that more of the nitrogen oxides were consumed at higher laser powers. Both the infrared and GC-MS analyses (Fig. 56) showed that nitrocyclobutane production rose slightly with the irradiation power increase. The production of 1-nitropropane and the mixed gases displayed no clear dependence on the laser power, as judged by GC peak areas. The amount of NO increased somewhat with increasing laser power (Fig. 57). Figures 58 through 61 show the production trends for formic acid, CO_2, 2-butene, and ethene. The data acquired for the power series of experiments are limited but the overall trends for the production of the compounds are believable in light of the similar production curves seen in the cyclopropane experiments and in the cyclobutane pressure experiments described above. Increasing the laser power seems to have the same effect on the product formation as increasing the cyclobutane pressure, which is not surprising since the cyclobutane is the energy absorbing species in the reaction mixtures.

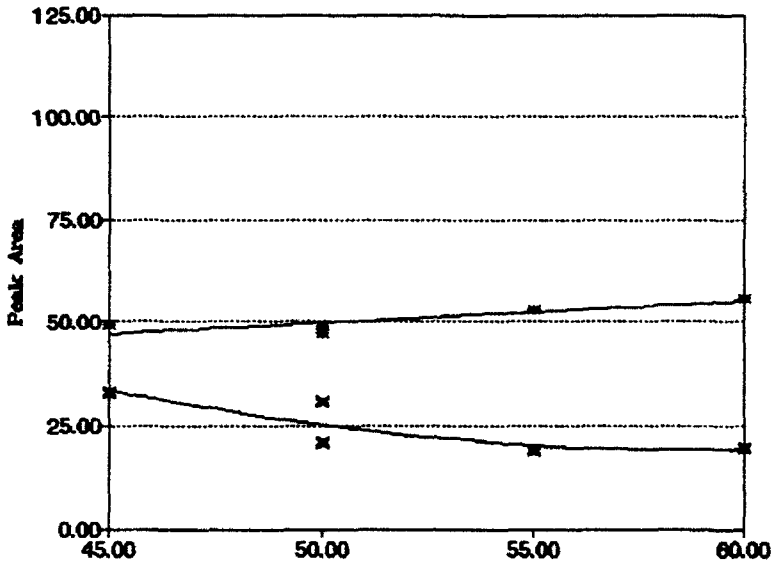

Figure 55. Nitrogen Oxides (40 Torr) Versus Incident Laser Power: $N_2O_4 + NO_2$ Infrared Peak Areas Before and After Irradiation of Mixtures Containing 179 Torr of Cyclobutane for 60 s Using the P(42) Line of the (00°1)-(10°0) Transition, 922.9 cm^{-1}

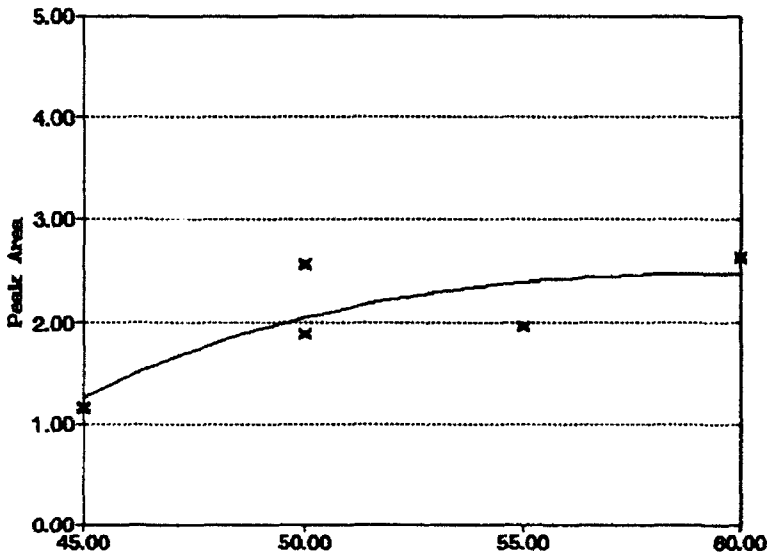

Figure 56a. Nitrocyclobutane Formation Versus Incident Laser Power: After Irradiation of Mixtures Containing 179 Torr of Cyclobutane and 40 Torr of Nitrogen Oxides for 60 s Using the P(42) Line of the (00°1)-(10°0) Transition, 922.9 cm^{-1}, Nitrocyclobutane Infrared Peak Areas

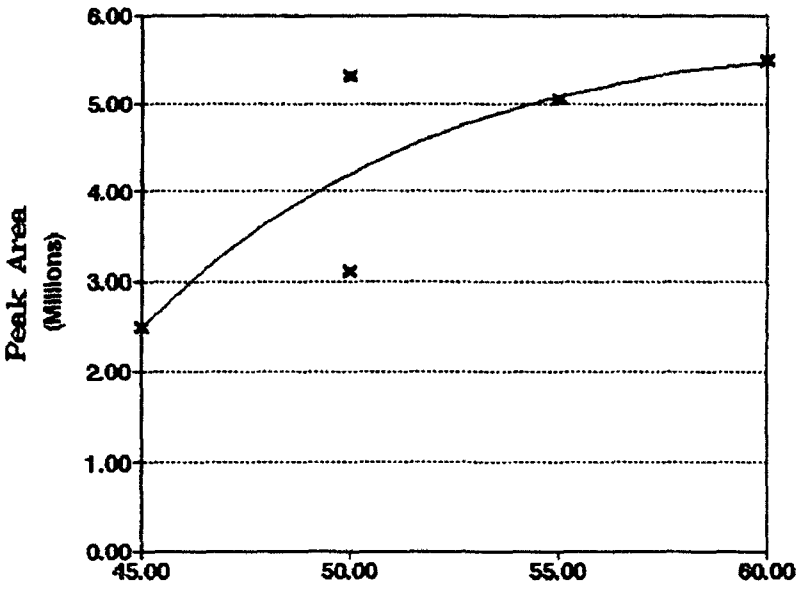

Figure 56b. Nitrocyclobutane Formation Versus Incident Laser Power: After Irradiation of Mixtures Containing 179 Torr of Cyclobutane and 40 Torr of Nitrogen Oxides for 60 s Using the P(42) Line of the (00°1)-(10°0) Transition, 922.9 cm^{-1}, Nitrocyclobutane GC-MS Peak Areas

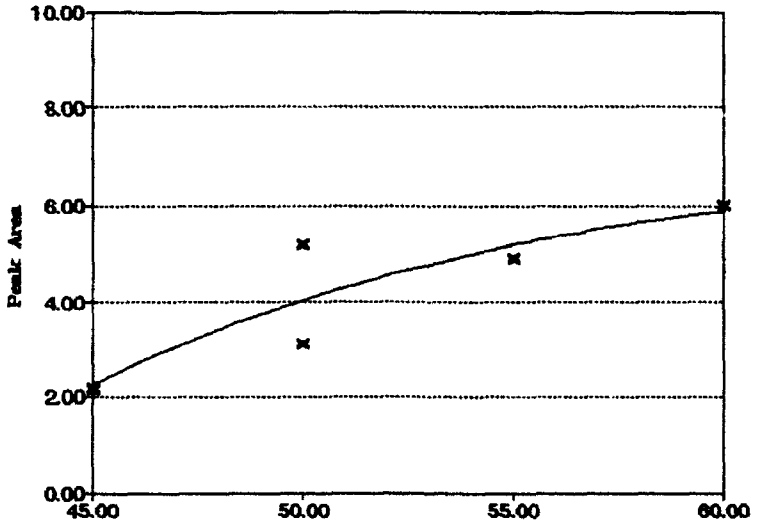

Figure 57. Nitrogen Monoxide Production Versus Incident Laser Power: Nitrogen Monoxide Infrared Peak Areas After Irradiation of Mixtures Containing 179 Torr of Cyclobutane and 40 Torr of Nitrogen Oxides for 60 s Using the P(42) Line of the (00°1)-(10°0) Transition, 922.9 cm^{-1}

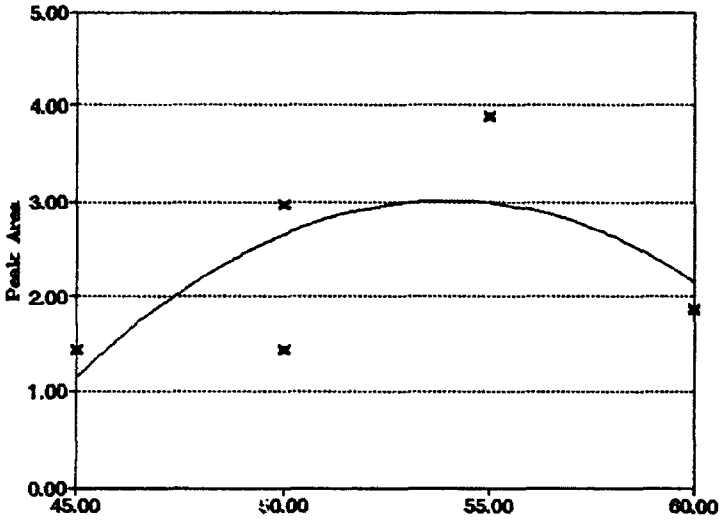

Figure 58. Formic Acid Production Versus Incident Laser Power: Formic Acid Infrared Peak Areas After Irradiation of Mixtures Containing 179 Torr of Cyclobutane and 40 Torr of Nitrogen Oxides for 60 s Using the P(42) Line of the (00°1)-(10°0) Transition, 922.9 cm^{-1}

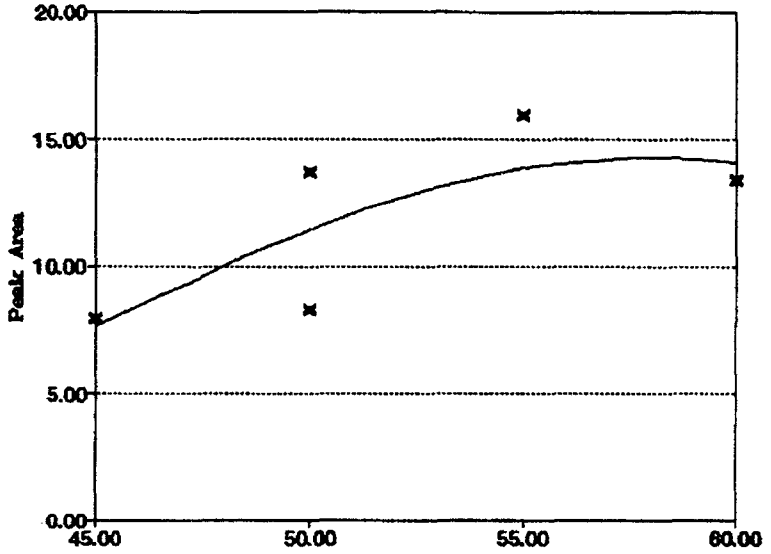

Figure 59. Carbon Dioxide Production Versus Incident Laser Power: Carbon Dioxide Infrared Peak Areas After Irradiation of Mixtures Containing 179 Torr of Cyclobutane and 40 Torr of Nitrogen Oxides for 60 s Using the P(42) Line of the (00°1)-(10°0) Transition, 922.9 cm^{-1}

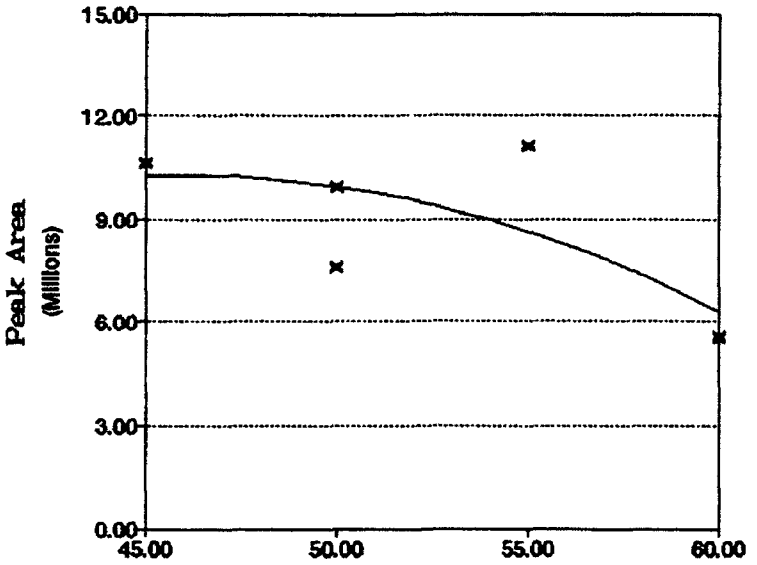

Figure 60. 2-Butene Production Versus Incident Laser Power: 2-Butene GC-MS Peak Areas After Irradiation of Mixtures Containing 179 Torr of Cyclobutane and 40 Torr of Nitrogen Oxides for 60 s Using the P(42) Line of the (00°1)-(10°0) Transition, 922.9 cm^{-1}

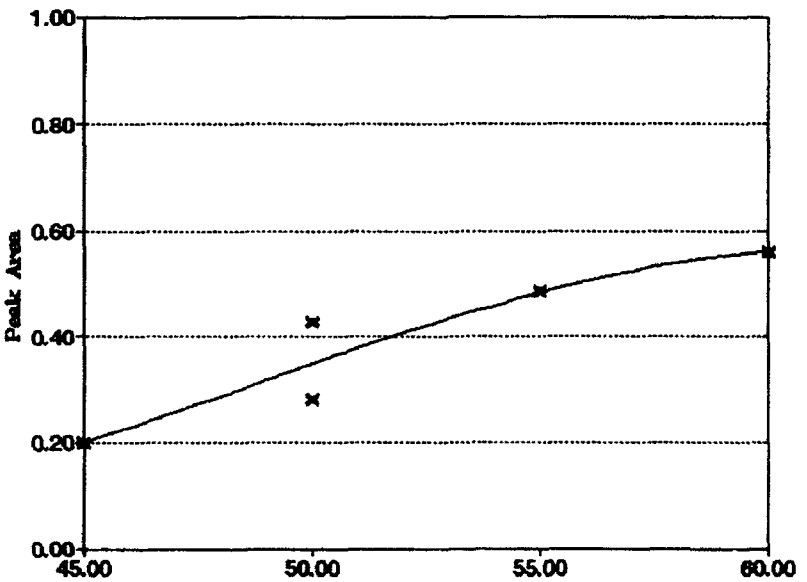

Figure 61. Ethene Production Versus Incident Laser Power: Ethene Infrared Peak Areas After Irradiation of Mixtures Containing 179 Torr of Cyclobutane and 40 Torr of Nitrogen Oxides for 60 s Using the P(42) Line of the (00°1)-(10°0) Transition, 922.9 cm^{-1}

We investigated the effect of varying irradiation times (30 - 120 s) on the trends of product formation using a series of experiments in which the cyclobutane and nitrogen oxide pressures were fixed at 179 and 40 Torr, respectively, and the laser power was set to 50 W/cm^2. The cyclobutane areas after irradiation were constant over the time range. Figure 62 shows the depletion curve for the nitrogen oxides. The amount of nitrocyclobutane formed increased only slightly, if at all, as the irradiation time increased over the 30 - 120 s range.

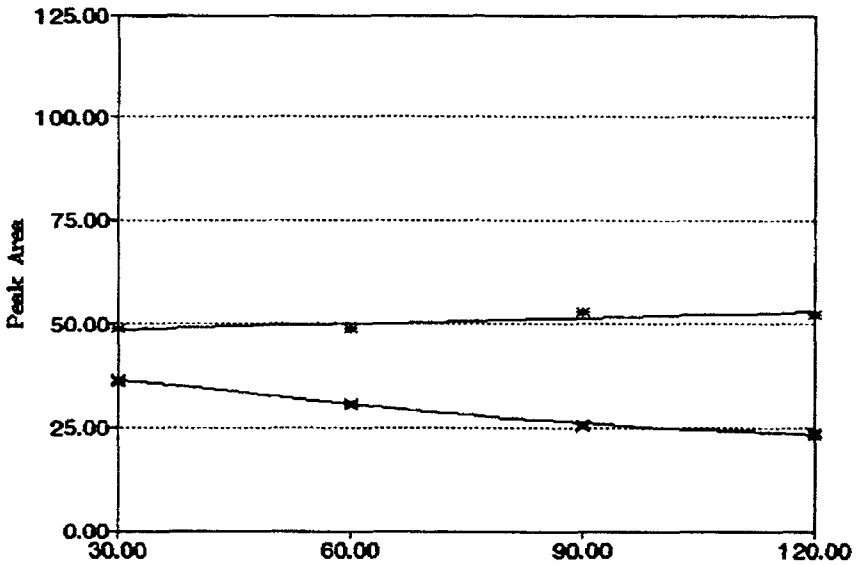

Figure 62. Nitrogen Oxides (40 Torr) Versus Irradiation Time: $N_2O_4 + NO_2$ Infrared Peak Areas Before and After Irradiation of Mixtures Containing 179 Torr of Cyclobutane at 50 W/cm^2 Using the P(42) Line of the (00°1)-(10°0) Transition, 922.9 cm^{-1}

Formic acid appeared to reach a maximum between 60 and 90 s (Fig. 63) while the CO_2 formation continued to rise over the time range (Fig. 64). Longer irradiation times favored the production of ethene (Fig. 65) perhaps at the expense of 2-butene (Fig. 66). The NO formation increased smoothly as the irradiation time increased (Fig. 67). The mixed gas and 1-nitropropane GC peak areas showed little, if any, dependence on irradiation time.

C. Cyclopentane

Cyclopentane has a single weak infrared absorption centered at 897 cm^{-1}, lying on the edge of the usable range of the carbon dioxide laser. Direct irradiation was possible only on the R-branch shoulder of the absorption band. To increase the efficiency of the irradiation of cyclopentane, an infrared sensitizer, sulfur hexafluoride, was sometimes introduced into the cyclopentane nitrogen oxide system. Sulfur hexafluoride has a strong infrared absorption (maximum at 945 cm^{-1}) permitting irradiation at 946.0 cm^{-1}, corresponding to the frequency of

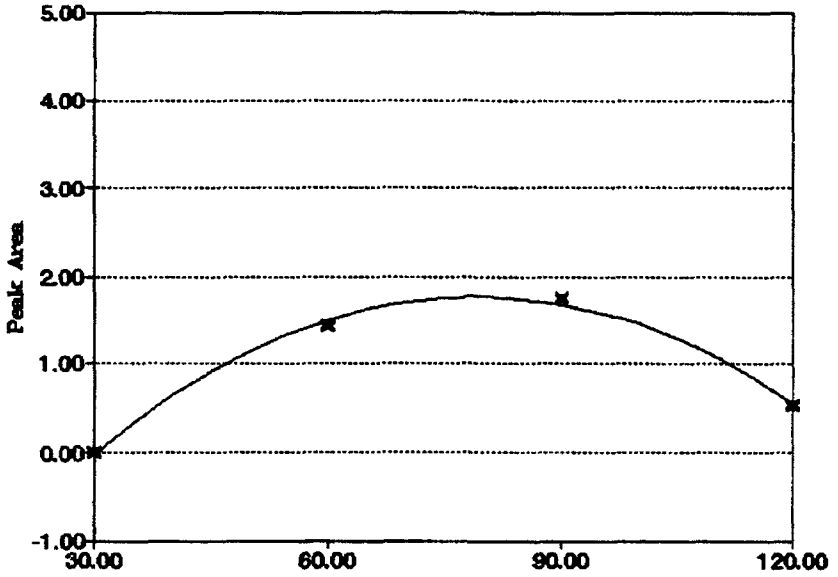

Figure 63. Formic Acid Production Versus Irradiation Time: Formic Acid Infrared Peak Areas After Irradiation of Mixtures Containing 179 Torr of Cyclobutane and 40 Torr of Nitrogen Oxides at 50 W/cm^2 Using the P(42) Line of the (00°1)-(10°0) Transition, 922.9 cm^{-1}

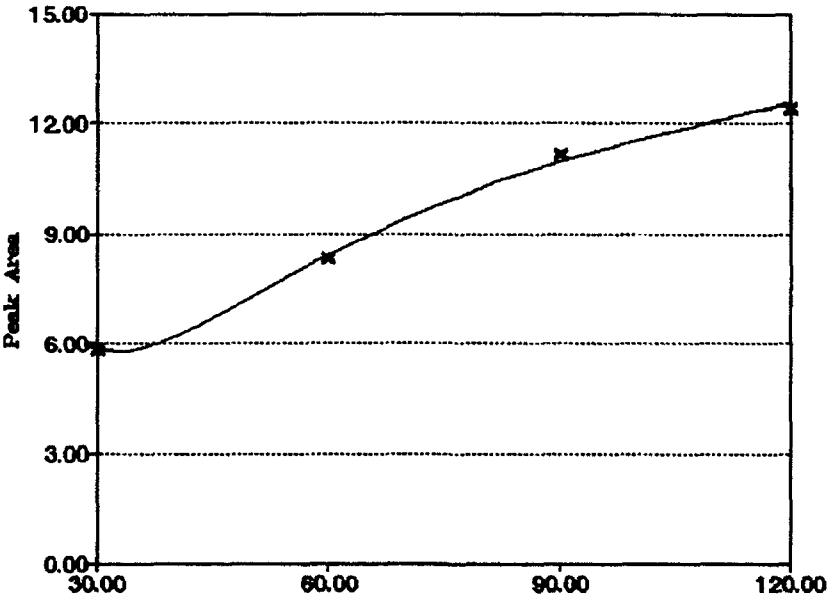

Figure 64. Carbon Dioxide Production Versus Irradiation Time: Carbon Dioxide Infrared Peak Areas After Irradiation of Mixtures Containing 179 Torr of Cyclobutane and 40 Torr of Nitrogen Oxides at 50 W/cm^2 Using the P(42) Line of the (00°1)-(10°0) Transition, 922.9 cm^{-1}

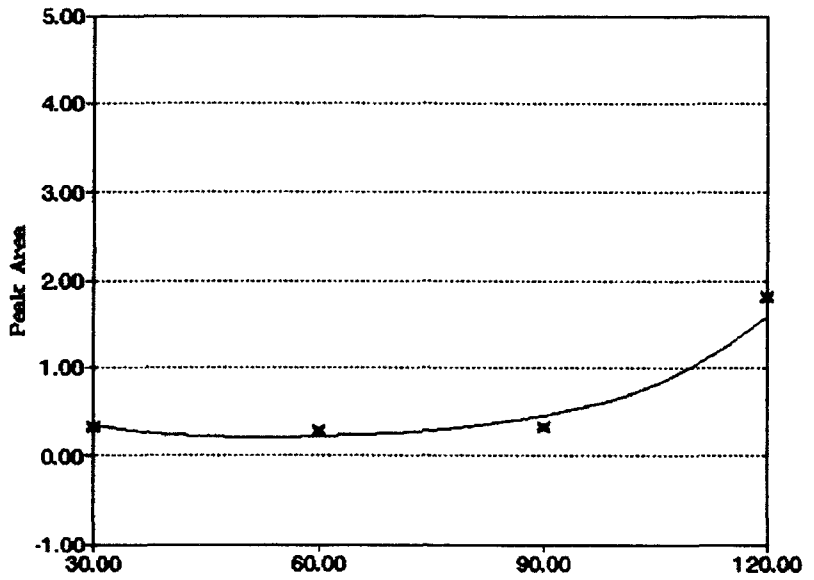

Figure 65. Ethene Production Versus Irradiation Time: Ethene Infrared Peak Areas After Irradiation of Mixtures Containing 179 Torr of Cyclobutane and 40 Torr of Nitrogen Oxides at 50 W/cm^2 Using the P(42) Line of the (00°1)-(10°0) Transition, 922.9 cm^{-1}

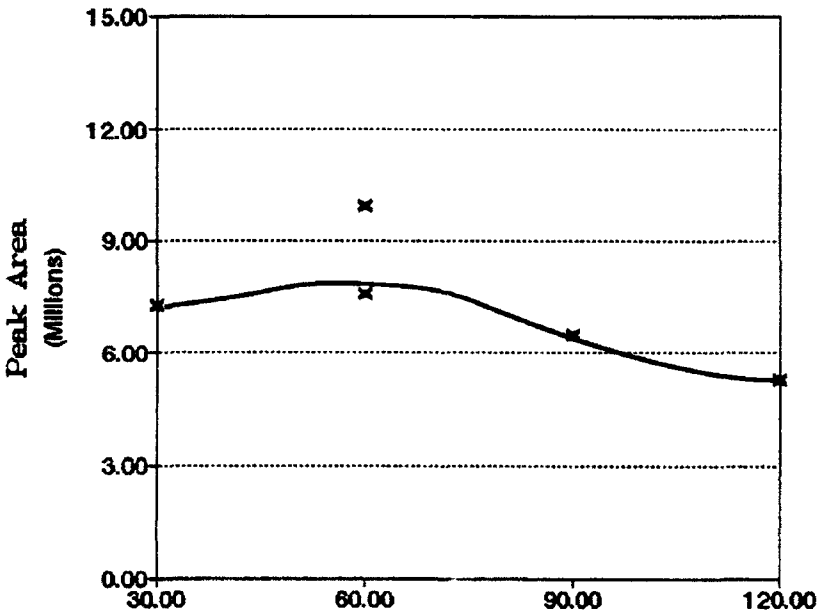

Figure 66. 2-Butene Production Versus Irradiation Time: 2-Butene GC-MS Peak Areas After Irradiation of Mixtures Containing 179 Torr of Cyclobutane and 40 Torr of Nitrogen Oxides at 50 W/cm^2 Using the P(42) Line of the (00°1)-(10°0) Transition, 922.9 cm^{-1}

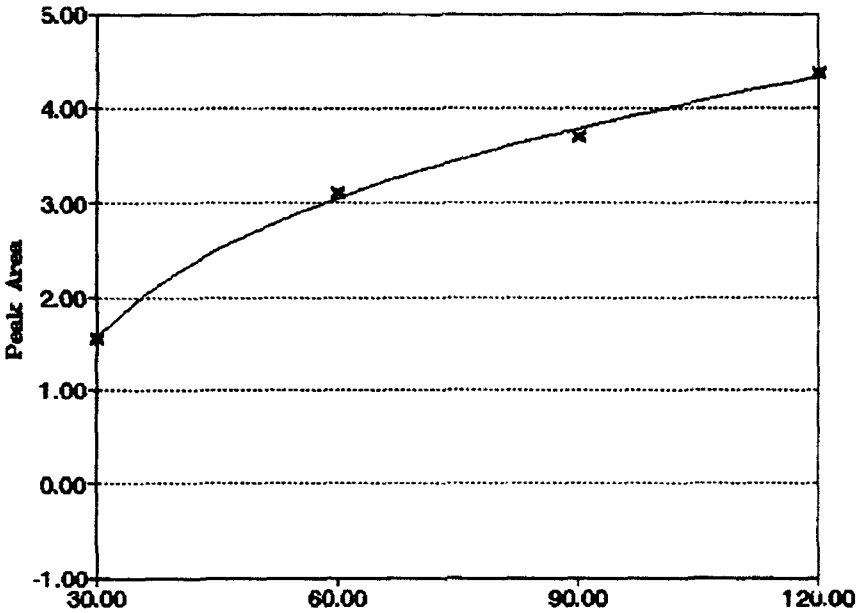

Figure 67. Nitrogen Monoxide Production Versus Irradiation Time: Nitrogen Monoxide Infrared Peak Areas After Irradiation of Mixtures Containing 179 Torr of Cyclobutane and 40 Torr of Nitrogen Oxides at 50 W/cm^2 Using the P(42) Line of the (00°1)-(10°0) Transition, 922.9 cm^{-1}

the P(18) line of the (00°1)-(10°0) band, an intense output line of the CO_2 laser. When the mixtures were irradiated using the P(18) line, the amount of energy absorbed by the system depended on the pressure of SF_6 rather than on that of cyclopentane. Mixtures of cyclopentane (180 Torr) and nitrogen oxides (25 Torr) were irradiated at 50 W/cm^2 with SF_6 present in small amounts (0.2 and 0.5 Torr). The frequency intervals over which integrals were acquired for the reactants, products, and sensitizer are in Table 3. The area of the sensitizer SF_6 remained flat over the irradiation time range 0 - 60 s, as Figure 68 indicates. This result was expected since a sensitizer should not participate chemically in the reaction. Cyclopentane areas appeared to remain constant over the entire time range (Fig. 69), but the amount of nitrogen oxides after irradiation (Fig. 70) diminished rapidly as the irradiation time increased, an effect that was especially dramatic in the reactions containing 0.5 Torr of SF_6. As determined by GC-MS analysis using the gas-sampling loop, irradiation of mixtures containing SF_6 at these two pressures produced significant quantities of nitrocyclopropane, as well as 1-nitrobutane and 1-nitropropane. The amount of nitrocyclopentane in the vapor phase reached a maximum earlier in the reactions containing 0.5 Torr of SF_6 (Fig. 71) with the quantity leveling off after a reaction time of about 15 s. When the SF_6 pressure was instead 0.2 Torr, the maximum nitrocyclopentane was reached at 45 s, but the same maximum amount of product was detected in both reactions.

Table 3. Infrared Frequency Regions (cm^{-1}) for Integrals of Reactants and Products in the Cyclopentane and Nitrogen Oxides Systems

Frequency Interval	Identity
2386.5 – 2294.0	CO_2
2143.6 – 2063.5	CO
1952.1 – 1871.6	NO
1286.8 – 1230.9	N_2O_4
1131.1 – 1071.3	Formic Acid
955.1 – 934.9	SF_6
920.4 – 871.2	Cyclopentane
779.1 – 720.8	$N_2O_4 + NO_2$
716.4 – 708.7	HCN

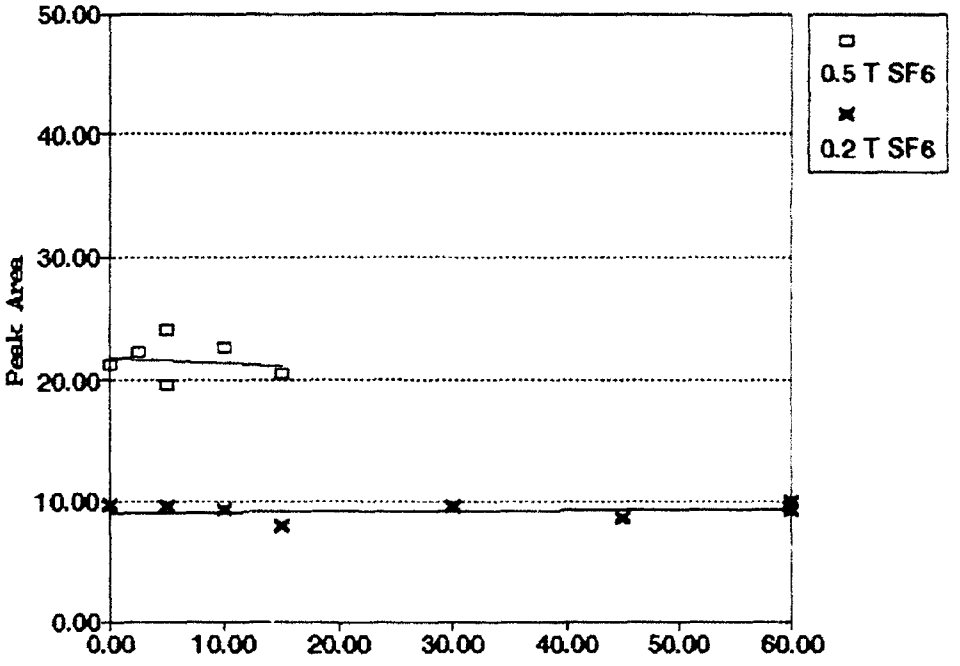

Figure 68. SF_6 Infrared Peak Areas Versus Irradiation Time at Two Different SF_6 Pressures (0.2 and 0.5 Torr): After Irradiation of Cyclopentane (180 Torr) and Nitrogen Oxides (25 Torr) at 50 W/cm^2 Using the P(13) Line of the (00°1)-(10°0) Transition, 946.0 cm^{-1}

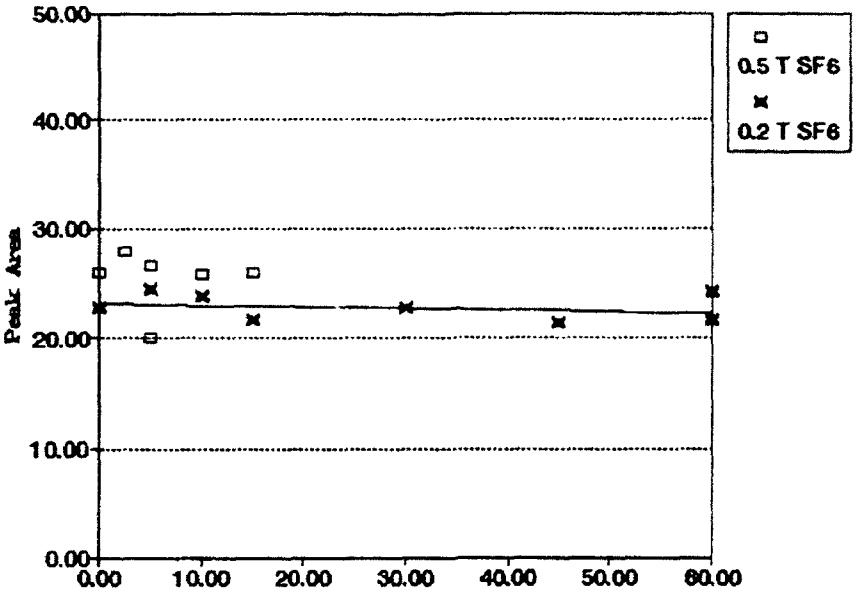

Figure 69a. Cyclopentane Versus Irradiation Time at Two Different SF_6 Pressures (0.2 and 0.5 Torr): After Irradiation of Cyclopentane (180 Torr) and Nitrogen Oxides (25 Torr) at 50 W/cm^2 Using the P(18) Line of the (00°1)-(10°0) Transition, 946.0 cm^{-1}, Cyclopentane Infrared Peak Areas

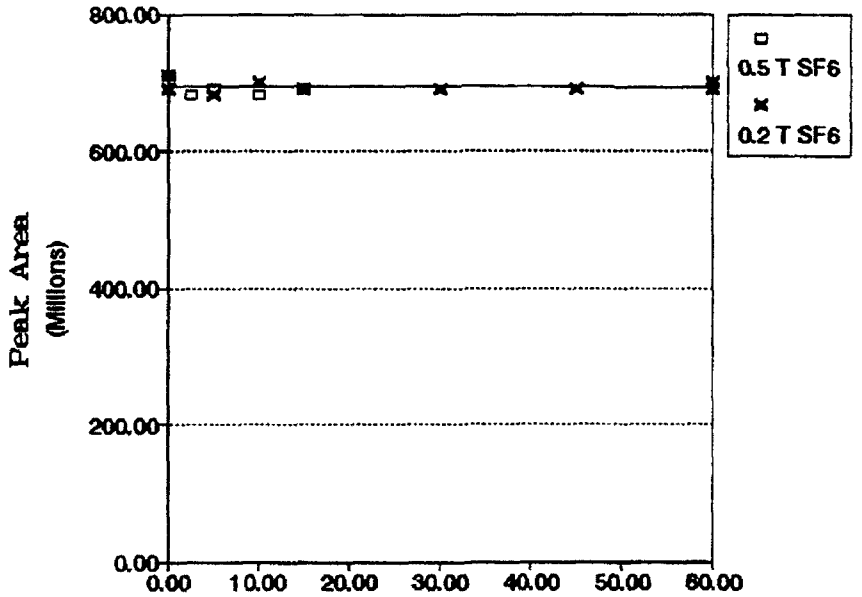

Figure 69b. Cyclopentane Versus Irradiation Time at Two Different SF_6 Pressures (0.2 and 0.5 Torr): After Irradiation of Cyclopentane (180 Torr) and Nitrogen Oxides (25 Torr) at 50 W/cm^2 Using the P(18) Line of the (00°1)-(10°0) Transition, 946.0 cm^{-1}, Cyclopentane GC-MS Peak Areas

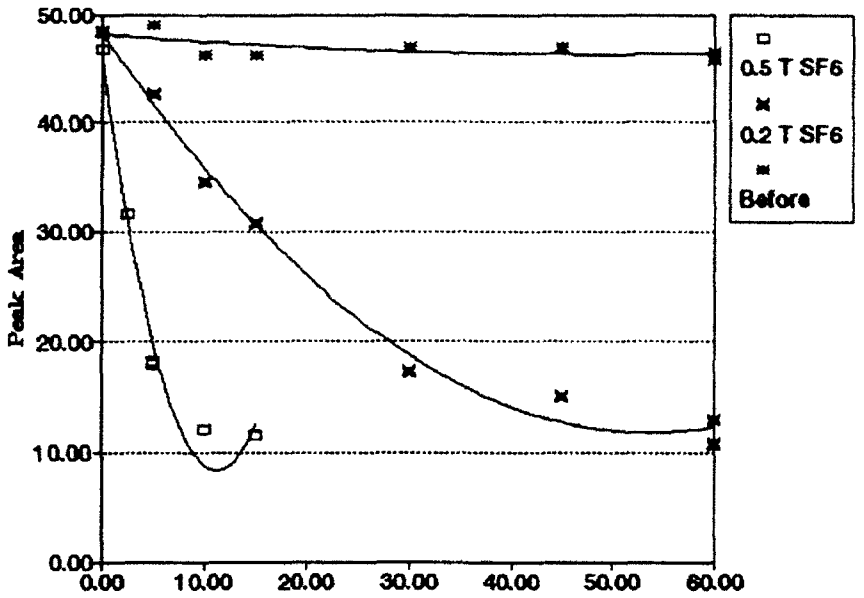

Figure 70a. Nitrogen Oxides Versus Irradiation Time at Two Different SF_6 Pressures (0.2 and 0.5 Torr): Before and After Irradiation of Cyclopentane (180 Torr) and Nitrogen Oxides (25 Torr) at 50 W/cm^2 Using the P(18) Line of the (00°1)-(10°0) Transition, 946.0 cm^{-1}, N_2O_4 Infrared Peak Areas

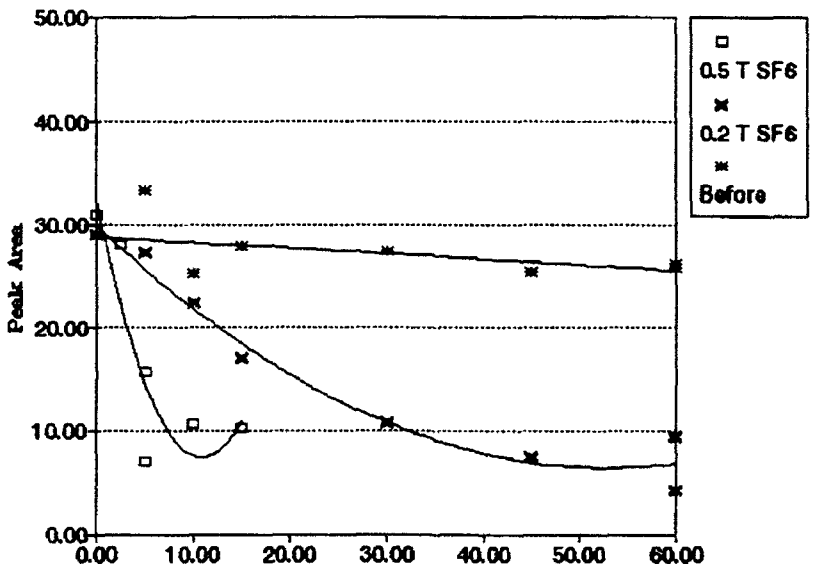

Figure 70b. Nitrogen Oxides Versus Irradiation Time at Two Different SF_6 Pressures (0.2 and 0.5 Torr): Before and After Irradiation of Cyclopentane (180 Torr) and Nitrogen Oxides (25 Torr) at 50 W/cm^2 Using the P(18) Line of the (00°1)-(10°0) Transition, 946.0 cm^{-1}, N_2O_4 + NO_2 Infrared Peak Areas

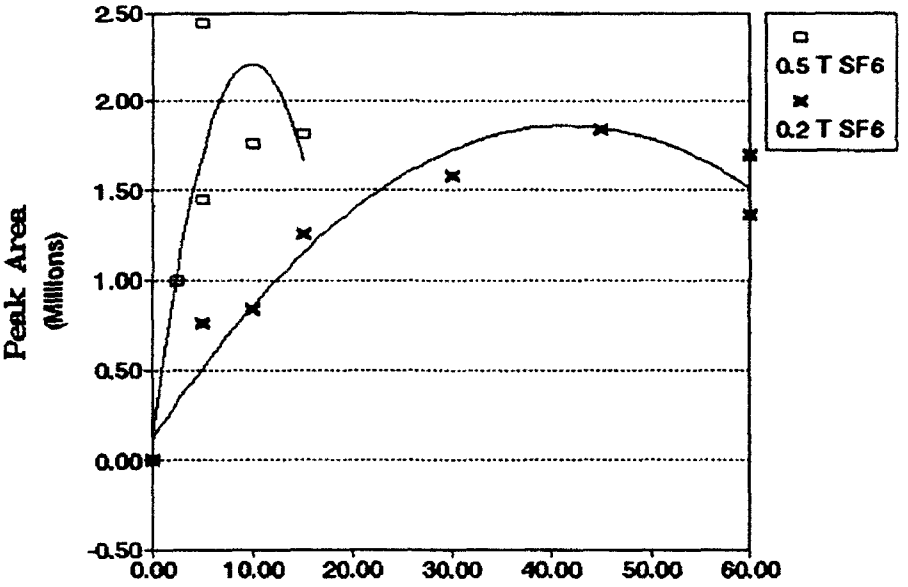

Figure 71. Nitrocyclopentane Formation Versus Irradiation Time at Two Different SF_6 Pressures (0.2 and 0.5 Torr): Nitrocyclopentane GC-MS Peak Areas After Irradiation of Cyclopentane (180 Torr) and Nitrogen Oxides (25 Torr) at 50 W/cm^2 Using the P(18) Line of the (00°1)-(10°0) Transition, 946.0 cm^{-1}

Figures 72 and 73 show that 1-nitrobutane and 1-nitropropane are formed earlier and in greater amounts when 0.5 Torr of SF_6 is present. The products reached a maximum at 10–15 s in the 0.5 Torr experiments and at 45 s in the 0.2 Torr experiments. Figures 74 through76 indicate that the gaseous products CO_2, CO, and NO, were formed in much the same manner. The GC mixed-gas peak showed the same pattern (Fig. 77). We did not monitor the production of nitroalkanes by infrared due to overlying absorbances in the regions of interest. Formic acid was monitored but the time dependency of its production could not be determined. As indicated by GC-MS results [4], pressures of SF_6 greater than about 1 Torr resulted in extensive fragmentation of cyclopentane and little nitrocyclopentane, making irradiation via the 946.0 cm^{-1} line less useful than we had hoped. The high absorptivity of the SF_6 band near the 946.0 cm^{-1} laser line coupled with the difficulty in controlling the laser power below about 25 W/cm^2, caused the reaction system to be too sensitive to small changes in the SF_6 pressures. We therefore sought conditions which would allow us to use higher SF_6 pressures.

The SF_6 absorption is narrow but extremely intense, so that significant laser power is absorbed by SF_6 even at frequencies offset from its maximum absorbance by more than 25 cm^{-1}. The P(46) line of the (00°1)-(10°0)

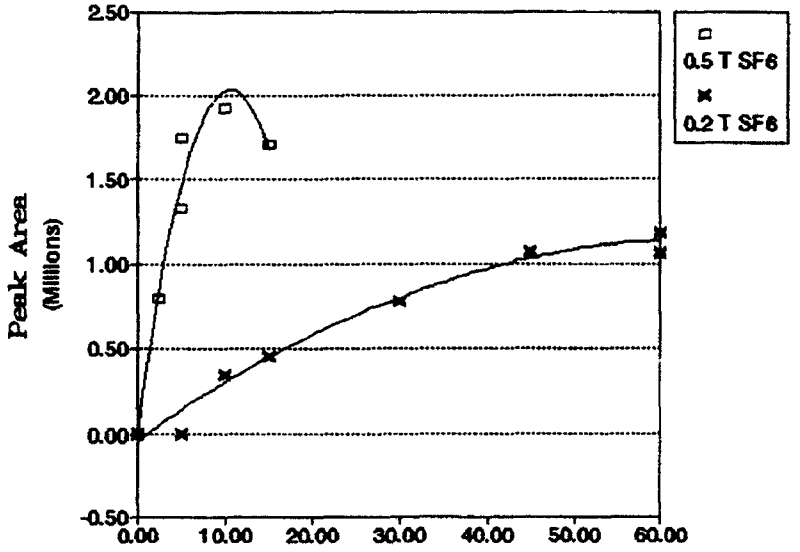

Figure 72. 1-Nitrobutane Formation Versus Irradiation Time at Two Different SF_6 Pressures (0.2 and 0.5 Torr): 1-Nitrobutane GC-MS Peak Areas After Irradiation of Cyclopentane (180 Torr) and Nitrogen Oxides (25 Torr) at 50 W/cm^2 Using the P(18) Line of the (00°1)-(10°0) Transition, 946.0 cm^{-1}

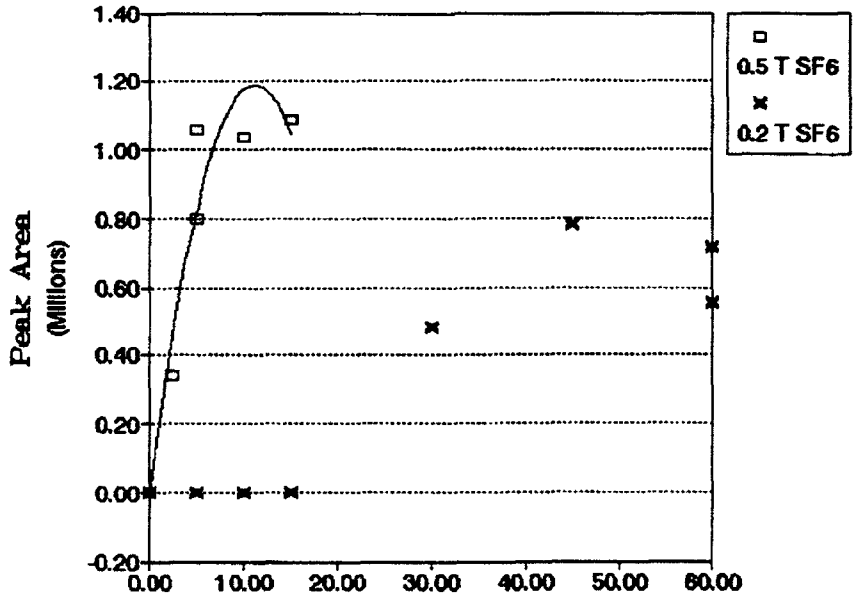

Figure 73. 1-Nitropropane Formation Versus Irradiation Time at Two Different SF_6 Pressures (0.2 and 0.5 Torr): 1-Nitropropane GC-MS Peak Areas After Irradiation of Cyclopentane (180 Torr) and Nitrogen Oxides (25 Torr) at 50 W/cm^2 Using the P(18) Line of the (00°1)-(10°0) Transition, 946.0 cm^{-1}

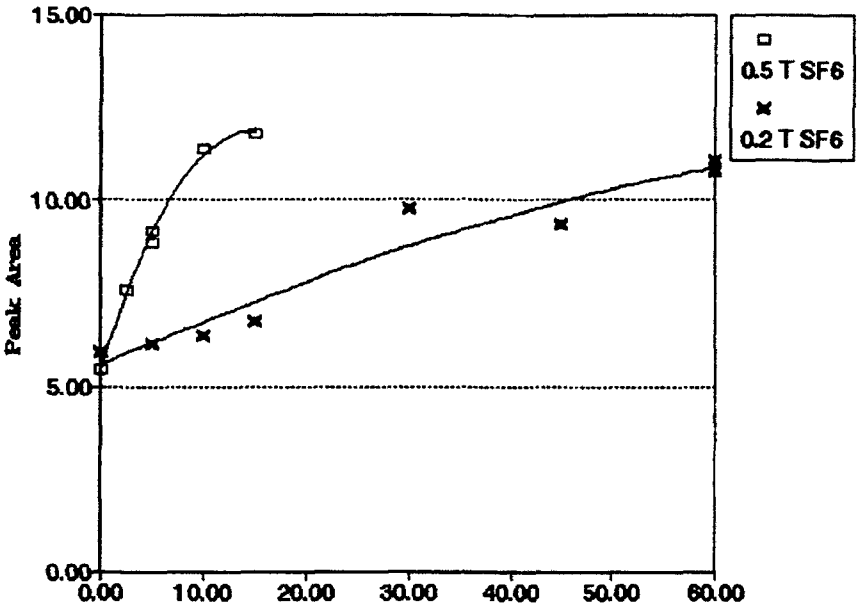

Figure 74. Carbon Dioxide Formation Versus Irradiation Time at Two Different SF_6 Pressures (0.2 and 0.5 Torr): Carbon Dioxide Infrared Peak Areas After Irradiation of Cyclopentane (180 Torr) and Nitrogen Oxides (25 Torr) at 50 W/cm^2 Using the P(18) Line of the (00°1)-(10°0) Transition, 946.0 cm^{-1}

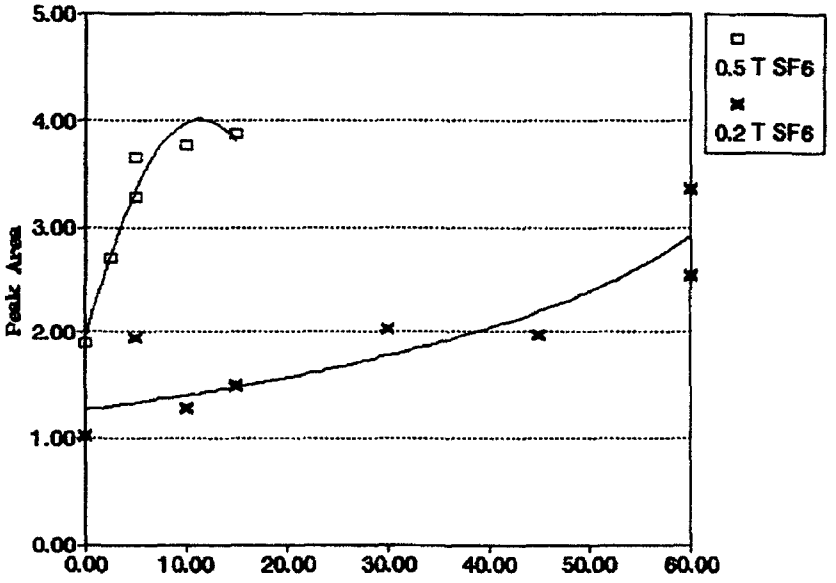

Figure 75. Carbon Monoxide Formation Versus Irradiation Time at Two Different SF_6 Pressures (0.2 and 0.5 Torr): Carbon Monoxide Infrared Peak Areas After Irradiation of Cyclopentane (180 Torr) and Nitrogen Oxides (25 Torr) at 50 W/cm^2 Using the P(18) Line of the (00°1)-(10°0) Transition, 946.0 cm^{-1}

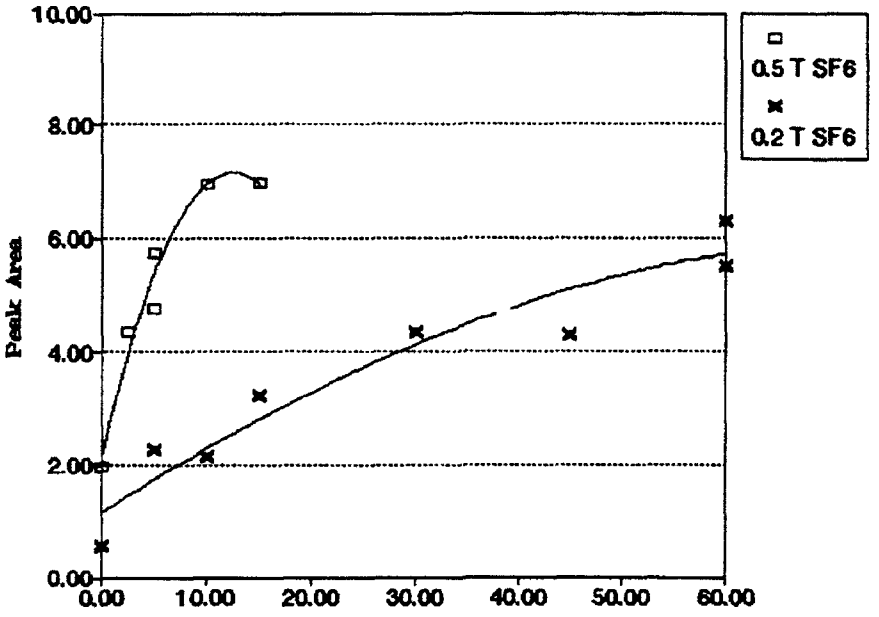

Figure 76. Nitrogen Monoxide Formation Versus Irradiation Time at Two Different SF_6 Pressures (0.2 and 0.5 Torr): Nitrogen Monoxide Infrared Peak Areas After Irradiation of Cyclopentane (180 Torr) and Nitrogen Oxides (25 Torr) at 50 W/cm^2 Using the P(18) Line of the (00°1)-(10°0) Transition, 946.0 cm^{-1}

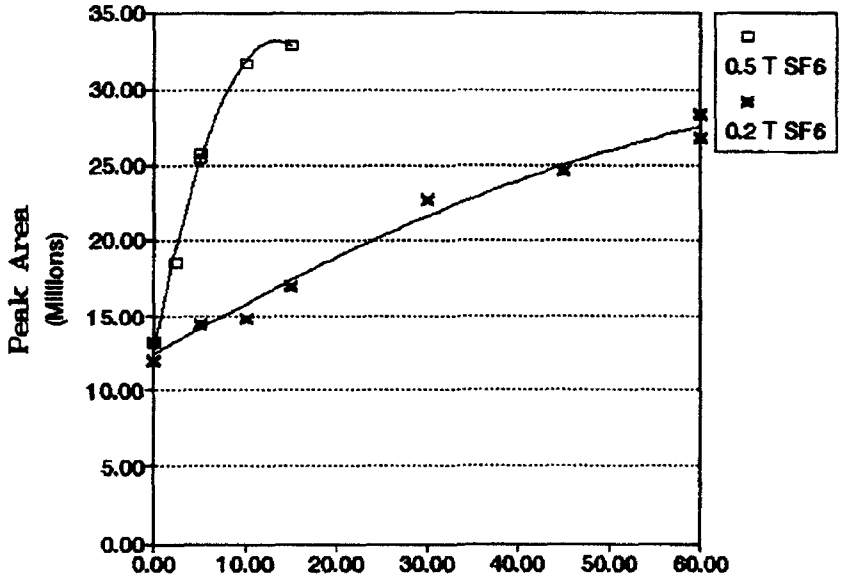

Figure 77. Mixed Gas Formation Versus Irradiation Time at Two Different SF_6 Pressures (0.2 and 0.5 Torr): Mixed Gas GC-MS Peak Areas After Irradiation of Cyclopentane (180 Torr) and Nitrogen Oxides (25 Torr) at 50 W/cm^2 Using the P(18) Line of the (00°1)-(10°0) Transition, 946.0 cm^{-1}

transition at 918.7 cm^{-1} provides access to the overlapping absorptions of SF_6 and cyclopentane, both of which absorb weakly at 918.7 cm^{-1} [3]. When irradiated using the P(46) laser line, cyclopentane absorbed enough energy so that nitration occurred even in the absence of SF_6. After mixtures of cyclopentane (180 Torr) and NO_2 (20 Torr) were irradiated at 45 W/cm^2 for times ranging from 0 to 120 s, the amount of cyclopentane remaining had not decreased significantly. The amount of nitrocyclopentane, the only nitroalkane detected in these mixtures, increased in the vapor phase up to about 60 s irradiation time, beyond which its production leveled off (Fig. 78). Mixed gas production followed the same pattern (Fig. 79). This result indicates that increasing the irradiation time does not strongly favor fragmentation processes.

Mixtures containing cyclopentane (180 Torr), nitrogen oxides (20 Torr), and varying amounts of SF_6 (0 – 3.0 Torr) were irradiated for 60 s at 45 W/cm^2 using the P(46) transition. The area of the GC peak from cyclopentane indicated

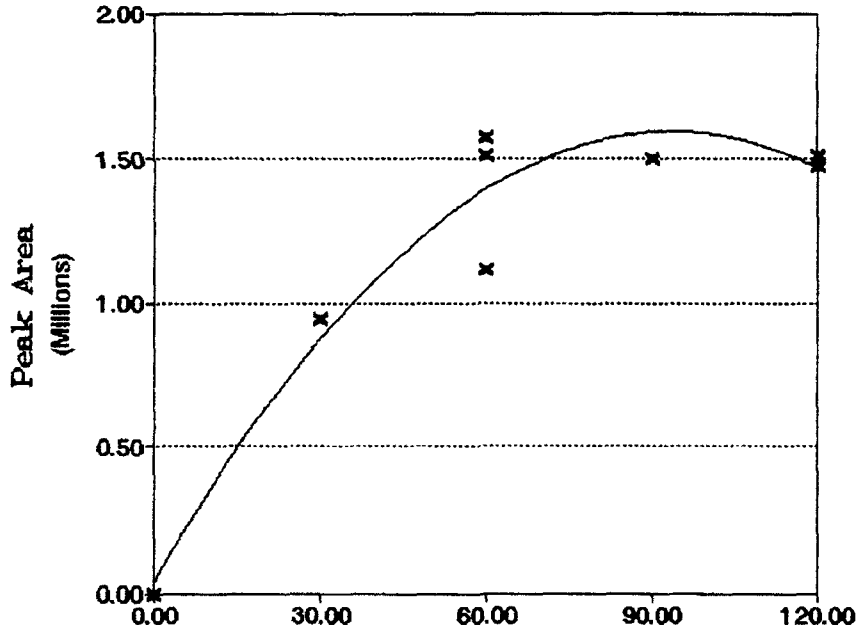

Figure 78. Nitrocyclopentane Formation Versus Irradiation Time: Nitrocyclopentane GC-MS Peak Areas After Irradiation of Cyclopentane (180 Torr) and Nitrogen Oxides (20 Torr) at 45 W/cm^2 Using the P(46) Line of the (00°1)-(10°0) Transition, 918.7 cm^{-1}

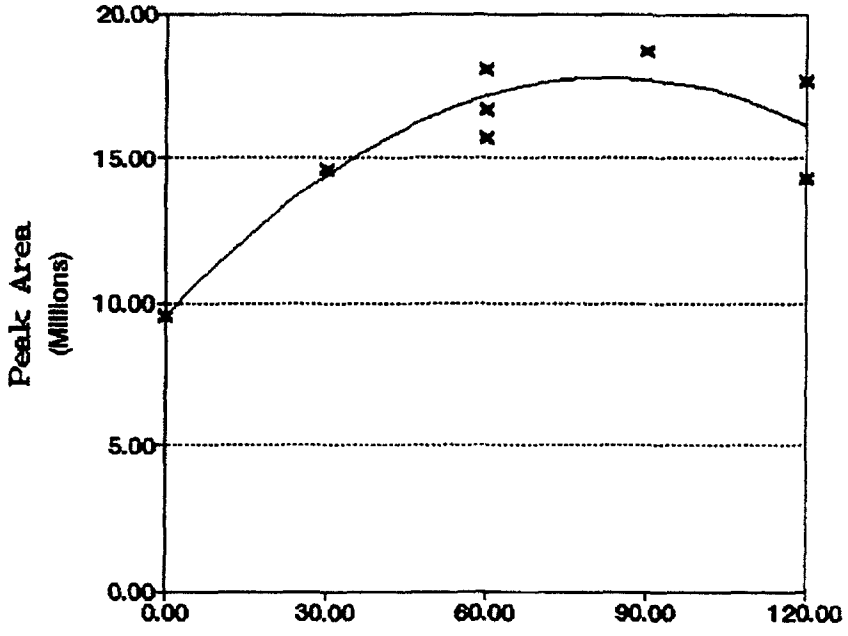

Figure 79. Mixed Gas Formation Versus Irradiation Time: Mixed Gas GC-MS Peak Areas After Irradiation of Cyclopentane (180 Torr) and Nitrogen Oxides (20 Torr) at 45 W/cm^2 Using the P(46) Line of the (00°1)-(10°0) Transition, 918.7 cm^{-1}

that more of it was consumed as the pressure of the sensitizer increased (Fig. 80). Using the P(46) laser line with 1.0 - 2.0 Torr of SF_6 facilitated the production of nitrocyclopentane (Fig. 81), but as more energy was absorbed by the system (higher SF_6 pressures) the amount of the nitrocyclopentane in the gas phase decreased. Moderate pressures of SF_6 also favored the production of 1-nitrobutane and 1-nitropropane: GC-MS analyses indicated that there was a narrow range of SF_6 pressures (between 1 and 2 Torr) over which the straight chain nitroalkanes could be detected. In contrast, s the amount of SF_6 in the system increased, mixed gas production rose sharply (Fig. 82), accounted for by fragmentations yielding small molecules, a process favored in the higher energy reactions.

Irradiation of the reaction mixtures containing SF_6 frequently produced visible quantities of a liquid on the potassium chloride windows. Since the vapor pressure of nitrocyclopentane is low (about 1 Torr) we were suspicious that some conditions contributed to formation of enough nitrocyclopentane for it to be present in both the vapor and the condensed phases. For this reason, we used the cell wash procedure described in the experimental section to monitor liquid phase products in the experiments that follow.

We investigated the effect of irradiation time with small amounts of SF_6 present, using the P(46) transition at 45 W/cm^2 to excite mixtures of cyclopentane (170 Torr), nitrogen oxides (30 Torr), and SF_6 (0.5 Torr). Irradiation times ranging

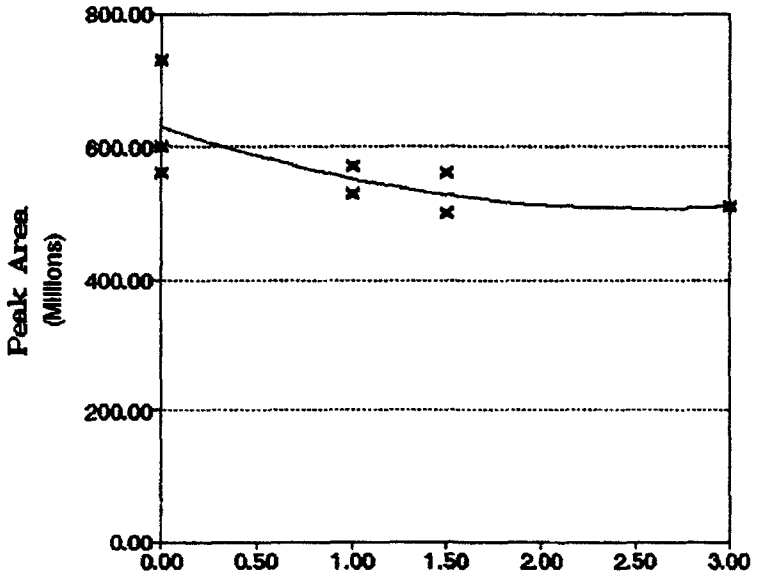

Figure 80. Cyclopentane Remaining Versus SF_6 Pressure: Cyclopentane GC-MS Peak Areas After Irradiation of Cyclopentane (180 Torr) and Nitrogen Oxides (20 Torr) at 45 W/cm^2 Using the P(46) Line of the (00°1)-(10°0) Transition, 918.7 cm^{-1}

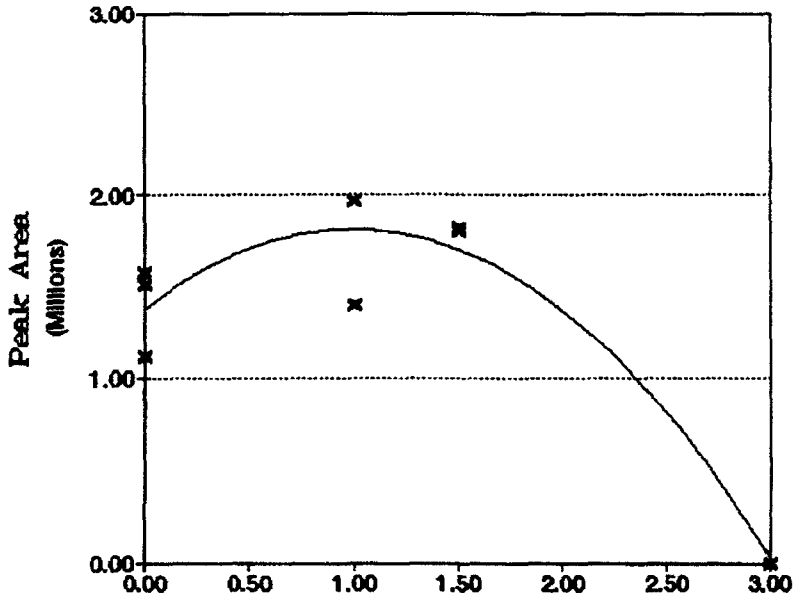

Figure 81. Nitrocyclopentane Production Versus SF_6 Pressure: Nitrocyclopentane GC-MS Peak Areas After Irradiation of Cyclopentane (180 Torr) and Nitrogen Oxides (20 Torr) at 45 W/cm^2 Using the P(46) Line of the (00°1)-(10°0) Transition, 918.7 cm^{-1}

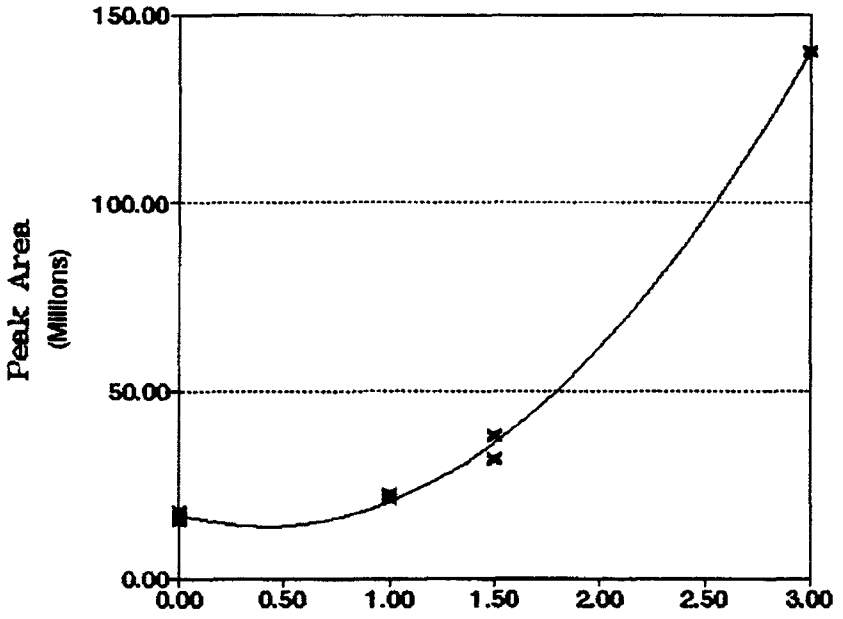

Figure 82. Mixed Gas Production Versus SF_6 Pressure: Mixed Gas GC-MS Peak Areas After Irradiation of Cyclopentane (180 Torr) and Nitrogen Oxides (20 Torr) at 45 W/cm^2 Using the P(46) Line of the (00°1)-(10°0) Transition, 918.7 cm^{-1}

from 60 to 240 s resulted in no detectable drop in cyclopentane peak areas as judged by both GC-MS and infrared analysis. The nitrogen oxide reactants were significantly depleted over this time range, however, as Figure 83 shows. Increasing the irradiation time beyond 60 s did not facilitate the nitrocyclopentane production. Figure 84 presents the results of the GC-MS analyses for nitrocyclopentane using the gas sampling loop. Following gas sampling, 2.0 mL aliquots of absolute ethanol were used as a cell rinse. Samples (0.5 ml of cell wash) were injected on the GC-MS, the replicate peak areas averaged, and the results plotted. Nitrocyclopentane was the only product detected in the cell wash. As Figure 85 indicates, irradiation times longer than 60 s did not result in more liquid nitrocyclopentane. The GC-MS areas in Figure 85 can be compared to those from the gas sampling experiment if we take into account the relative amount of samples injected by each method. In the cell-wash experiment a 0.5 ml injection represented 0.025 percent of the total sample; in the gas-sampling experiment a 0.250 mL aliquot represented 0.25 percent of the total sample. To compare results of the two types of experiments the peak areas in the cell-wash experiment must, therefore, be multiplied by 10. Figures 84 and 85 show that about 10 times as much nitrocyclopentane exists in the liquid phase as in the gas phase after 60 s of irradiation, and that irradiation for longer times does not alter the amounts of products formed in either phase. We were able to estimate the mass of nitrocyclopentane formed by mimicking the manner in which the cell washes

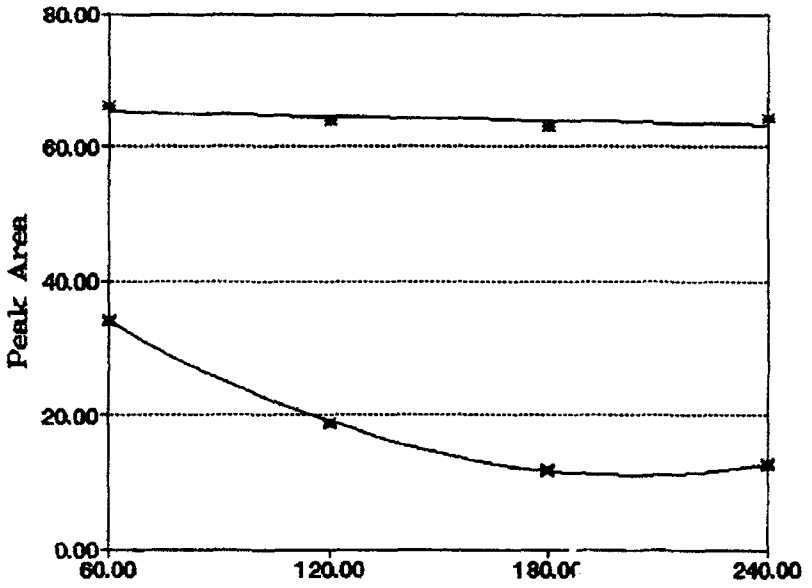

Figure 83a. Nitrogen Oxides (30 Torr) Versus Irradiation Time: Before and After Irradiation of Mixtures Containing 170 Torr of Cyclopentane and 0.5 Torr of SF_6 at 45 W/cm^2 Using the P(46) Line of the (00°1)-(10°0) Transition, 918.7 cm^{-1}, N_2O_4 Infrared Peak Areas

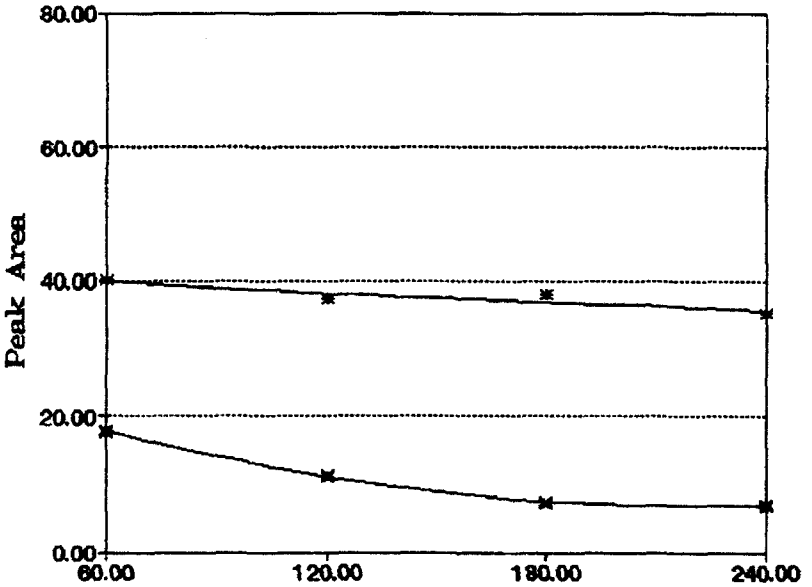

Figure 83b. Nitrogen Oxides (30 Torr) Versus Irradiation Time: Before and After Irradiation of Mixtures Containing 170 Torr of Cyclopentane and 0.5 Torr of SF_6 at 45 W/cm^2 Using the P(46) Line of the (00°1)-(10°0) Transition, 918.7 cm^{-1}, N_2O_4 + NO_2 Infrared Peak Areas

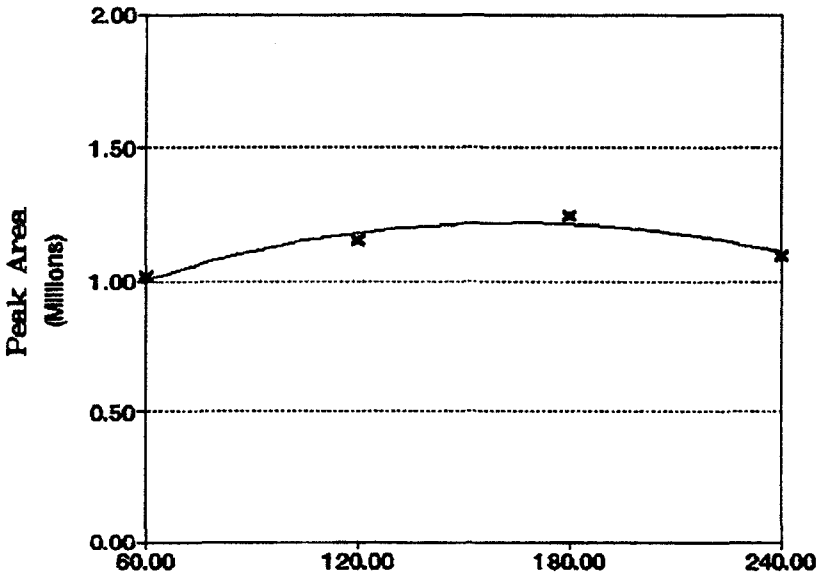

Figure 84. Nitrocyclopentane Vapor Versus Irradiation Time: Nitrocyclopentane GC-MS Peak Areas After Irradiation of Mixtures Containing 170 Torr of Cyclopentane, 30 Torr of Nitrogen Oxides, and 0.5 Torr of SF_6 at 45 W/cm^2 Using the P(46) Line of the (00°1)-(10°0) Transition, 918.7 cm^{-1}

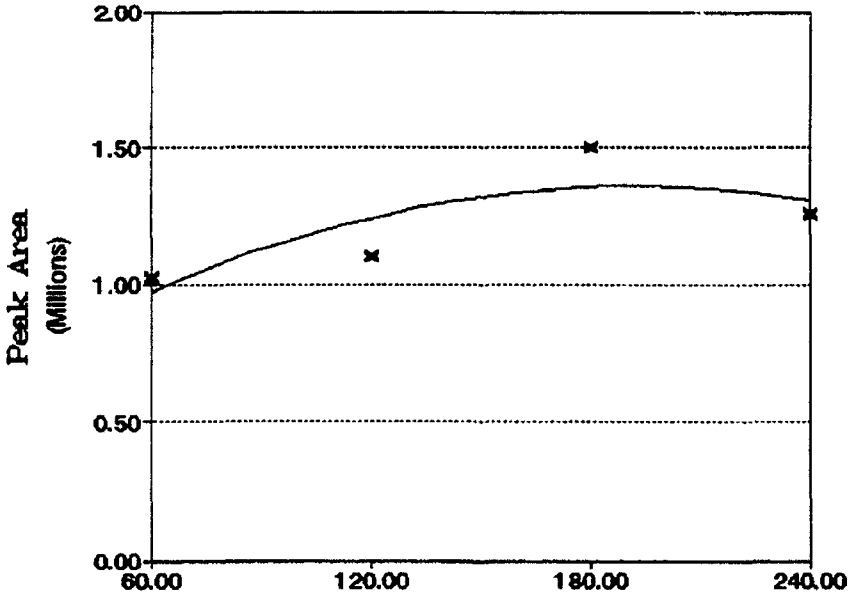

Figure 85. Nitrocyclopentane Liquid Versus Irradiation Time: Nitrocyclopentane Cell Wash GC-MS Peak Areas After Irradiation of Mixtures Containing 170 Torr of Cyclopentane, 30 Torr of Nitrogen Oxides, and 0.5 Torr of SF_6 at 45 W/cm^2 Using the P(46) Line of the (00°1) (10°0) Transition, 918.7 cm^{-1}

were conducted. A calibration curve (Fig. 86) was constructed as follows: volumes of neat nitrocyclopentane (1.0 - 8.0 ml) were added to the empty reaction cell, 2.0 mL of absolute ethanol added to this, the solution mixed by swirling, and then 0.50 ml samples of the "cell wash" injected on the GC-MS. Total ion counts were plotted vs. mls nitrocyclopentane/2.0 mL of solution. The peak area from the 60-s irradiation corresponded to about 1 mg of nitrocyclopentane (5 percent yield, based on moles of nitrogen oxides present initially). Although no other nitroalkanes were detected, increasing irradiation times did encourage formic acid, CO_2, and NO production (Figs. 87 through 89). The CO production did not appear to depend on irradiation time. The area of the mixed gas peak displayed, if anything, a slight decrease over irradiation times ranging from 60 to 240 s. This result supports previous observations: increasing the irradiation time does not as strongly favor fragmentation processes as does increasing the pressure of the sensitizer SF_6, which encourages the formation of the mixed gases through a strong energy absorbing effect.

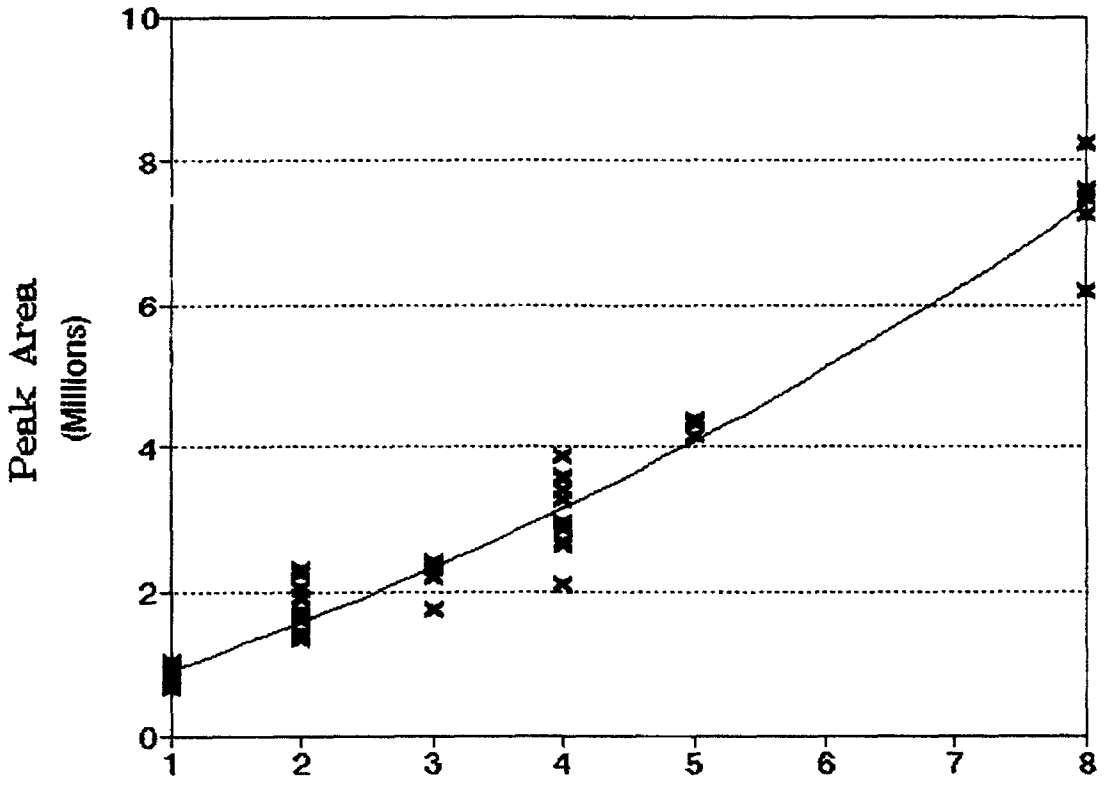

Figure 86. Calibration Curve for Nitrocyclopentane Solutions Using GC-MS Data

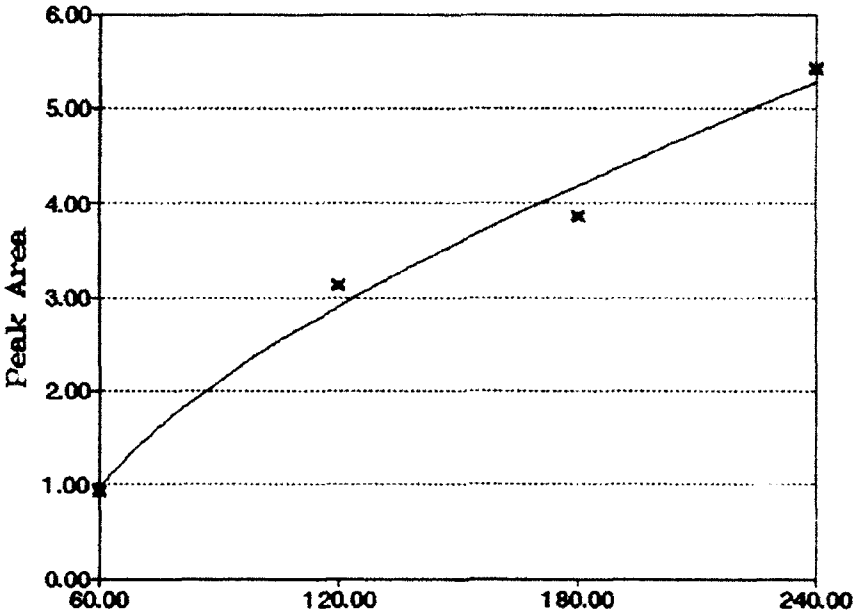

Figure 87. Formic Acid Production Versus Irradiation Time: Formic Acid Infrared Peak Areas After Irradiation of Mixtures Containing 170 Torr of Cyclopentane, 30 Torr of Nitrogen Oxides, and 0.5 Torr of SF_6 at 45 W/cm^2 Using the P(46) Line of the (00°1)-(10°0) Transition, 918.7 cm^{-1}

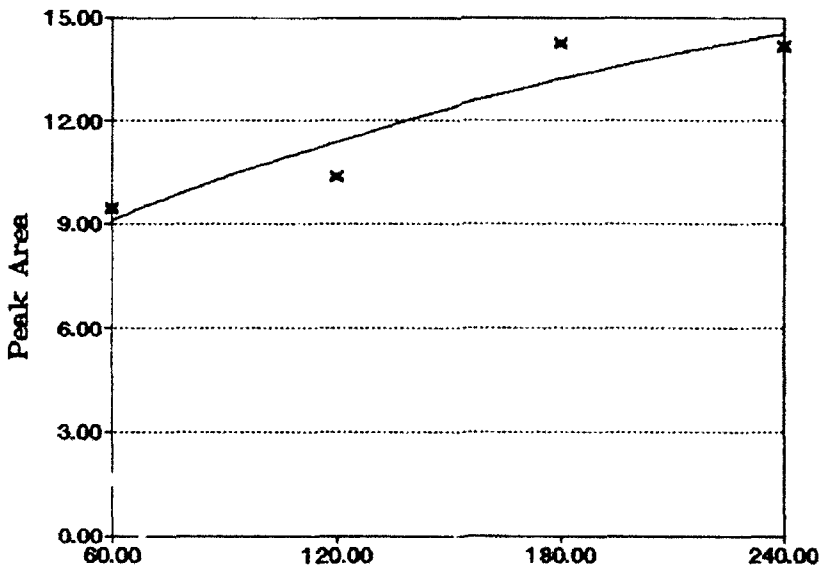

Figure 88. Carbon Dioxide Production Versus Irradiation Time: Carbon Dioxide Infrared Peak Areas After Irradiation of Mixtures Containing 170 Torr of Cyclopentane, 30 Torr of Nitrogen Oxides, and 0.5 Torr of SF_6 at 45 W/cm^2 Using the P(46) Line of the (00°1)-(10°0) Transition, 918.7 cm^{-1}

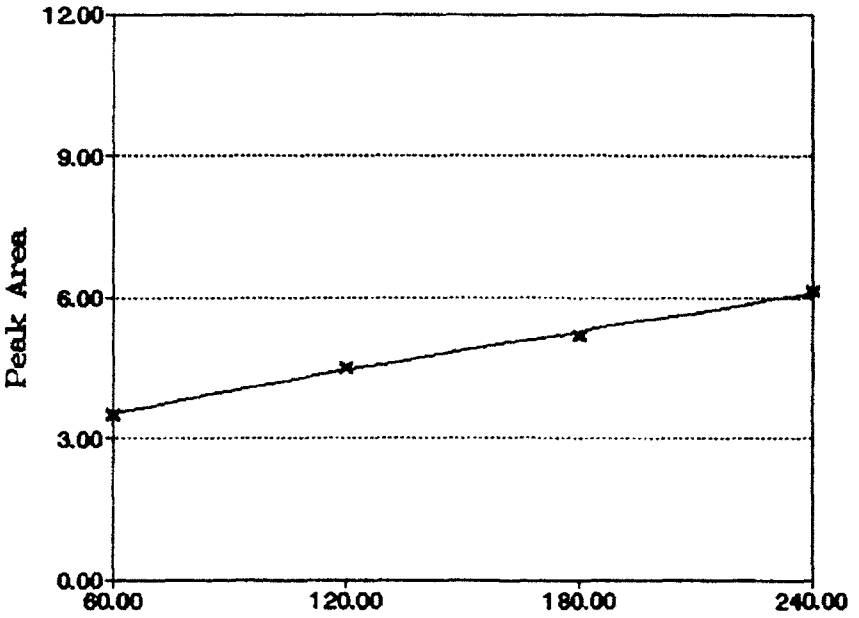

Figure 89. Nitrogen Monoxide Production Versus Irradiation Time: Nitrogen Monoxide Infrared Peak Areas After Irradiation of Mixtures Containing 170 Torr of Cyclopentane, 30 Torr of Nitrogen Oxides, and 0.5 Torr of SF_6 at 45 W/cm^2 Using the P(46) Line of the (00°1)-(10°0) Transition, 918.7 cm^{-1}

Results of previous experiments in which SF_6 pressure was varied, indicated nitrocyclopentane production had decreased as the SF_6 pressure exceeded 1.5 Torr, perhaps as a result of depletion of nitrogen oxides (initially, 20 Torr) from the reaction mixtures. Using infrared and GC-MS analyses, we examined the profiles of products resulting from a series of reaction mixtures in which the SF_6 pressure was carefully controlled (0 – 2.5 Torr), the cyclopentane pressure was 170 Torr, and the nitrogen oxides pressure was increased to 30 Torr. Irradiation was for 60 s at 45 W/cm^2 using the P(46) line. The areas of the SF_6 peaks increased linearly with the SF_6 pressure, and were the same before and after irradiation, showing the sensitizer's lack of involvement in chemical reactions. Cyclopentane areas in the product mixtures did not appear to decrease as the SF_6 pressure rose according to the GC-MS analyses. Our efforts to follow any decrease in cyclopentane using infrared integrals were hindered at higher SF_6 pressures by the production of ethene, many of whose infrared transitions fall in the same spectral region we were monitoring for cyclopentane, 920.4 – 871.2 cm^{-1}. The nitrogen oxides remaining showed a marked dependence on SF_6 pressure, having reacted almost completely at 2.0 Torr of SF_6 (Fig. 90).

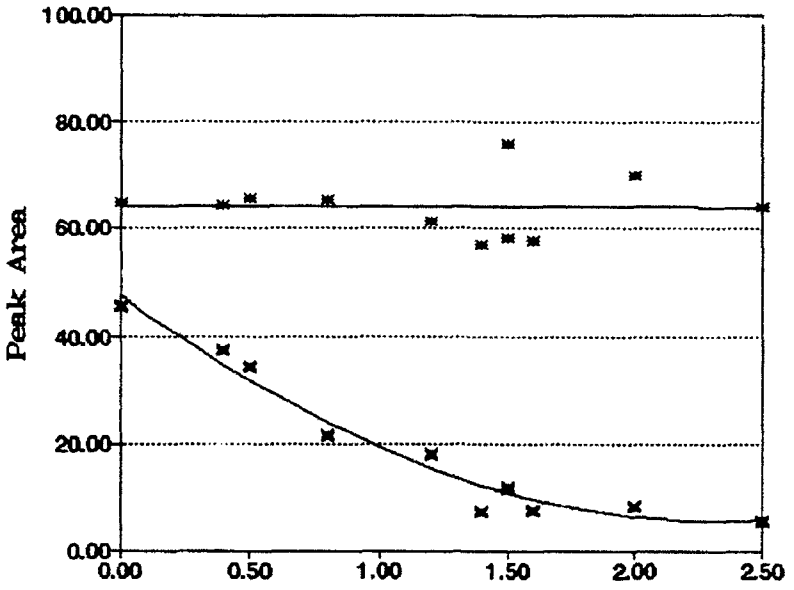

Figure 90a. Nitrogen Oxides (30 Torr) Versus SF_6 Pressure: Before and After Irradiation of Mixtures Containing 170 Torr of Cyclopentane for 60 s at 45 W/cm^2 Using the P(46) Line of the (00°1)-(10°0) Transition, 918.7 cm^{-1}, N_2O_4 Infrared Peak Areas

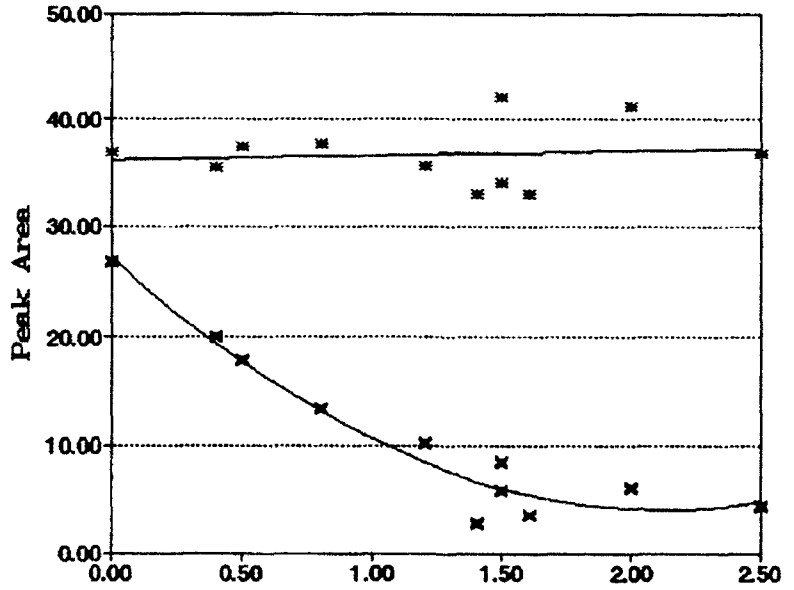

Figure 90b. Nitrogen Oxides (30 Torr) Versus SF_6 Pressure: Before and After Irradiation of Mixtures Containing 170 Torr of Cyclopentane for 60 s at 45 W/cm^2 Using the P(46) Line of the (00°1)-(10°0) Transition, 918.7 cm^{-1}, N_2O_4 + NO_2 Infrared Peak Areas

Nitrocyclopentane remained constant in the gas phase from 0 - 2.0 Torr of SF_6, and then decreased at 2.5 Torr (Fig. 91). The cell wash results help to explain the nitrocyclopentane production. Sufficient nitrocyclopentane had formed at 0 Torr of SF_6 for it to be detected in the condensed phase (Fig. 92), with the quantity in the liquid phase increasing up to about 1.5 Torr of SF_6 and the amount in the gas phase remaining constant and equal to the vapor pressure. From 1.5 to 2.5 Torr of SF_6, the nitrocyclopentane production fell off until none was detected in the liquid form and all that was produced was present in the vapor phase; at 2.5 Torr of SF_6 the reaction system was so energetic that products besides nitrocyclopentane were favored. Figure 93 in which the condensed phase areas are scaled (factor 10 x) displays a comparison of vapor phase and condensed phase nitrocyclopentane production. Linear nitroalkanes identified in this system were 1-nitrobutane and 1-nitropropane. Both products were undetected until the SF_6 pressure reached about 1 Torr, after which their production increased, peaking at about 1.5 Torr, and then decreased thereafter, until neither could be detected at 2.5

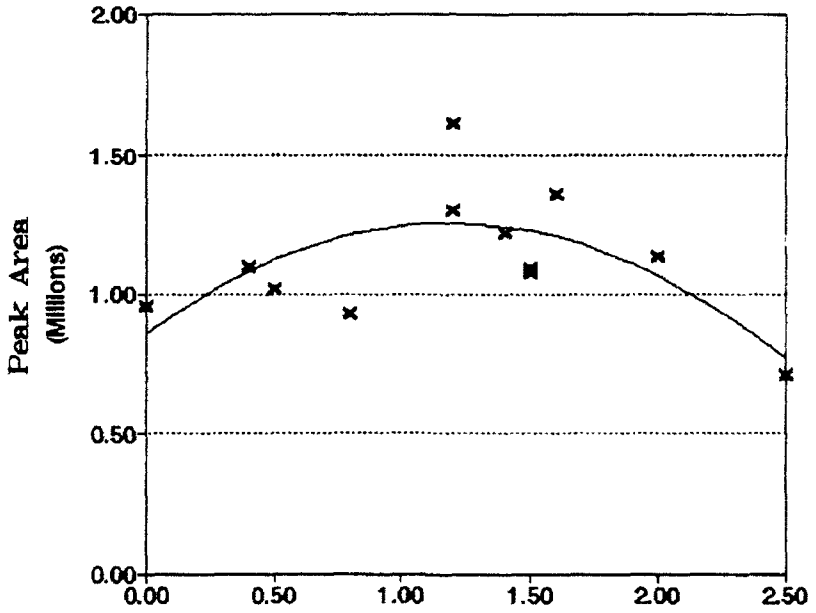

Figure 91. Nitrocyclopentane Vapor Versus SF_6 Pressure: Nitrocyclopentane GC-MS Peak Areas After Irradiation of Mixtures Containing 170 Torr of Cyclopentane and 30 Torr of Nitrogen Oxides for 60 s at 45 W/cm^2 Using the P(46) Line of the (00°1)-(10°0) Transition, 918.7 cm^{-1}

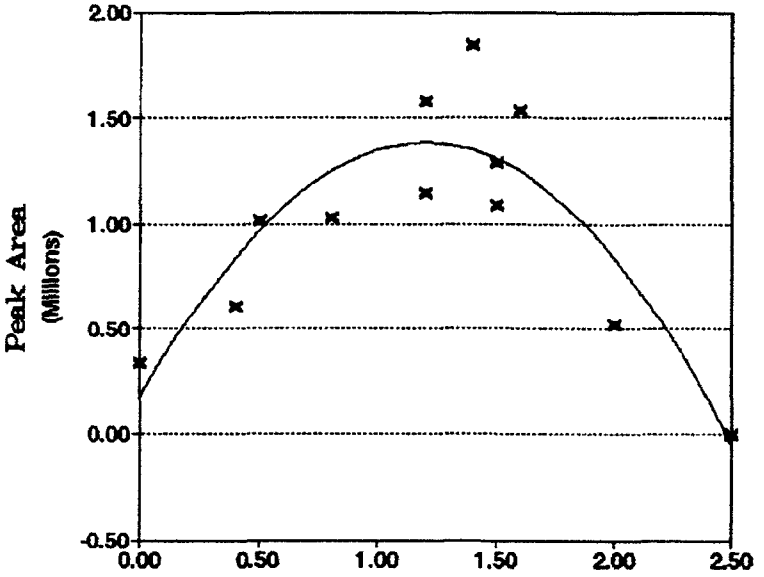

Figure 92. Nitrocyclopentane Liquid Versus SF_6 Pressure: Nitrocyclopentane Cell Wash GC-MS Peak Areas After Irradiation of Mixtures Containing 170 Torr of Cyclopentane and 30 Torr of Nitrogen Oxides for 60 s at 45 W/cm^2 Using the P(46) Line of the (00°1)-(10°0) Transition, 918.7 cm^{-1}

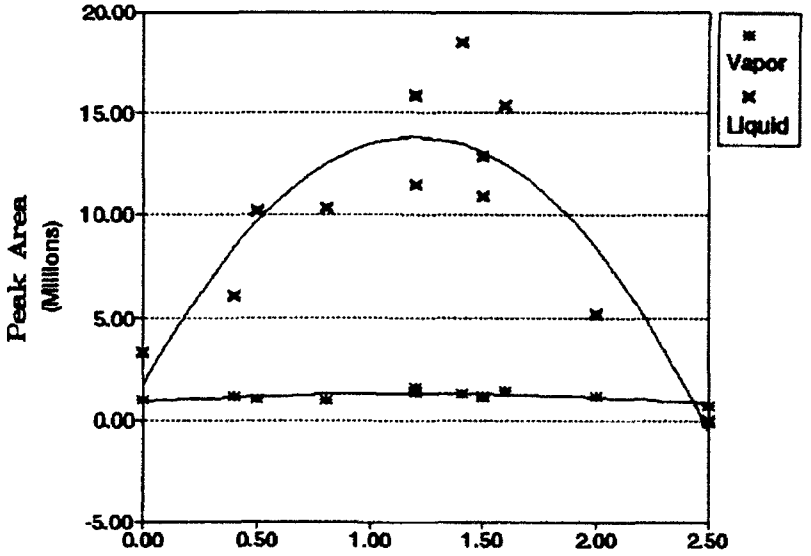

Figure 93. Nitrocyclopentane Vapor and Cell Wash (Scaled 10 x) Areas Versus SF_6 Pressure: After Irradiation of Cyclopentane (170 Torr) and Nitrogen Oxides (30 Torr) for 60 s at 45 W/cm^2 Using the P(46) Line of the (00°1)-(10°0) Transition, 918.7 cm^{-1}

Torr of SF_6 (Figs. 94 and 95). Formic acid and CO_2 production (Figs. 96 and 97) increased up to SF_6 pressures of about 2 Torr where the amounts leveled off, or perhaps decreased. In contrast, the amounts of CO and NO present in the product mixture continued to increase throughout the entire range of SF_6 pressures (Figs. 98 and 99). The GC mixed gas peak increased slightly up to about 1.5 Torr of SF_6 (Fig. 100), then inclined sharply when sensitizer pressures exceeded 1.5 Torr, a reflection of the increased fragmentation that occurred as the rate of energy absorbed by the system increased. Additional products resulting from the higher energy absorbed in the 2.0 and 2.5 Torr experiments were HCN, ethene, methane, and, tentatively, formaldehyde and NNO, as identified in the infrared.

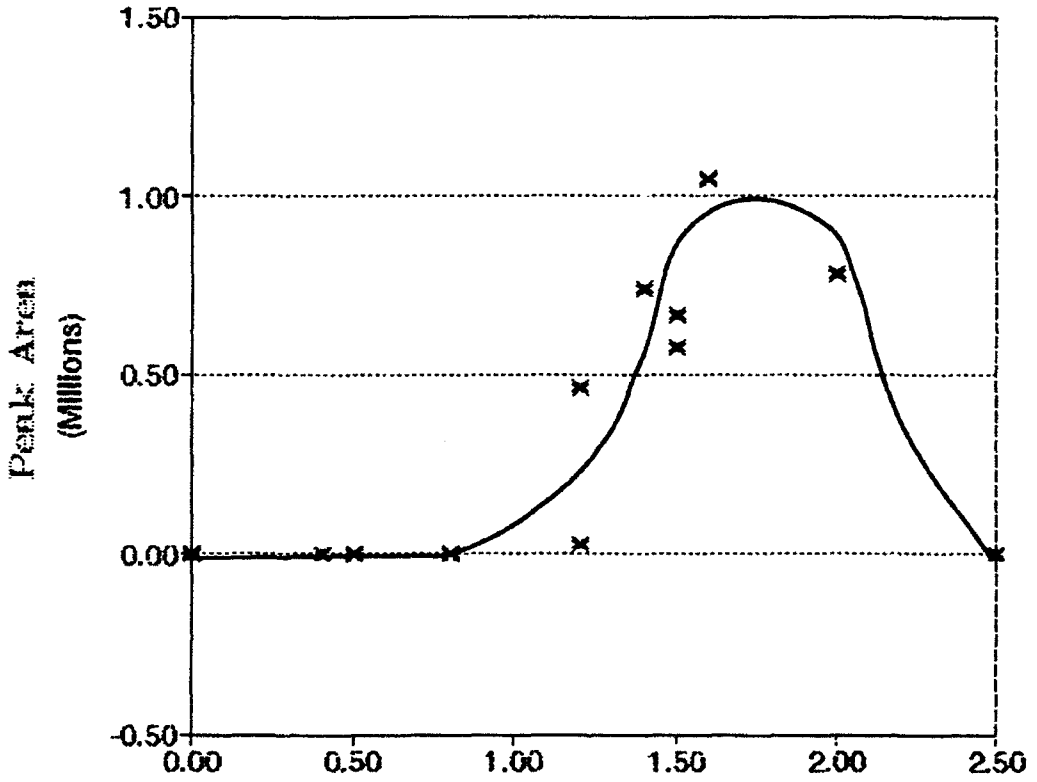

Figure 94. 1-Nitrobutane Versus SF_6 Pressure: 1-Nitrobutane GC-MS Peak Areas After Irradiation of Mixtures Containing 170 Torr of Cyclopentane and 30 Torr of Nitrogen Oxides for 60 s at 45 W/cm^2 Using the P(46) Line of the (00°1)–(10°0) Transition, 918.7 cm^{-1}

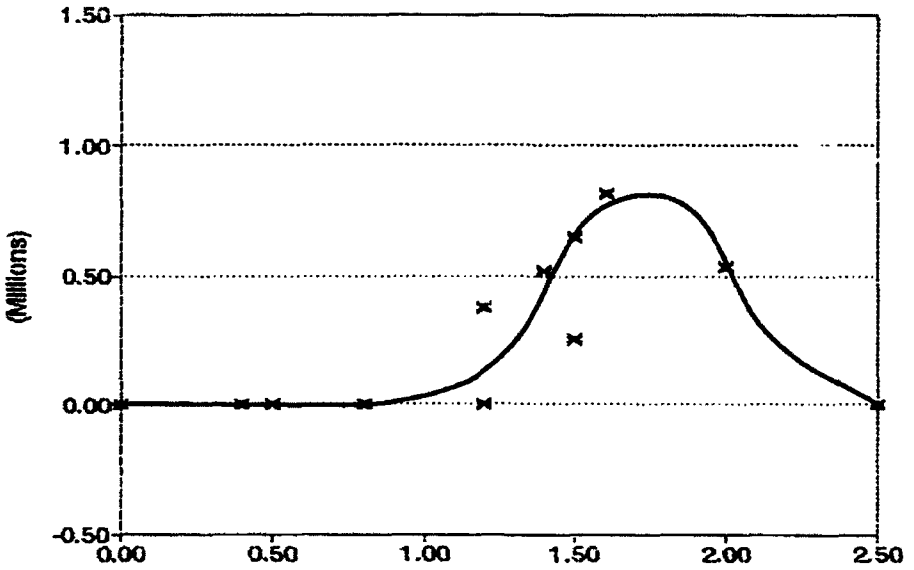

Figure 95. 1-Nitropropane Versus SF_6 Pressure: 1-Nitropropane GC-MS Peak Areas After Irradiation of Mixtures Containing 170 Torr of Cyclopentane and 30 Torr of Nitrogen Oxides for 60 s at 45 W/cm^2 Using the P(46) Line of the (00°1)-(10°0) Transition, 918.7 cm^{-1}

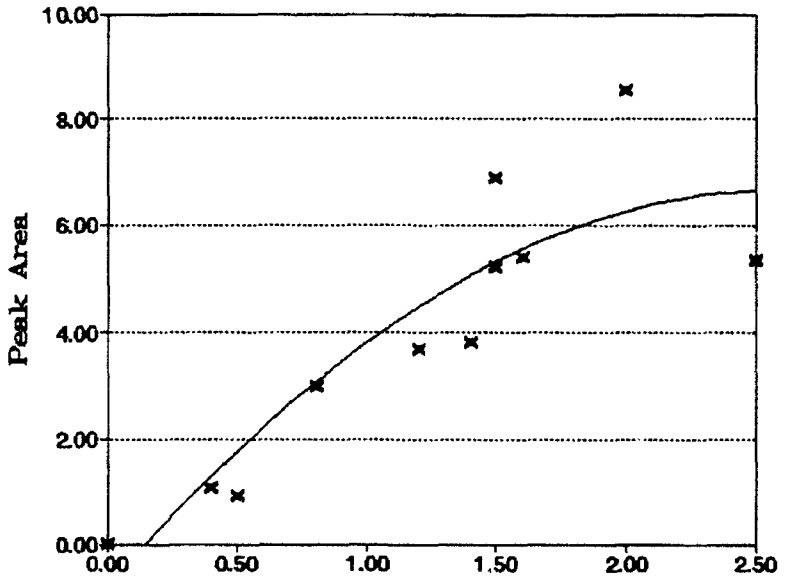

Figure 96. Formic Acid Versus SF_6 Pressure: Formic Acid Infrared Peak Areas After Irradiation of Mixtures Containing 170 Torr of Cyclopentane and 30 Torr of Nitrogen Oxides for 60 s at 45 W/cm^2 Using the P(46) Line of the (00°1)-(10°0) Transition, 918.7 cm^{-1}

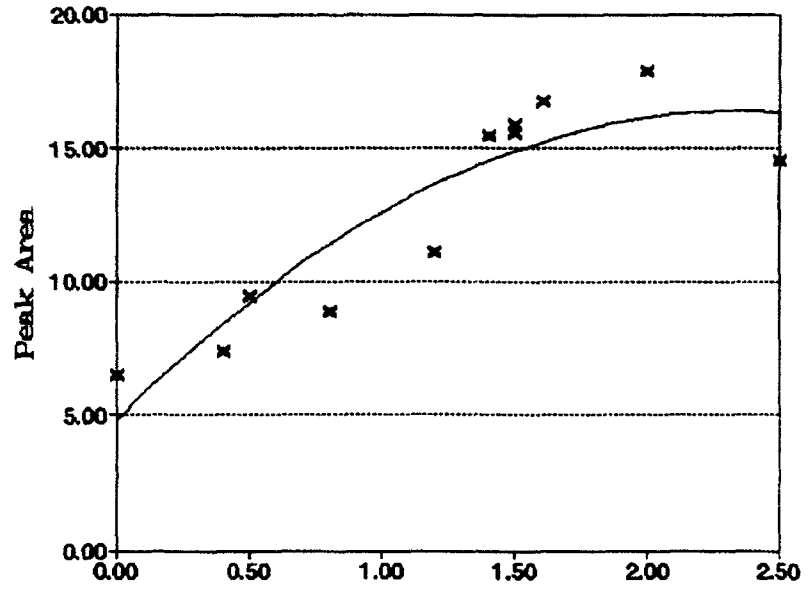

Figure 97. Carbon Dioxide Acid Versus SF_6 Pressure: Carbon Dioxide Infrared Peak Areas After Irradiation of Mixtures Containing 170 Torr of Cyclopentane and 30 Torr of Nitrogen Oxides for 60 s at 45 W/cm^2 Using the P(46) Line of the (00°1)-(10°0) Transition, 918.7 cm^{-1}

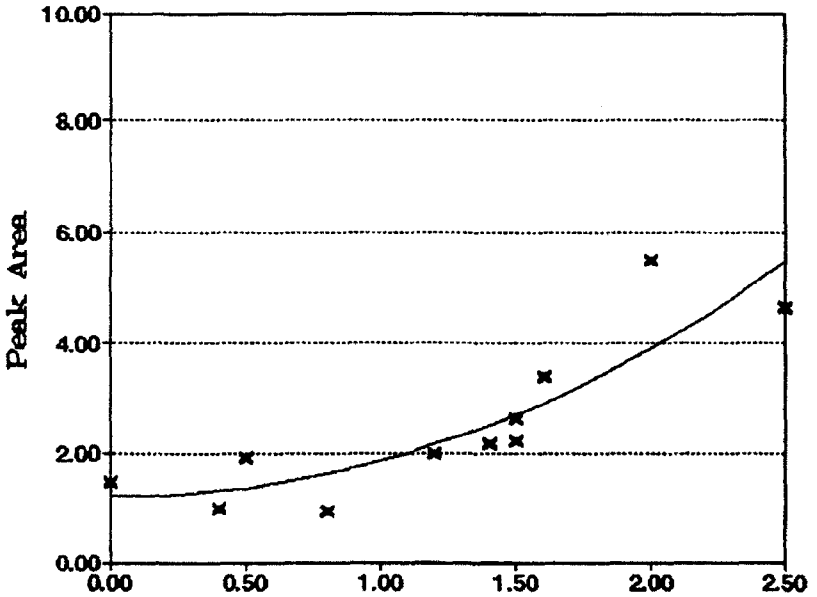

Figure 98. Carbon Monoxide Versus SF_6 Pressure: Carbon Monoxide Infrared Peak Areas After Irradiation of Mixtures Containing 170 Torr of Cyclopentane and 30 Torr of Nitrogen Oxides for 60 s at 45 W/cm^2 Using the P(46) Line of the (00°1)-(10°0) Transition, 918.7 cm^{-1}

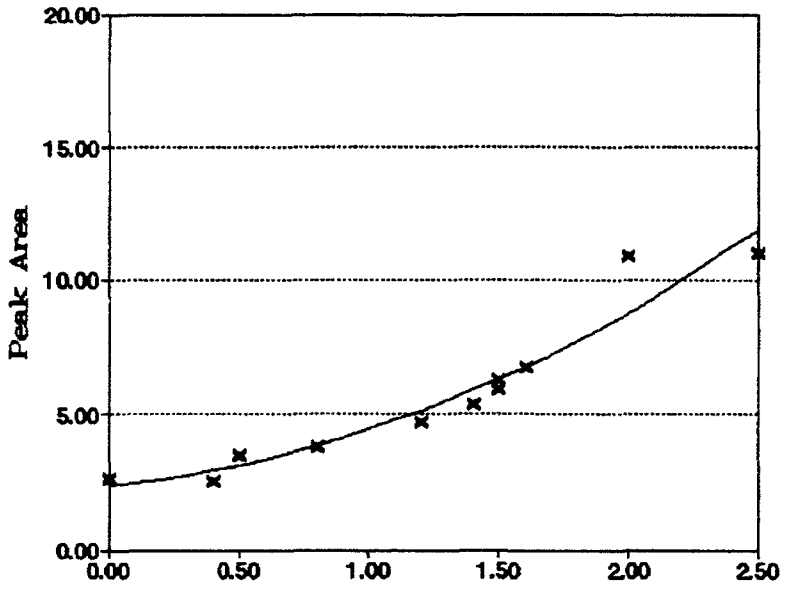

Figure 99. Nitrogen Monoxide Versus SF_6 Pressure: Nitrogen Monoxide Infrared Peak Areas After Irradiation of Mixtures Containing 170 Torr of Cyclopentane and 30 Torr of Nitrogen Oxides for 60 s at 45 W/cm^2 Using the P(46) Line of the (00°1)-(10°0) Transition, 918.7 cm^{-1}

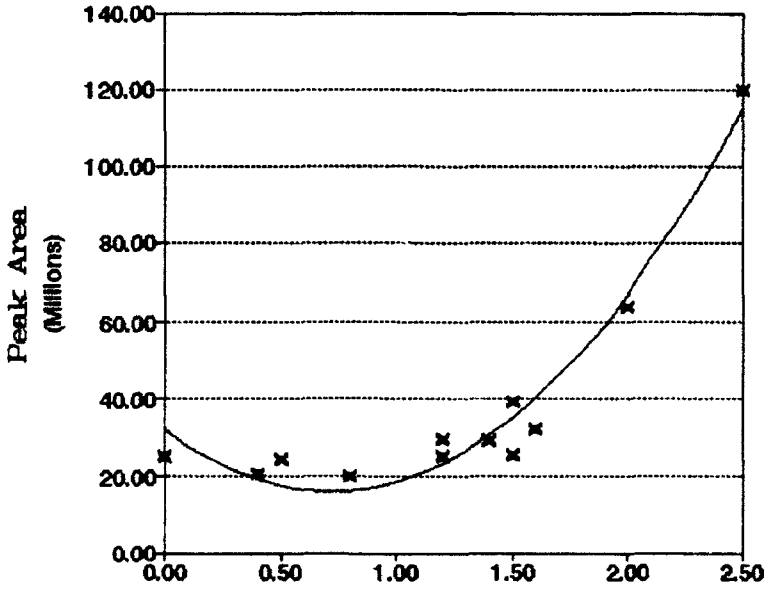

Figure 100. Mixed Gas Production Versus SF_6 Pressure: Mixed Gas GC-MS Peak Areas After Irradiation of Mixtures Containing 170 Torr of Cyclopentane and 30 Torr of Nitrogen Oxides for 60 s at 45 W/cm^2 Using the P(46) Line of the (00°1)-(10°0) Transition, 918.7 cm^{-1}

IV. CONCLUSIONS

We have carried out the CW, CO_2 laser induced nitration reactions between nitrogen oxides and cyclopropane, cyclobutane, or cyclopentane under a wide range of reaction conditions in order to evaluate the effectiveness and selectivity of the laser driven processes. We successfully monitored the impact of increased energy absorption on the products of greatest synthetic interest to us, the nitrocycloalkanes. Although the optimal conditions for nitration vary among the hydrocarbons, each has an optimal power window for producing nitrocycloalkanes without breaking down the precursors or products. For the cyclopropane experiments, the most favorable ratio of nitrocyclopropane to undesirable side products occurs when mixtures of cyclopropane (210 Torr) and nitrogen oxides (40 Torr) are irradiated at 25 W/cm^2 for 20 - 25 s using the P(18) laser line of the (00°1)-(02°0) transition. These conditions give no detectable amounts of side products that could pose separation problems, namely, propene, nitromethane, propenal, acetonitrile, and propenitrile, and reduce the amount of HCN to an almost undetectable level. Using the P(42) line of the (00°1)-(10°0) transition, mixtures of cyclobutane (180 Torr) and nitrogen oxides (40 Torr) when irradiated at 50 W/cm^2 for 60 s, favor nitrocyclobutane production while minimizing 1-nitropropane. If 1-nitropropane can be tolerated in the product mixture, raising the power to 60 W/cm^2 while increasing the cyclobutane pressure to 200 Torr increases the amount of both nitroalkanes. In the cyclopentane nitration, the most favorable pressures are 170 Torr of cyclopentane, 30 Torr of nitrogen oxides, and 1.0 Torr of SF_6 with irradiation at 45 W/cm^2 for 30 s using the P(46) line of the (00°1)-(10°0) transition of the CO_2 laser. These conditions yield nitrocyclopentane while eliminating detectable amounts of 1-nitrobutane and 1-nitropropane. Only at high SF_6 pressures (2.0 Torr) did we detect HCN in the infrared.

From the GC-MS and infrared analyses, the dependence of the quantity of reactants and products formed as a function of either variations in the incident laser power or on changes in pressures of the cyclic hydrocarbons, sensitizer, and nitrogen oxides was determined. The product yields, especially those of the nitrocycloalkanes, are highly sensitive to changes in the reaction systems, and therefore, serve as a probe of the energy state of the reaction. Energy absorption is increased by (a) irradiation for longer times while holding the pressures of the reactants and the incident power constant, (b) increase of the incident laser power, (c) increase of the pressure of the energy absorbing hvdrocarbon, or (d) increase of the sensitizer pressure. Of these, increased irradiation time is unique in that it increases the total energy absorbed by the system without increasing the power absorbed (energy per unit time). Under a given set of pressures and incident power, the amount of nitrocycloalkane depends on irradiation time to the extent that the nitrogen oxides are still available in the reaction system. In fact all the products, except ethene forming from cyclobutane, follow this pattern: the products reach their maximum yields by the time the areas of the nitrogen oxides decrease and level off, indicating that nitrogen oxides are required in the reaction paths of each of them.

Increased hydrocarbon pressure, incident laser power, and sensitizer pressure all have the effect of increasing the rate of energy absorbed. In order to vary the power significantly by varying the hydrocarbon pressure a wide range of pressures have to be employed. The resulting variation in total pressure and in ratio of reactants complicates the determination of power dependence. As expected, increasing the hydrocarbon pressure favors the production of nitrocycloalkanes, at least up to a point. When cyclopropane pressure is varied, nitrocyclopropane yield increases up to the cyclopropane pressure at which the nitrogen oxides reach a minimum: the nitrating agent is essentially depleted so nitration ceases. In the cyclobutane pressure series, the nitrocyclobutane production also mirrors the nitrogen oxide use. Though nitrogen oxides do not absorb the CO_2 laser output directly, the nitrogen oxides pressure has an important effect on the cyclopropane reaction system. Increasing the nitrogen oxides pressure over the range studied has no discernible effect on the yield of vapor phase nitrocyclopropane; however, some other products are dramatically encouraged by increasing nitrogen oxides pressure, namely propene, acetonitrile, propenitrile, nitromethane, and propenal. Therefore, in a utilitarian sense, the nitrogen oxides pressure should be strictly controlled at an appropriately low level to minimize these side products.

Variation of the incident laser power over a limited range of powers allows the most direct access for determining power dependence. Instrumental limitations restricted us to 20 - 25 W/cm^2 on the low power side, below which lasing could not be sustained, and 100 W/cm^2 on the high power side for the strongest laser emissions. The CO_2 transitions available to directly irradiate the cyclic hydrocarbons are not among the strongest output bands and correspond to weak hydrocarbon absorbances. Even so, we can extract some information about the dependence of nitrocycloalkane formation on incident power using data from the cyclopropane and cyclobutane experiments. Increasing the irradiation power favors the production of nitrocycloalkanes until sufficient power is absorbed that fragmentation reactions predominate. A number of fragmentation products can be detected only after a certain threshold power and increase rapidly thereafter. There is, therefore, a narrow range of powers that optimizes nitrocycloalkane production: the incident power must be high enough to support nitration but low enough not to exceed the threshold that promotes excessive fragmentation.

Cyclopentane has weaker absorption bands than do cyclopropane or cyclobutane in the frequency range accessible through direct irradiation using the CO_2 laser. A sensitizer helps to overcome some of the limitations encountered in adjusting the laser output by providing a flexible, though indirect, means of varying power. The CO_2 laser has several emissions overlying an intense absorption region of SF_6, which also overlaps with a weak absorption band of cyclopentane. The frequency of irradiation can be varied so that SF_6 absorbs more or less of the energy. Alternatively, the pressure of SF_6 can be changed while keeping the ratio of nitrating agent to hydrocarbon constant and, at the low pressures of SF_6 required, keep the total pressure essentially constant. Varying the power with the aid of the sensitizer has an analogous effect to increasing

incident power, that is, there is a narrow range of sensitizer pressures that favors nitrocyclopentane production and limits fragmentation. The most pronounced effect on fragmentation is observed when energy absorption is increased using a sensitizer.

Nitrocyclopentane formation is so favored, especially with SF_6 present, that the reaction cell becomes saturated with the vapor and the nitrocyclopentane begins condensing on the container walls. Using the cell-wash procedure, it was shown to be true for nitrocyclopentane, which has a vapor pressure of about 1 Torr, and it is possible that it can occur for the lower molecular weight nitroalkanes too, though their vapor pressures are higher. Even at optimum pressures of SF_6 (1.0–1.5 Torr), nitrocyclopentane was the only nitroalkane detected in the condensed phase, evidence for the high selectivity of the laser-induced nitration process. The yield of nitrocyclopentane, based on the calibration curve, was 10-12 percent under optimum conditions, based on nitrogen oxides, the limiting reagent. Pure samples of nitrocyclopropane and nitrocyclobutane were unavailable for use as standards to determine their percent yields. However, this 10-12 percent yield is better than the 3.6 - 5.0 percent yield [1] obtained in the thermal nitration of nitrocyclopropane. Because of the favorable yields in the cyclopentane reaction and the selectivity of the laser induced nitration of the cyclic hydrocarbons, the possibility exists for a continuous process in which liquid nitrocycloalkanes can be recovered free of contamination.

It is our opinion that with continued research in this area, these laser-induced nitrations could be driven to even higher yields. The lessons learned from the use of SF_6 with cyclopentane could be applied successfully to both cyclopropane and cyclobutane. It is also likely that this process could be successfully extended to other classes of compounds, including aromatics. Finally, it would be interesting to evaluate the coincident excitation of both reactants using the appropriate lasers.

REFERENCES

1. Hass, H. B. and Shechter, H., J. Am. Chem. Soc. **75**, 1382 (1953).

2. Stanley, A. E. and Godbey, S. E., Appl. Spectrosc. **43**, 674 (1989).

3. Stanley, A. E., Godbey, S. E., Bonicamp, J. M., and Ludwick, L. M., Spectrochim. Acta., in press, 1992.

4. Stanley, A. E., Ludwick, L. M., White, D., Andrews, D. E., and Godbey, S. E., Appl. Spectrosc., in press, 1992.

5. Khalit, S. M. and Jarjis, H. M., Z. Naturforsch **46**, 898 (1991).

6. Lifshitz, Assa, "Shock Initiated Pyrolsis of Nitrocyclopropane," Final Technical Report, U. S. European Research Office, London, England, December 1966.

7. Sverdlov, L. M., Kovner, M. A., and Krainov, E. P., *Vibrational Spectra of Polyatomic Molecules* (John Wiley & Sons, New York, 1974) and references therein.

8. Smith, D. C., Chi-Yuan Pan, and Nielson, J. R., J. Chem. Phys. **18**, 706 (1950).

9. Durig, J. R., Smooter Smith, J. A., Li, Y. S., and Wasac, F. M., J. Mol. Str. **99**, 45 (1983).

10. Arakawa, G. T. and Nielsen, A. H., J. Mol. Spectrosc. **2**, 413 (1958).

11. Begun, G. M. and Fletcher, W. H., J. Mol. Spectrosc. **4**, 388 (1960).

12. Durig, J. R., Sun, F. Y., Li, Y. S., and Bush, S. F., J. Ram. Spectrosc. **13**, 290 (1982).

13. Gilkut, K. E. and Borden, W. T., J. Org. Chem. **44**, 659 (1979).

14. Norton, R. H. and Beer, R., J. Opt. Soc. Am. **66**, 259 (1976).

DISTRIBUTION

	Copies
Director U.S. Army Research Office ATTN: SLCRO-PH P. O. Box 12211 Research Triangle Park, NC 27709-2211	1
Director U.S. Army Research Office ATTN: SLCRO-CB/R. Ghirardelli P. O. Box 12211 Research Triangle Park, NC 27709-2211	1
Headquarters Department of the Army ATTN: DAMA-ARR Washington, DC 20310-0623	1
Headquarters OUSDR&E ATTN: Ted Berlincourt The Pentagon Washington, DC 20310-0623	1
IIT Research Institute ATTN: GACIAC 10 W. 35th Street Chicago, IL 60616	1
Director Defense Advanced Research Projects Agency 1400 Wilson Boulevard Arlington, VA 22209	1
Commander U. S. Military Academy Department of Chemistry West Point, NY 10996–1785	1
Commander U. S. Army Chemical Research and Development Center ATTN: SMCCR-RS/E. J. Poziomek SMCCR-RSC/William S. Magee SMCCR-RSL-A/Steven Christensen SMCCR-RSP-B/Edward W. Stuebing Aberdeen Proving Ground, MD 21010-5423	 1 1 1 1

DISTRIBUTION (Cont'd)

	Copies
Commander Naval Research Laboratory 4555 Overlook Avenue, S.W. Washington, DC 20375–5015	1
Commandant HQ, U.S. Marine Corps ATTN: Code LMW-5 Washington, DC 20380–0001	1
U. S. Army Material System Analysis Activity ATTN: AMXSY-MP (Herbert Cohen) Aberdeen Proving Ground, MD 21005	1
Middle Tennessee State University Department of Chemistry and Physics ATTN: Judith M. Bonicamp Murfreesboro, TN 37132	25
Eastern Kentucky University Department of Chemistry ATTN: Susan E. Godbey Richmond, KY 40475	25
Tuskegee University ATTN: Larry M. Ludwick Tuskegee, AL 36088	25
Augusta College Department of Chemistry and Physics ATTN: Janice M. Turner Augusta, GA 30904	1
The University of Alabama in Huntsville Department of Chemistry ATTN: Samuel P. McManus Huntsville, AL 35899	1
U. S. Army Strategic Defense Command ATTN: DASD-H/Jimmy Barnett P. O. Box 1500 Huntsville, AL 35807-3801	1

DISTRIBUTION (Cont'd)

	Copies
AMSMI-RD, Dr. McCorkle	1
Dr. Rhoades	1
AMSMI-RD-PR, W. Stephens	1
AMSMI-RD-PR-T, L. Asaoka	1
AMSMI-RD-PR-M, K. McGuire	1
AMSMI-RD-CS-T	1
AMSMI-RD-CS-R	15
AMSMI-GC-IP, Fred Bush	1
AMSMI-RD-WS, W. Wharton	1
J. Bennett	1
S. Troglen	1
AMSMI-RD-WS-CM, Ann E. Stanley	25